Data-Driven Optimized Operation of Buildings with Intermittent Renewables and Application to a Net-Zero Energy Library

Vasken Dermardiros

A Thesis
In the Department
of
Building, Civil and Environmental Engineering

Presented in Partial Fulfillment of the Requirements
For the Degree of
Doctor in Philosophy (Building Engineering) at
Concordia University
Montreal, Quebec, Canada

December 2020

CONCORDIA UNIVERSITY

School of Graduate Studies

This is to certify that the thesis prepared

By: *Vasken Dermardiros*

Entitled: *Data-Driven Optimized Operation of Buildings with Intermittent Renewables and Application to a Net-Zero Energy Library*

and submitted in partial fulfillment of the requirements for the degree of

DOCTOR OF PHILOSOPHY (Building Engineering)

complies with the regulations of the University and meets the accepted standards with respect to originality and quality.

Signed by the final examining committee:

Dr. Youmin Zhang	Chair
Dr. Gregor P. Henze	External Examiner
Dr. Nawwaf Kharma	External to Program
Dr. Radu Zmeureanu	Examiner
Dr. Bruno Lee	Examiner
Dr. Andreas K. Athienitis	Thesis Co-Supervisor
Dr. Scott Bucking	Thesis Co-Supervisor

Approved by Dr. Michelle Nokken
Graduate Program Director

December 11, 2020 Dr. Mourad Debbabi
Interim Dean, Faculty of Engineering and Computer Science

Abstract

Data-Driven Optimized Operation of Buildings with Intermittent Renewables and Application to a Net-Zero Energy Library

Vasken Dermardiros, Ph.D.
Concordia University, 2020

We are at the intersection of three major trends in the built environment where: (i) occupants' comfort, health and safety requirements are needed to support a productive workplace while maintaining a low operating cost, (ii) economic and environmental advantages are favouring an increased use of renewable energy generation and to reduce our reliance on fossil fuels, and (iii) major utilities will require regulation and are gradually shifting towards a more dynamic energy market. This thesis contributes a modelling and control framework that unifies and addresses these three points together.

This thesis contributes a methodology for the development of a bootstrapped ensemble-based low-order data-driven grey-box thermal models for supervisory-level optimal controls. The model is integral to a robust sampling-based predictive control (MPC) framework. This approach is directly applicable to most commercial buildings operating on a schedule and can be extended to consider occupant-driven spaces.

The methodology is applied to the Varennes Net-Zero Energy Library: Canada's first institutional net-zero energy building. Exogenous inputs are modelled to consider likely probabilistic outcomes for ambient temperature, cloudiness and interior plug loads. Bounding cases are simulated to contrast the proposed approach against conventional methods. MPC is applied to minimize various cost functions and emphasis is placed on a flexible profile-

tracking cost function. The profile to track can be an open-market electrical price or a demand response signal thus improving the grid's flexibility while satisfying the building constraints and better utilizing its systems and storage. In a morning peak demand reduction case, given at least a 4-hour notice, our method is able to pre-heat the building, use minimal energy on-peak and yield the full benefits. Considering a profile tracking case to reduce grid interaction, a 10-12% total energy reduction was achieved for winter where the space was gradually heated in the morning and evening while maximizing HVAC utilization during periods of large photovoltaic generation promoting self-consumption. A similar strategy would be near-impossible to handcraft without optimization-based approaches.

This proposed methodology can guide later implementations in the development of the next generation of low-cost cloud-connected controllers that are easy to deploy and can be adapted dynamically.

Acknowledgements

I thank my supervisors Drs. Andreas K. Athienitis and Scott Bucking for their guidance and support throughout the PhD. My training as a researcher and scientist was sharpened through Prof. Athienitis' networking, encouragement to participate and gain exposure to international conferences held in Montreal, Ottawa, Toronto, New York, San Francisco, Atlanta, Orlando, Bern, Torino and Rome. Thank you for showing me the world! Prof. Bucking has honed my thinking and approach towards that of a computer and data scientist and has greatly encouraged me to explore the domain of artificial intelligence and its application to our built environment. The age of AI-assisted design and operation is upon us.

I would like to acknowledge the financial support received from the NSERC Alexander Graham Bell Doctorate Scholarship, the Hydro-Québec Engineering and Computer Science (ENCS) Entrance Scholarship, the Professor Hugh McQueen Award of Excellence, the Concordia Faculty of ENCS Graduate Scholarship, and through funding received through the Research Chair. Without this generous support, this work could not have been completed. Thank you firmly for putting faith in my work.

This thesis is part of an ongoing research project at Concordia University funded under a NSERC/Hydro-Québec Industrial Research Chair held by Dr. Athienitis which aims to improve the efficiency of buildings and their interactions with the grid through optimized controls. The Chair includes fundamental and experimental works to accelerate the implementation and demonstrate the effectiveness of advanced controls.

I acknowledge the help and support from Dr. Jiwu Rao from Concordia University for helpful discussions and analysis of the library data and for retrieving and processing weather data from the local airport weather station. Judith Frappier, Stéphane LaBarre, Raphaël Jacques from the city of Varennes for granting us access to the building data and for the

help in understanding the operation of the systems, and our partners from Régulvar, Marc Dugré and Gabriel Mainville, for connecting us to the building's BAS, offering training for their interface and explaining the implementation of the controls and their strategies. Also for thinking about the control systems to come to enable the wide adoption of the proposed methods herein. I acknowledge the help and discussions from the whole Hydro-Québec LTE research team, in particular Drs. Jocelyn Millette and Jonathan Bouchard; from the CanmetENERGY Varennes team, in particular Drs. Jose Candanedo and Vahid Dehkordi. I acknowledge the creators, developers and package maintainers of: python, pandas, matplotlib, cvxpy, scikit-learn, lmfit, emcee, bokeh, seaborn, plotly, cufflinks, git, spacemacs and org-mode – the last two have had a measurable positive impact in my life.

I would like to thank Prof. Annamaria Buonomano for the final encouragement to wrap up the thesis and submit for publication. Your positive influence is greatly cherished. I would like to thank Prof. Costa Kapsis for our long chats about dreaming what the future holds for buildings and the human experience. And I would warmly like to thank my friends and lab mates for the deep discussions and ideation sessions usually around a beer or three, particularly thinking of you Harry Vallianos, Nunzio Cotrufo, Olesia Kruglov, David Sun, Cristobal Guerrero, Bruno Marcotte, Fatima Amara, Tasos Papachristou, Efstratios (Stratos) Dimitrios Rounis, Zissis Ioannidis, Ali Saberi, Sam Yip, Jennifer Date, Remi Dumoulin, Camille John, Navid Morovat, Matin Abtahi, Mathieu Pellissier and James Bombara.

I would also like to thank my family for not asking too many questions.

Finally, a humongous thank you to Elsa Monanteras for standing by me and tolerating the struggles of the PhD life. I'm sorry if I've complained a bit too much. With your help, I've learned how to turn negative rants into positive action.

The thesis is in reality the tip of the iceberg: the 10% observable. The journey was arduous and cycled through euphoria and despair. Through it, I learned and discovered my own self. How to be organized, efficient, productive, self-motivated and, most importantly, persistent. It forced me to strengthen my beliefs, forge a vision and to lead my own path forward.

Quae quaestio.

Contents

List of Figures

List of Tables

Nomenclature

Acronyms

AHU	Air handling unit
(A)NN	(Artificial) neural network
(B)EMS	(Building) energy management system
AIC	Aikaike information criterion
AR/MA/X	Autoregressive/moving average/exogenous input (model)
BAS	Building automation system
BIC	Bayesian information criterion
BIM	Building information modelling
BIPV	Building-integrated photovoltaic
BIPV/T	Building-integrated photovoltaic with thermal (heat recovery)
COP	Coefficient of performance: heating/cooling effect over compressor work
CV(RMSE)	Coefficient of variation of the root mean squared error
DALI	Digital addressable lighting inferface
DE	Differential evolution: meta-heuristic optimization method
DOAS	Dedicated outdoor air system
DHI	Diffuse horizontal irradiance, W/m^2
DNI	Direct normal irradiance, W/m^2
EUI	Energy use intensity, kWh/m^2yr
FDD	Fault detection and diagnosis
FMI	Functional markup interface
GHI	Global horizontal irradiance, W/m^2
GHG	Greenhouse gas

GLM	Generalized linear model
GP	Gaussian process
GSHP	Ground-source heat pump
HP	Heat pump
HVAC	Heating, ventilation and air conditionning (systems)
IoT	Internet of things
MAE	Mean absolute error
MAP	Maximum *a posteriori* probability
MAPE	Mean absolute percentage error
MC	Monte Carlo
MCMC	Markov chain Monte Carlo
ML/AI	Machine learning/artificial intelligence
MLE	Maximum likelihood estimate
MPC	Model(-based) predictive control
MSE	Mean squared error
NetZEB	Net-zero energy building
NMBE	Normalized mean bias error
NSERC	Natural Sciences and Engineering Research Council of Canada
OLS	Ordinary least squares
P/PI/PID	Proportional-integral-derivative (control)
PCM	Phase-change material
PSO	Particle swarm optimization: meta-heuristic optimization method
PV	Photovoltaic (solar panels)
RC	Resistor-capacitor (network)
RL	Reinforcement learning
RMSE	Root mean squared error
RNN	Recurrent neural network
RTU	Roof-top prepackaged unit
SI	System identification
SMPC	Stochastic model(-based) predictive control

SNEBRN	Smart Net-Zero Energy Buildings Research Network
SS	State-space (model)
SVM	Support vector machine

Symbols and Variables

T	Temperature, $°C$
Q	Heat power, W
X	Independent variable, or system variable in state-space model
U	Controllable variable
W	Exogenous input
Y	Dependant variable, or model output in state-space model
subscript, n	Index, n^{th} variable or parameter
superscript, t	Index, time step
superscript, x^*	Optimal value of x
prefix, Δ	Difference
underscript, $\underline{x}$	Lower limit of x
overscript, $\overline{x}$	Upper limit of x
overscript, $\hat{x}$	Estimate of x
β	Parameter
ϵ	Residual, error
μ	Mean
$\mathcal{N}(\mu, \sigma^2)$	Normal (Gaussian) distribution with mean μ and standard deviation σ^2
σ	Variance

Chapter 1

Introduction

1.1 Mission Statement

How can we improve the operation of buildings for their occupants, owners, the utilities and the environment as renewable sources are increasingly employed and operational data is more abundantly available? How can we, on a massive scale, build control-oriented models and drive control decisions to improve grid regulation, reduce operational costs and guarantee occupant comfort? This thesis aims to help answer these questions.

1.2 Problem Statement

Electrical energy production and consumption do not always match. There are moments where the consumption demand peaks and puts a strain on the electric grid. During those periods, most utilities are forced to either purchase power from neighbouring grids at a premium, turn on gas-fired peaking power plants and/or ask large clients registered to a demand response program to reduce their demand and be compensated. Currently, generators are scheduled via contracts for the next few days and will curtail over-generation. The grid is not yet flexible.

The future of the grid is tending to be a transactional grid where energy and information will be exchanged among buildings in an open market; going from a larger community towards the micro- and nano-grid, see Figure 1.1. The nano-grid can be as simple as a single building

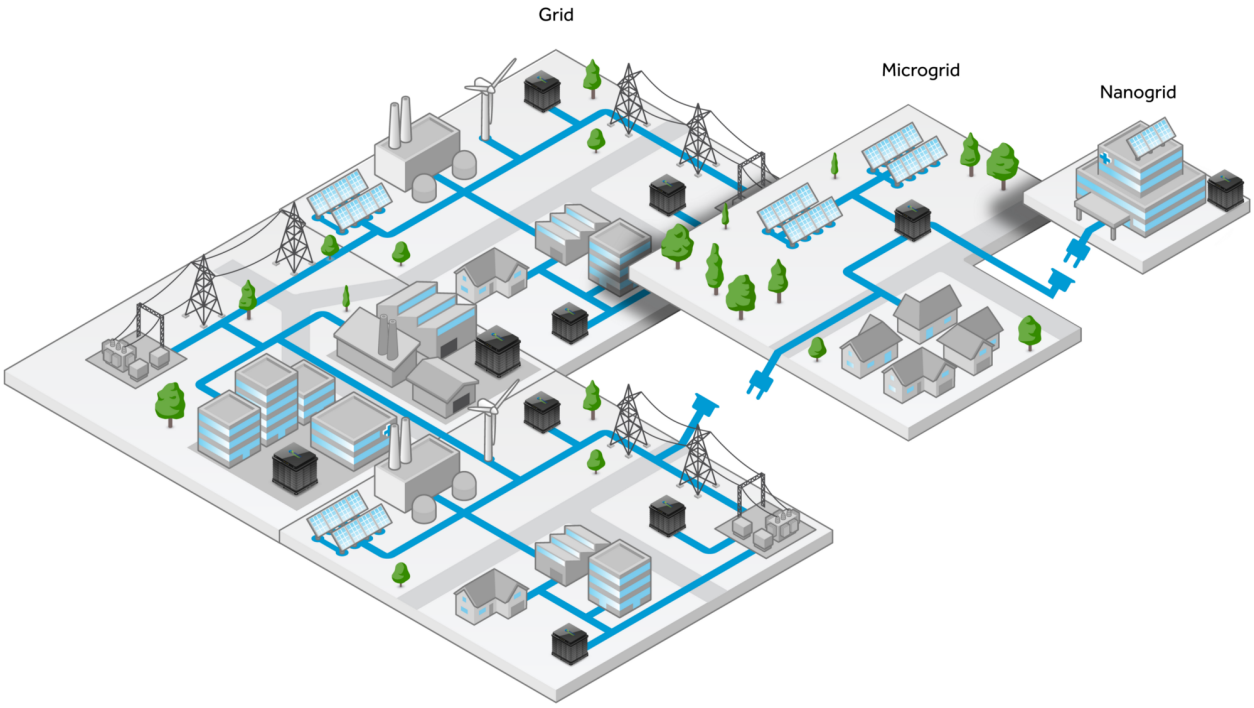

Figure 1.1: Transactional grid compartmentalization (Kabessa, 2017).

with its on-site renewable energy production and storage solution. In this thesis, the Varennes library is used as a case study, the first institutional net-zero energy building in Canada located just off Montreal in the city of Varennes, Quebec (Dermardiros et al., 2019). The building acts as a nano-grid with its on-site photovoltaic (PV) generation and has a thermal energy storage solution as part of its structure. There is no electrical storage system on-site, but can be considered for a future add-on. The work presented here can be transferable to other buildings running on a schedule since the library is first conditioned based on the time of day and then based on occupancy.

In a transactional grid, buildings must be dynamic and connected. They need to be *energy flexible* which is defined as the "ability to adapt the energy profile without jeopardizing technical and comfort constraints" (Aduda et al., 2016; Reynders et al., 2018).

Throughout the world, polluting power plants are being replaced by renewable energy sources. The price of PV solar panels has been dropping exponentially since the late '70s due to technological and manufacturing advancements (Kavlak et al., 2018). Solar energy has reached cost parity in most localities globally, beating coal, with a record lowest large-

scale installed cost at 1.79 cents/kWh in Saudi Arabia as of late 2017 (Graves, 2017). In Quebec where electricity is the cheapest in North America, cost parity is expected in 2023[1]. The utility power mix is not always clean (Bucking et al., 2016) and renewable sources can mitigate the problem.

The drawback of solar energy comes from its intermittent nature and unavailability during the night. California is actively integrating renewable energy more so than any other State. From the utility production in March 2017 shown in Figure 1.2, solar production peaks during noon. However, looking at the bottom subplot, we can observe a strong negative price signifying a phase misalignment of peak production and peak consumption. Closer to 5 PM, the price peaks due to net consumption ramping back up. Focusing on an average profile, in Figure 1.3 we can see the net power demand during the day throughout the years. As more and more solar panels are deployed, the utility-side net power demand is further reduced during the day. This leads to two issues: (1) it creates an exaggerated ramp during the evening and (2) it starts interfering with the utility's baseload power production, which is partly nuclear in California and cannot be modulated. Both problems force the utility to discount electricity during noon but must ramp up power plants – if possible – in the evening, which was previously not the case. The example shown is for the shoulder season when the cooling load is expected to be low and the least amount of electricity would be consumed. This circumstance foreshadows what is to be expected the rest of the year as renewable energy production is increased without electrical storage.

In Quebec, due to the low cost of electricity, solar is lagging. The climate is cold to very cold and the grid's peak demand occurs in winter mornings and evenings due to residential loads where heating is typically supplied using electric resistance and due to office and retail buildings starting up. See the power demand curve for a very cold day in Figure 1.4. Regarding the utility, the use of PV in Quebec does not aid with the morning peak in winter and may make matters worse during the evening similarly as above by depressing the noon-time utility output resulting in a larger ramp up. As the provincial utility, Hydro-Québec remains a provincial government-owned corporation. Although they claim 99% of their power is pro-

[1]Noted during a presentation by J. Millette, then researcher at Hydro-Québec's research office "Laboratoire des technologies de l'énergie (LTE)", at the Mission Innovation 7 workshop, 2018-09-27

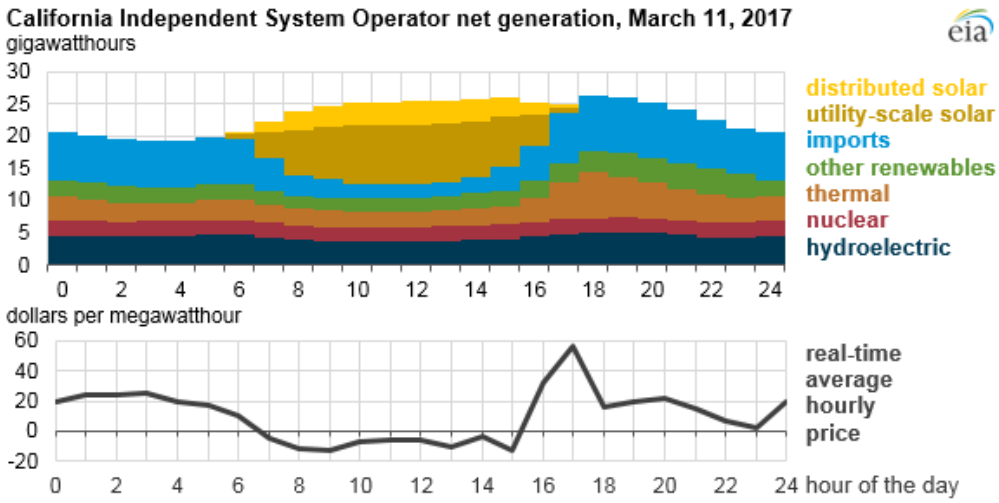

Figure 1.2: California power mix includes large central and distributed solar generation. Notice the negative electrical prices in the bottom subplot near noon and a peak close to 5 PM (EIA, 2017).

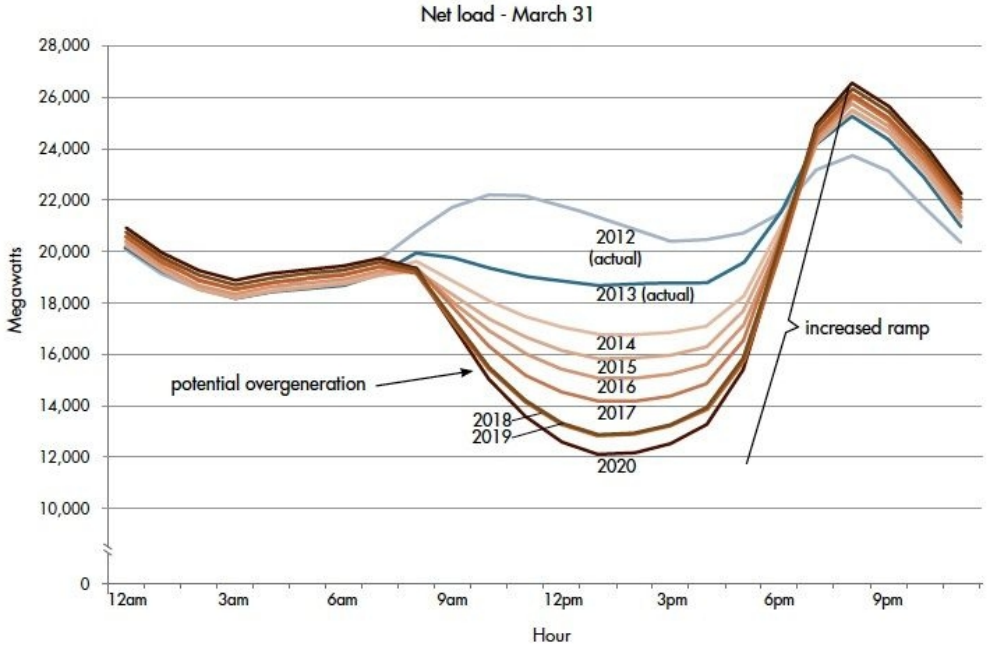

Figure 1.3: California grid duck curve. Comparing the 2012 load curve to the projected 2020 curve, a large evening ramp up period is created (EERE, 2017).

duced through renewable sources, the power source mix on the grid cannot be determined since a significant portion is imported from neighbouring provinces and states that rely on

fossil fuels. To reduce greenhouse gas emissions, the high-level objective should be to rely more on hydroelectricity with a flatter demand curve and to export more clean energy to neighbouring provinces and states during their peak periods to defer their use of fossil fuel burning peaker plants.

One solution to the peaking problem would be to install utility-scale storage systems, but they remain costly. Recently, Google DeepMind is in talks with UK's National Grid to help balance their electricity demand due to their larger reliance on energy from intermittent renewable sources (Thomas, 2017). As of the date of this publication, no follow-up reports have been released on the outcome of this collaboration.

Regulation can also occur on the consumption side through incentives – demand response and energy conservation programs – and direct links with intelligent thermostats. Intelligent buildings and homes can aid the utility by relying on energy flexibility concepts such as optimally controlling their thermal and/or electrical storage systems (Denholm and Hand, 2011; Jensen et al., 2017; Lund et al., 2015; Moslehi and Kumar, 2010). Buildings should be able to see the price of electricity, aid the utility by responding to demand response signals, anticipate its internal needs due to occupancy and weather forecasts, learn and know the intricate behaviour of its mechanical and electrical systems and act accordingly. Even with dedicated electrical or thermal storage including phase-change materials (Dermardiros, 2015; Dermardiros et al., 2016; Dermardiros and Athienitis, 2015; Dermardiros et al., 2015), a suitable whole sub-building and building models will inevitably be required to capture the thermal interactions and fulfill all the above requirements.

Current practice relies on specially designed rules from building operators or from control companies relying heavily on expertise where weather and occupancy predictions are rarely utilized. Research, on the other hand, focuses on simulation engines which are over-parameterized and are difficult to calibrate to an existing building: they are made for design purposes. Tailored models have their use but can only be afforded by boutique clients. We need general models to be trained on building data which can be scaled with cheap computational power throughout the years.

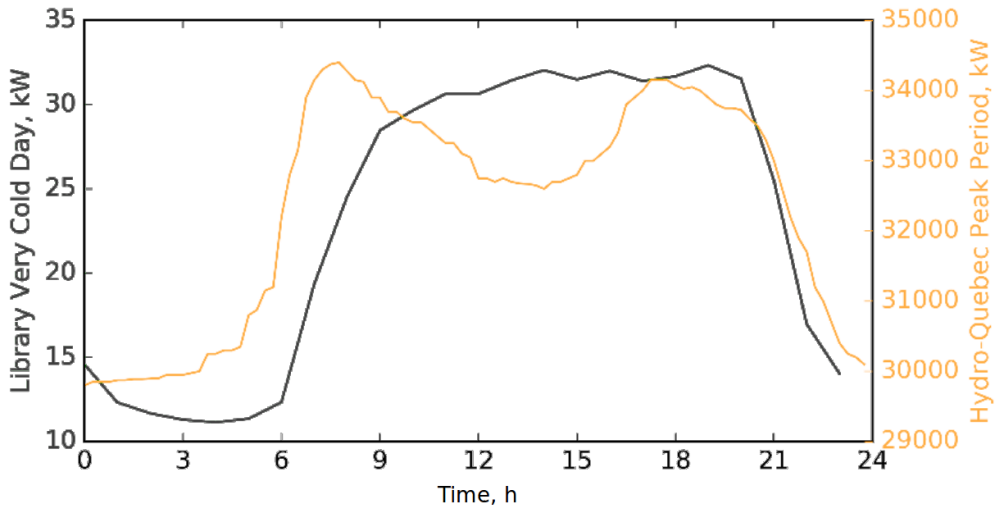

Figure 1.4: Library electrical demand and grid demand for an extreme winter day, Hydro-Québec data from 2011 (Laperrière and Brassard, 2011).

1.3 Method

Computational power has been growing exponentially for the past 120 years per unit dollar following Moore's Law. Data storage and networking follow a similar trend. Because of smart phones, the cost of sensors are also decreasing while becoming more precise and power efficient. Data is generated quickly and flexible models are needed to extract information. The field of deep learning has had another resurgence because of the alignment of all the above factors (LeCun et al., 2015; Goodfellow et al., 2016).

Buildings are unique and modelling each one individually is far from being cost-effective given the relative cost of energy compared to engineering fees. General data-driven models that can be broadly applied are needed. The data would first be analyzed to identify the most influential variables that explain the desired outcome. Depending on the scale of the model – room-level vs. floor-level vs. building-level – the selected variables will differ. The variables would then be input to a data-driven grey-box or black-box model. Various models will be compared and depending on the availability of data, some are likely to perform better due to the "No Free Lunch" theorem (Wolpert and Macready, 1997).

The models will serve to drive control decisions via model-predictive controls (MPC) to improve comfort, minimize peak power and energy demand while minimizing operating

costs. The models can also be used for fault detection and diagnostics (FDD) and for helping in the early design stage especially in complementing community design tools (Bucking and Dermardiros, 2018), but these objectives will remain secondary herein. Conventional reactive controls seldom make use of occupancy and weather predictions to drive control sequences and would fail or be too conservative under uncertainty.

As of this writing, we are in a pandemic. The way buildings are used has drastically changed and will continue to change particularly with work-from-home policies and social distancing measures needing to be imposed while at the office. The residential sector will evolve since they will be occupied for more hours during the day and there will be a need for a home office to perform work, while office buildings will become less dense and may primarily be used for work and meetings that will need to be done in person. Internet of things (IoT) sensors need to be applied to better assess occupancy and be supported by domain expertise and artificial intelligence (AI) to achieve the goals of flexibility, sustainability, comfort and, most importantly, health.

1.4 Thesis Structure

The thesis is structured in chapters. The chapters are published or under review in well-established journals, however the chapters herein include more details and supplemental information.

This introduction chapter gives an overall perspective of the way the electrical grid is transforming: there is an increased use of renewable energy sources and buildings can aid in the grid regulation well before necessitating electrical storage solutions. The following chapter reviews the current literature state-of-the-art. The subsequent three chapters elaborate on the central thesis of this work: given a building, how should it be analyzed, what modelling methodology should be used that best forecasts the building power and thermal state under uncertainty and how to apply it in a model-based predictive controls framework. The final chapter gives directions for future work on how to expand the proposed methodology in breadth and reach to scale to more buildings and to more archetypes of buildings.

Chapter 1 Introduction. States the mission and problem with a brief explanation of meth-

ods used. The electric grid is transforming and buildings will play a central role in its regulation.

Chapter 2 Literature Review. Pertinent references and review of current state-of-the-art highlighting research needs by this work and prospectively. Chapter focuses on time-series prediction and control methods specifically applied to buildings and thermal systems. Handling uncertainties and assuring efficient and scalable processing is emphasized through model simplification and iterative convex optimization methods.

Chapter 3 Energy Performance, Comfort and Lessons Learned from a NetZEB. A description and exploratory data analysis is applied to the case study Varennes Net-Zero Energy library. Methodology is formulated for schedule-driven buildings and pre-processing step for building transitional models. This approach is generic and general.

Chapter 4 Establishing Low-Order Models for Building Power and Thermal State Forecasting. A parametric study analysis and comparison is performed between physics-based and physics-free approaches. Model calibration metrics and approaches are proposed. The stability and spread of the model forecasts are analyzed when relying on a distribution of parameter weights.

Chapter 5 Sampling-Based Model Predictive Controls. A model-based predictive control framework is formulated for noised instances utilizing an ensemble-based model under various cost functions. Emphasis is given on the profile-tracking cost function that can represent the energy flexibility of the building given uncertain predictions of consumption and energy production.

Chapter 6 Conclusion and Directions for Future Work. Potential for future work and extended application of methods applied towards other buildings is discussed. The support from the industry and standardization bodies is indispensable to accelerate widespread adoption. The lasting research contributions are presented.

Appendix A Varennes Library Supplementary Information. The details on the lighting, natural ventilation, hydronic radiant slab, ground-source heat-pump and building-integrated photovoltaic and thermal (BIPV/T) system are expanded.

Appendix B Supplementary Models and Assumptions. Details are included on the causal effects between input features, on the modelling approaches for the library models and estimating its parameter posterior distributions, for modelling the BIPV/T system, on the exterior ambient temperature forecasts and on the cloudiness prediction model.

Appendix C Publication Contributions and Significance. A list of publications completed as part of this thesis and details of my personal contributions therein.

Chapter 2

Literature Review

This chapter provides background on current control practices in buildings and why there is a need for model- and prediction-based strategies. Section 2.1 states the current operational practice. Section 2.2 details what is model-based predictive controls (MPC) giving a brief historical perspective and the challenges that lie ahead. In section 2.3, the approaches to MPC are broken down into subsections covering categories of models, physics-based models, model calibration, simplifications to modelling including low-order models, typical day operational modes, hierarchical approaches and then consideration of model and prediction uncertainties. A subsection on pure data-driven approaches including reinforcement learning is also given. Section 2.4 discusses the financial advantage of MPC in the sustainable marketplace. Section 2.5 summarizes and links the material to then establish the research plan and objectives in sections 2.6 and 2.6.1.

2.1 Current Practice

Typically, buildings are controlled to match deterministic setpoints. The setpoints can be different for an occupied or vacant room and occupancy is usually either scheduled, measured through occupancy detectors or inferred from CO_2 readings. The latter would offer the largest energy savings since fresh air is only admitted based on demand.

The setpoints are met using closed-loop control in most cases, *i.e.* the controlled object needs to make the measured point match the setpoint, *e.g.* a supply warm-air damper is

opened/closed to make the room air temperature match a setpoint. To attain the setpoint, terminal equipment rely on proportional (P), proportional-integral (PI) and proportional-integral-derivative (PID) loops, *i.e.* depending on the setpoint error – the difference between the measured point and setpoint – a proportional amount of heating is applied; the smaller the difference, the lower the heating. Purely proportional control leads to oscillatory behaviour due to system response times – referred to as *setpoint hunting*. The integral and derivative terms are added to dampen this effect. PID controls are suitable for fast responding local loops but tend to fail for slower systems (Afram and Janabi-Sharifi, 2014).

Open-loop control is often used supplementary upstream. Continuing with the warm-air example, the temperature of the warm-air supply is a function of exterior air: the colder it is outside, the hotter the supplied air. However, if no zone requires heating, determined by having the terminal dampers at the minimum position, the hot air temperature is lessened. This process is called a *temperature reset*. Similarly, if air demand is low, the supply fans can reduce their speeds to save energy; called a *pressure reset*; reset strategies detailed in (Montgomery and McDowall, 2008).

Alternatively, expertly-derived supervisor-level controls exist, especially in cases where there are thermal storage solutions on site – chiller-priority vs. storage-priority cooling – or demand response participants – when signal comes through, a schedule turns off non-critical equipment decided by the building operator or consultant engineers. For a more comprehensive list of supervisory controls, refer to ASHRAE (2015, see chap. 42 Supervisory Control Strategies and Optimization). However, implementing supervisory controls require a non-negligible investment from the building owner. Smaller commercial, municipal and residential sectors, cannot justify the cost-benefit over the steep consultancy fees.

2.2 The Need for Model-Based Predictive Controls

Most large commercial and institutional building constructions contain significant thermal mass in the form of exposed concrete, thermal and/or electrical storage solutions, and large slow responding systems where P/PI fail (Afram and Janabi-Sharifi, 2014; Candanedo et al., 2011; Athienitis et al., 1990). A model-based predictive control system can be used to

better utilize the thermal/electrical storage and the algorithm can also be used to discover optimized supervisory controls depending on the requirements of the building owner/client. Additionally, occupants have an increasing demand for customized comfort controls and workspaces which can lead to increased productivity (WGBC, 2013). Knowing occupants' preferences and their likely schedules can also be used for pre-conditioning a space and to sequence the HVAC system's operation to reduce costs.

Lastly, the grid is slowly transforming with an increased use of renewable energy. In a previous work, we have analyzed the primary energy factor of electricity on Canadian province Ontario's grid (Bucking et al., 2016) to determine periods when the grid is less reliant on fossil fuels and to design buildings that would be net-exporting clean energy during those periods and be net-importing when the grid is cleaner. In a follow-up paper, St-Jacques et al. (2020) have mapped and analyzed the flow of electricity on the macro-level grid among the various sectors of the province of Ontario and its neighbouring provinces and states. Following this work, a building or a renewable farm designer can rely on the spatial and temporal information of the grid to drive design decisions: which orientation should have PVs, which city would benefit from wind turbines, and so on. This information can also be used within the context of MPC to operate clusters of buildings to aid the utility reduce its greenhouse gas emissions and to alleviate energy flow bottlenecks within a power sector.

2.2.1 Historical Notes on Model-Based Predictive Controls

Model-based predictive controls – or receding horizon control – were applied in the oil and petrochemical industries as early as the 1950s. Until the mid-70s, massive mainframe computers were required to compute the process settings. Since, the arrival of cheaper, more reliable and powerful microprocessors greatly aided the development and implementation of MPC. Through time, process stability was addressed by developing robust MPC and, later, nonlinear MPC. By the end of the 90s, with the improvement of the optimization algorithms and processing power, MPC has matured to a technology used in various fields, such as: medicine (real-time insulin regulation), finance (revenue management, product pricing, credit assessment), buildings (maximize comfort, reduce power demand and energy use), among countless examples. The control industry sometimes refers to it as *real-time embedded*

$$J(x_0) = \min_{u_0,\ldots,u_{N-1}} \sum_{k=0}^{N-1} l_k(x_k, u_k) \quad \text{Cost function} \quad (1)$$

$$\text{subject to} \quad (x_k, u_k) \in \mathcal{X}_k \times \mathcal{U}_k \quad \text{Constraints} \quad (2)$$

$$x_0 = x \quad \text{Current state} \quad (3)$$

$$x_{k+1} = f(x_k, u_k) \quad \text{Dynamics} \quad (4)$$

Common types of cost functions.

Cost function type	Mathematical description
Quadratic cost	$l_k(x_k, u_k) = x_k^T Q x_k + u_k^T R u_k$
Linear cost	$l_k(x_k, u_k) = c^T u_k$
Probabilistic cost	$l_k(x_k, u_k) = \mathbb{E}[g_k(x_k, u_k)]$

Common types of constraints.

Constraints type	Mathematical description
Linear constraint	$Ax_k \leq b$
Convex quadratic constraint	$(x_k - \bar{x})^T Q (x_k - \bar{x}) \leq 1, Q \succcurlyeq 0$
Chance constraint	$\mathbb{P}[Ax_k \leq b] \geq 1 - \alpha, \alpha \in (0, 0.5]$
Second order cone constraint	$\|Ax_k + b\|_2 \leq Cx_k + d$
Switched constraint	if *condition*, then $A_1 x_k \leq b_1$ else $A_2 x_k \leq b_2$
Nonlinear constraint	$h(x_k, u_k) \leq 0$

Figure 2.1: Generic model-based predictive controls framework from (Oldewurtel et al., 2012). The total cost function (1) corresponds to a loss function over a prediction horizon $N-1$ with common types shown on the top left. The constraints (2) limit the search space to be within the domain of acceptable comfort and equipment limits and are typically linear. The current state (3) constraint is to initialize the boundary condition. The dynamics (4) is the system model that the MPC will use to predict the future quantities used in the optimization. In this thesis, it is a time-invariant RC thermal circuit represented by a state-space model with x_k being state variables and u_k, controllable variables.

optimization with solving times in the milli- to microseconds (Lee, 2011; Qin and Badgwell, 2003; Boyd, 2008). Coffey *et al.* noted the earliest application of MPC as supervisory control for a building was from 1988 (Coffey et al., 2010). However, due to computational requirements, it did not receive much attention until the 2000s. MPC has numerous advantages over conventional schedule-based P/PI/PID controls. First, we describe what is MPC.

2.2.2 What is MPC?

Model-based predictive controls is an optimization-based control framework where control actions are optimized over a prediction horizon to minimize a cost function given constraints. It relies on a model describing the system dynamics in combination of constraints limiting the actions to allowable or desired ranges. Future estimates of exogenous inputs and disturbances are included, *e.g.* weather forecast, occupants' behaviours (Wetter, 2009).

Specifically, the design of an MPC algorithm requires a discrete time predictive model of the system to be controlled, weights or coefficients of the cost function of the optimization

problem, and constraints (Rawlings and Mayne, 2009; Camacho and Bordons, 2007; Borrelli et al., 2012). When applying the optimal control sequence to the real system the resulting evolution must be as close as possible to the time-series prediction. In such a dynamic optimization problem, the objective or cost function, J, is minimized over a prediction horizon, $N-1$, see Figure 2.1 for more detail including mathematical descriptions of common types of cost functions and constraints for a discrete-time MPC framework (Athienitis and O'Brien, 2015, chap. 6.3) (Lee, 2011; Qin and Badgwell, 2003; Camacho and Bordons, 2007). Applied to buildings, the cost function can be the actual operating cost based on electrical rates, which can be variable to include demand response signals and can have a reward for promoting self-consumption of renewable energy. They can aid the utility by relying on energy flexibility concepts such as optimally controlling their thermal and/or electrical storage systems (Denholm and Hand, 2011; Jensen et al., 2017; Morales et al., 2014; Aduda et al., 2016; Reynders et al., 2017, 2018). The constraints, which can be formulated both on system input and output, typically include temperature range restrictions for occupant comfort or safety reasons, equipment capacity limitations, cycling limitations and as required. The process to be controlled is modelled as a linear time-invariant discrete time system. Specifically, the state of the system for an incremental time step is returned by the model, $f(x_k, u_k, w_k)$, of the system where x_k are system variables which track the system dynamics, u_k are the control inputs or variables that can be manipulated to improve the building performance, and w_k are the time series of exogenous inputs that can be observed but not controlled, *e.g.* weather. The system constraints can be softened into penalties on the objective function where violations result in a worsened objective value instead of an infeasible solution. In general, the objective function and constraints should be convex, *e.g.* quadratic costs and linear costs, in order to use highly efficient solvers. In cases of non-convex problems, iterative methods can be used considering a convex problem for the given iterative optimization step (Boyd and Vandenberghe, 2004; Rawlings and Mayne, 2009; Camacho and Bordons, 2007; Borrelli et al., 2012). To consider time-varying components, such as operable windows a set of time-invariant parameters can be trained and these parameters selected based on the state of the windows.

Although not central to this thesis, optimization methods can be used to aid the design of a

building. Machairas et al. (2014) reviews and details a plethora of optimization and modelling methods which can be transferred for building operation. For more concrete examples, see (Bucking et al., 2014; Magnier and Haghighat, 2010).

2.2.3 Advantages and Limitations

The MPC framework makes the operating intent *explicit*: the cost is what needs to be minimized, the constraints are the limits of the system and the variables are what can be controlled. In the conventional scheduled operation, the control desires are *implicit* in how the sequences are programmed and can be cumbersome to comprehend especially if they contain many heuristics. The owner can only hope occupants will remain comfortable during a demand response event; whereas using MPC, the cost function would force to reduce demand during a demand response event but the constraints would guarantee comfort.

What is interesting from the outcomes of MPC is, that in some cases, well-known heuristic rules are discovered by the algorithm. In Kelman and Borelli (2011), the MPC algorithm was able to systematically reproduce well-known heuristics such as demand limiting, economizer cycles, temperature reset and pre-conditioning of spaces; the heuristics were manifested based on what was the cost function. The authors state that a limitation in this paper is that uncertainties were not considered and can negatively affect the strategy's performance, *e.g.* pre-cooling too much in anticipation of large solar gains that do not occur thus resulting in discomfort and would be considered in a future work[1]. In May-Ostendorp et al. (2011), well-known heuristics were also discovered by MPC and the authors argue that the utilization of MPC can be automated, replicated, is more intuitive and cheaper than expert-derived heuristics.

Shaikh et al. (2014) reviewed the state-of-the-art and lists advantages and limitations of MPC compared to conventional controls:

Advantages

1. MPC considers disturbance predictions – that are occupancy profiles, weather, etc. – in trying to regulate, appropriately, the control activities along with the convex

[1] A technical report can be found: `http://www.mpc.berkeley.edu`.

optimization strategy.

2. It usefully exploits the building's thermal mass compared to the conventional controls – such as PID, weather compensated or rule-based control.

3. It can take account of the energy price variation and can be easily employed in the optimization problem formulation.

4. Shifting and minimization of the energy peak loads can be handled within a definite period due to the selection of the tariff and least operational cost.

5. Optimization can be carried out from a pool of predefined signals and it can select the appropriate signal.

6. The distributed control strategy can also be formulated; thus, the computational load has been split among various solvers.

Limitations

1. MPC technology requires a model of the system which involves huge costs for modelling, data collection, expert monitoring and deployment; due to which, it is not worth-it for medium-sized buildings. Therefore, narrowing down the system cost and complexity is essential to determine a minimized optimization domain and a critical degree of freedom.

In addition, in comparison to conventional controls – such as PID, weather-compensated or rule-based control –, MPC usefully exploits the building's thermal mass (Hu et al., 2019). MPC techniques have shown encouraging results in simulation frameworks to control dynamic heating and cooling activating thermal mass as a measure of load shifting according to a given cost function (Wolisz et al., 2020). In fact, it can take account of the energy price variation and can be easily employed in the optimization problem formulation. Thus, shifting and minimization of the energy peak loads can be handled within a definite period due to the selection of the tariff and least operational cost. In addition, the optimization can be carried out from a pool of predefined signals, selecting the appropriate signal. Finally,

distributed control strategies can also be formulated, splitting the computational load among various solvers to increase the control feasibility. On the contrary, the MPC technique shows several limitations. With respect to classical control schemes, which are generally model-free, MPC requires models that may be difficult to develop for complex building systems. Their development involves costs for modelling, data collection, monitoring and deployment and can become cost-prohibitive for smaller buildings unless certain simplifications are made and the process is approached in a systematic way. Therefore, narrowing down the system cost and complexity is essential to determine a minimized optimization domain and a critical degree of freedom (Paris et al., 2010).

A limitation not mentioned is that to apply MPC, a separate computer is needed to calculate the optimal control profile and to then transfer the results to the BAS by either overwriting the normal operation schedule or directly overwriting setpoints or equipment statuses. No off-the-shelf MPC controller exists in the current market; there exists many start-ups, two in Montreal[2] as of this writing, offering supervisory-level controls and analytics. The approach is to first connect, collect and analyze the building data, build a model of the building, run the MPC algorithms in the cloud, where computing power can be scaled, and transfer the results back to a local controller. Digital privacy can become an issue when building data is transferred out and an internet-connected building can become a target to network attacks.

Regardless, the main limitation of MPC is the need of a model and there exist many approaches.

2.3 Approaches to MPC

Literature suggests that depending on the complexity of the system to be controlled or for a more practical implementation, some simplifications can be made: (1) the modelling approach used to describe the system dynamics can start with a calibrated detailed model and later simplified by using results from a sensitivity analysis to reduce the number of

[2]BrainBox AI `https://www.brainboxai.com/` which is part of the Canadian IVADO `https://ivado.ca/` AI research super-cluster

inputs/features, (2) the control problem can be divided or clustered into different operational scenarios and made into rules or a simplified function, (3) the problem can be split into a hierarchical system, (4) special attention needs to be taken to consider uncertainties to improve robustness, and (5) data-driven models and reinforcement learning can be used.

These approaches are detailed next with their advantages and limitations and which approaches were chosen for the thesis. The reader is encouraged to first read Chapter 3 which details the main case study: the Varennes library.

2.3.1 Categories of Models

The main limitation of MPC is the requirement of a model. All modelling approaches have fundamentally the same purpose: they need to predict the thermal state of a building and its energy demand. White-box modelling approaches are generally exploited in building energy performance simulation tools aiming at obtaining an accurate description of the occurring transient physical phenomena (*e.g.* spatial gradients through the building elements, dynamic heat transfer loads, etc.) over a wide range of operating conditions and for preliminary design purposes (Amara et al., 2015). Conversely, black-box models have simpler structures and flexible mathematical formulations with a large degree of freedom to be able to model any sort of phenomenon, guaranteeing generality and flexibility. Nevertheless, such models are purely data-driven and, since they are tailored to the building operating conditions on which they are trained, require a long training period and wide forecasting range to reduce prediction errors (Bohlin and Graebe, 1995). In fact, to train a black-box model on a specific case, diverse data are needed to learn the parameter values that minimize the prediction error. This model essentially must learn the underlying data generating distribution or structure (physics) to make predictions (Rätz et al., 2019). Since black-box models lack knowledge about the physical structure of the system, semi-physical (grey-box) models, basically based on a reduced physical descriptions of building dynamics, are preferable due to the possibility to derive simplified mathematical energy building models via reverse engineering methods, to drastically reduce the computation time to assess building energy performance in case of large scale simulations, as well as to design advanced model-based controllers (Shaikh et al., 2014). In a specialized white- or grey-box model, the modeller uses domain-expertise to

describe the physical phenomena resulting in a system with less degrees of freedom requiring less data to calibrate. Both approaches are invaluable, it all depends on whether there is a budget to develop a tailored model or whether there is enough data to train a generic one. But when it comes to performing an optimization, execution speed and convexity become limiting factors. For a more in-depth description, refer to Dermardiros et al. (2015, chap. 2.4) and Candanedo (2011, chap. 2.2).

Effective grey-box, or semi-physical, models are necessary to design and implement efficient and reliable control algorithms for building energy performance analysis (Wang and Zhai, 2016). The proper design of the control law, the tuning of its gains toward the efficient simulation of the closed-loop dynamics, are not easy tasks. This is particularly true for the efficient application of MPC algorithms which require for reduced-order building models capable to properly predict the building dynamics and its energy needs with minimal computational effort, especially for large scale simulations (Prívara et al., 2012). Thus, it is useful to develop reduced order predictive models that are accurate and simple to solve the trade-off between results precision and computing time.

2.3.2 Physics-Based Models

The advantage of a physics-based model is that, once defined, can be used to predict the full behaviour of the system in any event. The disadvantage is that it takes a large effort to correctly define all the parameters of the model relying heavily on the experience and expertise of the modeller (Chwif et al., 2000). Building simulation software such as TRNSYS, EnergyPlus, ESP-r, eQuest and Modelica require the building modeller to specify all data concerning the building enclosure construction, internal loads, occupancy schedules, equipment schedules, weather, and so forth to simulate the energy use and thermal behaviour of the modelled zone. Many of these variables, possibly unknown, are either left to their default values or, at worst, erroneously input by the modeller. The objective of building simulation is to obtain insight on how a building reacts to various internal and external profiles to assess as to what would be the best solution or most economical satisfying the occupants' comfort requirements, the Code (CNRC-NRC, 2015; ASHRAE, 2016), or other special needs prescribed by the client. These detailed programs are more suitable for aiding

design decision over being used for controls although there has been work using these engines for that end (Zhao and Magoulès, 2012).

2.3.3 Model Calibration

The models will need to be calibrated to match the *in-situ* operation of the buildings and systems they are representing. For both physics-based and physics-free methods, the metric is what is minimized to assure a proper fit of the model parameters onto the data. Coakley et al. (2014) reviewed modelling and calibration methods used in the building energy simulation community. They stated that there are no thorough procedural standards for calibration and such standards are expensive to develop. They observed that there is a poor integration among the various design software – preliminary design to detailed design to building energy performance simulation pipeline –, and furthermore "there are few studies which account for uncertainty in model inputs and predictions leading to a lack of confidence in building energy simulation outputs". Calibrations can be off by up to a 100% difference.

To assure models are stable for longer prediction and not just for one step, Žáčeková et al. (2011); Prívara et al. (2012) have extended a mean squared error over a prediction horizon as a metric to minimize to train simple models for MPC.

Current calibration practice relies on minimizing calibration metrics. Calibration metrics include what is proposed by ASHRAE Guideline 14, namely using the NMBE and CV(RMSE) metrics. Garrett and New (2016) have shown that the ASHRAE Guideline metrics are not necessarily stronger indicative calibration metrics than the other metrics they have tested – correlation, kurtosis, MAPE, MBE, RMSE. They concluded that "the correlations between input and output error measures were not statistically significant, implying that the metrics put forth in ASHRAE Guideline 14 are as good as any of the 4 other binary metrics tested." They suggested more effort should be spent on calibrating the inputs to models; to perform a sensitivity analysis to determine the most influential parameters and their realistic value range. Let us not forget Goodhart's Law where "when a measure becomes a target, it ceases to be a good measure". Which can be interpreted that the conventional approaches are sufficient, however, all metrics should be consulted since they provide different information on the fit and that the objective of a fit is to obtain a useful model and not something that

minimizes an artificial or surrogate metric.

2.3.4 Simplified Models

For MPC to be effective, the underlying models need to be simple and fast for the algorithm to converge to a solution (Oldewurtel et al., 2012; Cigler and Prívara, 2010; Moroşan et al., 2010; Candanedo and Athienitis, 2010). The models can either be simple in themselves or simplified for a given simulation timestep. The optimal or near-optimal values would then be sent to the Building Automation System (BAS).

Work from Heidarinejad et al. (2017) studied the behaviour of buildings given the time-granularity of the data and how they may affect the outcome of MPC. Plant-level consumption data can be expressed in hourly and daily figures while zone-level consumption needs to be at a finer resolution. Modelling can be broken down and simplified accordingly. In this regard, physical simplifications and model order reduction techniques are more often considered. Physical simplifications are generally achieved by a linearization scheme and pre-processing, so that the detailed nonlinear model can be derived into a linear and time-invariant system by using fewer component models (Bourdeau et al., 2019). This approach is demonstrated in chapter 4.

Simplified models are easier to interpret and calibrate in an installed system since they contain fewer parameters to adjust. The parameters can be learned in real time – online calibration – with data from the BAS. The discrepancies can be due to construction, installation, renovations or system tolerances.

Oldewurtel et al. (2012); Lehmann et al. (2013) and the OptiControl team have been working closely with the Swiss weather agency MeteoSwiss, Siemens and other organizations to develop and implement MPC algorithms to buildings. They have developed a detailed thermal resistor-capacitor (RC) model. The nonlinearities were linearized within the operating range. They used a stochastic MPC (SMPC) strategy to consider the uncertainty due to weather variability. The objective function was to minimize energy consumption while limiting the number of thermal comfort violations. They report that SMPC outperforms current control practices. Kelman and Borelli (2011) has also used an RC model and obtained satisfactory results. Bacher and Madsen (2011) have developed multiple RC models

of varying detail to identify the most suitable model for a building. The selection is based on whether the added detail improved the information gained given the added complexity via a likelihood ratio test. They show empirically that there is a preferred trade-off. Similar work on low-order models has also been reported by Fonti et al. (2017), with a two-part review paper and experiment by Viot et al. (2018b,a), see Table 1 in their first paper for a list of low-order models from the literature. The most complex model reported was 38R12C – 38 resistances and 12 capacitances – that modelled a building with operable windows and included the ventilation system, while the simplest one was 1R1C for a passive house. In this thesis, the most detailed model used is 4R3C representing a simplified high-level model of the Varennes library separating the main subsystems.

Henze et al. (2010) have studied near-optimal control strategies for various types of commercial buildings in four climate zones offering different electrical tariffs. They have analyzed, through fractional factorial analysis, the most influential parameters in medium sized offices. The four factors derived from the fractional factorial analysis are the mass level, internal loads, equipment efficiency, and equipment part-load performance. From very detailed models, they have trained simplified models on the four factors to replicate the results of MPC getting up to 90% of the performance. Modern office buildings are well insulated and therefore independent to weather but highly dependent on internal loads. Proper utilization of thermal mass can result in cost savings if it can be effectively charged and discharged. The savings occur by being able to operate chillers at part load. Chillers are typically more efficient at part load since more surface area of the evaporator and condenser can be used for heat exchange. The peak savings are insensitive to the building enclosure: wall thermal resistance, window U-value, window-to-wall ratio, building shape surface area-to-volume ratio, or plenum configuration. However, the enclosure has a significant impact on the building load and energy consumption. On the other hand, peak savings due to thermal mass charge and discharge are most sensitive to utility rates, then by the amount of mass and internal gains. Strong incentives, especially with low off-peak rates, produce lower pre-cooling temperatures. Pre-cooling is less aggressive when there are significant off-peak energy rates, even in the presence of high demand rates.

Gunay et al. (2016) has looked at influential parameters by first developing and analyzing

12 different grey-box models with varying complexity and trained using an extended Kalman filter and a particle filter. The objective was to access the amount of detail required to model the thermal characteristics of an individual office to be used for controls. The grey-box models are either first- or second-order. The range of models incrementally add building measurement data. They showed that the inclusion of plug-in loads in the models had the greatest effect. Plug loads are indicators of occupancy presence which signifies the occupant drives the loads of his or her office.

By applying a simple correlation or a more thorough sensitivity analysis, Nguyen et al. (2014) have shown that the number of input variables can be reduced from more than 100 to the 21 highly significant ones. In other cases, they have reported works that reduce the number of inputs by nearly half. Garrett and New (2016) also push forward the need to do a sensitivity analysis to reduce the input-side error and to obtain weights for the inputs based on their influence on the output. Therefore, instead of blindly using all the available data into the model, a sensitivity analysis, such as fractional factorial analysis, should be performed to tease away input features that are not impactful.

A technique of simplifying the model is using system identification (SI) (Ljung, 1987). The method consists of relating controllable inputs to outputs of interest, essentially, transforming the detailed modelled to a simple black-box model. The simplified model would then be used in the MPC optimization algorithm. Candanedo et al. (2013) has used this technique to study the near-optimal use of an ice storage bank for a medium office building. Ma et al. (2012) have extended the method by applying SI at every simulation timestep. Essentially, SI would be applied to the EnergyPlus model, then, the MPC algorithm would determine the near-optimal control parameters. The parameters would be applied to the original EnergyPlus model to verify the result, after which the process would be repeated. They calculated around 25% of cost savings compared to common controls. Bernal et al. (2012) have developed an MPC pipeline in MATLAB called MLE+[3] to simulate a building in EnergyPlus, apply SI to simplify the model, run MPC and then send the optimal control profiles to the building via the BACnet stack. The proposed methodology was complete and their complete work uploaded to GitHub, however development has stopped in 2013 and uncertainties were not

[3] `https://github.com/mlab-upenn/mlep_v1.1`

thoroughly considered. MPCPy[4] (Blum and Wetter, 2017) does a similar attempt to bridge a simulation software, OpenModelica, with MPC. What was interesting in their work was the modular approach of MPC where the model, optimization method, exogenous data import, calibration and building communication are separate modules and can be swapped in and out. Future researchers can improve specific modules. The modules are connected together with Python. The team has also released a testing environment[5] where researchers can compare different modelling and control approaches and have a unified benchmark (Blum et al., 2019). The work relies on EnergyPlus, OpenModelica and the Functional Markup Interface (FMI). In their plans, EnergyPlus will be replaced with the Spawn-of-EnergyPlus (USDOE, 2019) which offers a modular approach to modelling. MPCPy was difficult to setup and get it running, I was unable to change the solver used and instead went with a different solver using Python.

Works from Blum et al. (2019) and Garrett and New (2016)[6] also put emphasis on the repeatability of work and to have baselines for fair comparisons of modelling and control methods. The latter have opened the database of building data they have used for their paper and have developed a systematic testing methodology called the Trinity test. Garrett *et al.* are providing a way for researchers to share their buildings' data and to be all tested similarly so that researchers can: (1) replicate the work of other researchers; and (2) have a common ground to compare calibration techniques.

Low-order models for control applications can be determined during the design phase of the building, thus combining design with operation. Recent work by Andriamamonjy et al. (2019) aims at obtaining RC models from Building Information Modelling (BIM) models. BIM is becoming the industry standard for design documentation being able to combine all construction domains – architecture, engineering, construction – into a single location. It can be used to build a construction schedules, material takeoffs for budgeting and this model can be maintained up to date as the building evolves. These models are highly detailed and

[4] `https://github.com/lbl-srg/MPCPy`

[5] `https://github.com/ibpsa/project1-boptest`

[6] More information and other publications found: `https://energy.gov/eere/buildings/downloads/autotune`, their Github repository: `https://github.com/ORNL-BTRIC/Autotune`, and for testing calibration systematically: `http://bit.ly/trinity_test`.

the authors of the paper have developed an approach to simplify surfaces and zones into controllable spaces extending the usefulness of BIM into building operation. The grey-box models are developed in Modelica, and can be used in MPCPy. Unfortunately, the library case-study was designed and drafted on CAD and this approach cannot be used.

Grey-box models rely on simplified physical representations. The dependency on physics makes it difficult to model stochastic processes. Massa Gray and Schmidt (2018) have developed a hybrid approach where a grey-box state-space model is used to capture the building physics, followed by a black-box Gaussian process model trained on the model residuals to capture the stochasticity due to occupancy and the weather. Alternatively, a black-box model can be trained on data and later used to extract physical information about the system modelled and used elsewhere in controls (Brastein et al., 2018; Naveros et al., 2015). A hybrid approach is most promising for scenarios where there is a strong influence of occupancy on the building operation, such as closed offices and/or intermittently used spaces like conference rooms; for a library building operating on a schedule, this uncertainty is not as firm and so I have not used a hybrid method.

Hovgaard et al. (2013) have applied a non-convex MPC strategy for commercial refrigeration units. The systems were modelled using heat balance equations without linearization. The non-convexity was treated by solving a sequential convex optimization problem. A 30% cost savings would be achieved in a time-of-use priced electricity locality.

Nguyen et al. (2014) reviews work that show optimization results from using surrogate models trained on EnergyPlus models and the results from EnergyPlus were comparable for testing cases which means surrogate models are good approximations and are conducive for controls.

The above cases show that it is possible to apply MPC on a detailed model or on a surrogate grey-box or black-box model trained on the detailed model. It was also shown that rules can be extracted to obtain an offline MPC approach.

2.3.5 Operational Modes, Typical Days and Extracted Rules

Literature suggests using an offline approach to ease and simplify the implementation of MPC.

Parisio et al. (2014) simplified the MPC problem into cases. The authors explored the possibility of using MPC under two scenarios where the airflow or required load is governed by either fresh air requirements – CO_2 levels – or by thermal comfort requirements. They have used a stochastic approach to model occupancy loads and the weather. The chance constraints were transformed into deterministic constraints through a sampling-based approach.

Although the authors did not apply it, a clustering method – which is an unsupervised learning approach as part of ML – could have been used to bin consumption profiles into typical type of days and then design the control strategies based on the type of day.

May-Ostendorp et al. (2011) have applied MPC on a building with operable windows to minimize energy use. They relied on EnergyPlus and its Energy Management System (EMS). EnergyPlus is computationally expensive to run and for the optimization method, the underlying heat transfer equations remain hidden and cannot be exploited. The authors had to rely on a meta-heuristic search technique – particle swarm optimization (PSO) – to solve for the optimal control sequence. This method cannot be run in real time so the authors ran the MPC algorithm for various cases and used the results to train a generalized linear model (GLM) that would approximate MPC. The variables chosen to train the GLM consists of data readily available in most buildings as well as time delayed values. Several models relying on different variables were trained to assess as to how many measurements would be required to obtain results approaching the full-MPC case. They used a step-wise regression technique that minimizes the Akaike's Information Criterion (AIC). The AIC is a statistical figure of merit that objectively measures the model's ability to reproduce the variance of the observations with the fewest model parameters. The simplified trained GLM can very closely mimic the general characteristics of the optimizer results, achieving 70 to 90% of the energy savings, at a small fraction of computation.

Similarly, but simplified even further, in a paper and in his thesis, Coffey (Coffey et al., 2010; Coffey, 2012) has extended the capabilities of GenOpt – a building design optimization framework – to include a controls layers called SimCon. The controls layer can utilize MPC or other user-defined strategies. In his work, he relies on TRNSYS to run the MPC algorithm on various conditions, after which he obtains optimal control trajectories. The trajectories are then compiled into a large lookup table, interpolated between the various

conditions simulated to approximate the current online conditions, and used in real time in the actual building through the building energy management system (BEMS). This results in an offline MPC which was estimated to capture 59 to 94% of the savings of an online approach. May-Ostendorp et al. (2011) applied MPC to an EnergyPlus model as-is. Although the computational time was long, their objective was to then extract simplified control rules that can be implemented in the BEMS today. Drgoňa et al. (2018) have trained a state-space model using stochastic gradient decent, ran MPC for multiple scenarios and finally trained a neural network able to yield actions based on the current system state and future predictions.

In the application chapter – chapter 5 –, the electrical consumption of the building and the solar radiation received has been modelled using typical days and clustering. This simplifies what needs to be predicted to use MPC.

Extracting rules from MPC into a decision tree would serve as an analysis tool for understanding which actions lead to an optimal behaviour. Rules are simple to program in existing controllers.

2.3.6 Hierarchical Approach

Scattolini (2009) reviews and classifies decentralized, distributed and hierarchical control architectures. The main purpose of breaking down a large-scale MPC problem into smaller systems is to ease the computational complexity – more efficiently solved sub-problems, high/low-levels on different time scales and solving horizons – and simplify communication – each subsystem can be operated independently. The subsystems can either minimize a local performance index – *independent* algorithms – or a global index – *cooperating* algorithms. In the independent case, a high-level controller would dispatch the constraints to the subsystems to optimize in a master/slave configuration. In the cooperating case, both high and low levels will all together optimize an overall cost function. In the latter case, there will also be competition/cooperation between each sub-level system that may lead to operational instabilities. To improve stability, the author refers to many papers that tackle the problem. One of which is to have a high-level *negotiator* interacting with the low-level *autonomous agents* until a consensus on the actions is attained. Many hierarchical MPC frameworks do not have theoretical guaranteed stability properties. There is work to apply

results from robust MPC onto hierarchical MPC but robustness naturally leads to conservative results yielding unacceptable real-world performance. Lastly, the author suggests more work to be done on *reconfigurable control structures and hybrid systems* like being able to add or remove actuators and sensors in a plug-and-play fashion and have the MPC adjust automatically. Other suggestions include exploring optimization algorithms, state estimation methods, control structure selection methods and synchronization and communication protocols.

Similarly, Thieblemont et al. (2017) reviews that one of the ways to overcome modelling complexity is to have several simple models and select them depending on the mode of operation; still in the context of MPC. Another solution is to break down the approach into a high- and low-level MPC. The high-level would deal with long term objectives such as determining if there will be enough renenewable energy generation, how to best use it, when to purchase or sell to the grid; *i.e.* it optimized the plant and storage systems. The low-level would deal with short term objectives such as tracking the building temperature setpoints and/or energy consumption. We could interpret this as the low-level MPC is given an energy budget by the high-level MPC to work with.

The library is considering purchasing batteries for electrical storage. Once they do, a hierarchical approach can be used to plan the charging and discharging of this system. A hierarchical approach can also be used to consider the library in more detail going down to the actuator level where the high-level MPC used in this thesis would allocate a budget to the low-level zone-level controller to use. This remains a future work.

2.3.7 From Model & Prediction Uncertainties to Operational Robustness

The statistician George Box said "all models are wrong, but some are useful". What is meant by this quote is that models represent a simplification of the complex world that can be more easily understood and made useful. How the complexities and interconnections are enclosed into the model is sometimes arbitrary or convenient. When the modelling purpose is to gain insight into non-observable parts of a system, many different and non-equivalent

model architectures can be designed that essentially yield the same output (Coakley et al., 2014). Thus, mathematical formalisations of partially-observed experiments, even for well-defined or closed systems, can generate non-equivalent descriptions of these system (*i.e.* , models whose outputs are compatible with the same set of observations but whose structures are not reconcilable with one another). This has also been referred to as equifinality or model indeterminacy. Therefore, the task of the modeller is to not only pick and design a model that best describes the phenomena, but to have in mind the end use of the model and to take in considerations the ease of use, mathematical complexity, stability and speed of execution.

MPC requires optimal control techniques to generate the optimal control sequence. Nevertheless, the accuracy of the building model has a high impact on the quality of the optimal operation strategies (Liu and Henze, 2004). In fact, changes in the operating condition and/or disturbances in real scenarios may influence the closed-loop behaviour resulting in control sequences which can be very different from those that are optimal. Thus, novel data-driven feed-forward decision frameworks are proposed to determine the set of operation decisions with uncertainties (Wei et al., 2018). Maasoumy et al. (2014) have studied the effects of uncertainty onto the predictions which can have a large impact. The impact of uncertainties on the energy performance of buildings can be mitigated by considering different techniques, like fuzzy programming models (Mavrotas et al., 2008) optimization techniques integrated into simulation analysis (Nguyen et al., 2014), chance constrained programming (Zakaria et al., 2020), robust optimization (Kuznetsova et al., 2014; Costa-Carrapiço et al., 2020), reinforcement learning (Hu, 2015; Rätz et al., 2019).

Models are not perfect and the predictions MPC relies on are not guaranteed. In Coakley et al. (2014), uncertainty sources were grouped in 4 categories: specification, modelling simplification and assumptions, numerical, and scenario which accounts for external conditions and occupancy. Basically, the model structure can be mis-specified, its parameters can be tuned incorrectly through a local minima, the simulation results can be divergent due to numerical reasons, the weather, occupancy and energy costs are noisy predictions. Therefore, instead of attempting to converge on a singular result, most engineering answers should instead be expectations and have a mean value with a certainty range. Concretely, instead of inputting the U-value of a wall assembly into a grey-box model, it would be preferable to

input likely values based on domain knowledge which will result in a likely range of interior temperatures.

Reddy et al. (2007) have identified that most calibration studies have overlooked uncertainty analysis. In their work, Reddy *et al.* assigned ranges of variation to influential inputs parameters to produce multiple possible solutions. The authors selected the top 20 solutions rather than selecting a single solution.

Nature has published a few papers on the importance of being uncertain to ascertain the correct use of statistical metrics, see (Krzywinski and Altman, 2013; Herzog and Ostwald, 2013; Nuzzo, 2014).

The uncertainties in weather need to be considered where there is a strong dependence of energy use with outside temperature and when there is a PV system. Lazos et al. (2014) reviews forecasting and modelling techniques like Zhao and Magoulès (2012). Climate prediction will lead to better load management: *e.g.* predicting solar availability and cloud coverage will help predict PV production.

The optimization algorithm will minimize the cost function as much as possible without violating the constraints. This usually means the building is operated hugging the permissible bounds which makes the optimal control sequence very sensitive to the predictions. In Kelman and Borelli (2011), the authors state that if uncertainty is not considered, savings cannot be attained: the building would be over-cooled in anticipating a larger-than-occurred solar heat gains, resulting in a need to heat the erroneously over-cooled space to maintain comfort.

Occupants' behaviour remains the largest uncertainty in office buildings. (Gunay et al., 2014). Erickson et al. (2011) have created agent-based models to simulate occupants. The models would be refined over time with the addition data. A better prediction of where occupants will be and what they will do will yield a better control of the HVAC system and result in increased comfort and productivity. Jia and Spanos (2017) have applied a queuing-based approach to model occupancy.

Ma et al. (2015) presented an SMPC approach for building controls. The uncertain load forecasts were modelled by finitely supported probability density functions which were updated as new information is made available. Due to the complexity of the overall system, system nonlinearities and chance constraints need to be handled to enable real-time im-

plementation. The paper focused on the trade-off between computational tractability and conservatism. Finally, the SMPC was compared to alternatives. The thermal zones of the building – a library – were modelled using the ARMAX model. The model was trained using data from unoccupied periods. Ambient weather and internal gains were modelled using a predicted mean and forecast error. Thermal bounds served as a proxy for thermal comfort and were softened. The rest of the constraints guaranteed proper system behaviour. To transform the chance constraints, two methods were utilized where one, the discrete method, relied on the probability density function and the other was a sampling-based method. Ma *et al.* showed that an MPC algorithm not considering uncertainties performed worst at maintaining comfort than conventional building controls. The discrete method consumed less energy whereas the sample-based method had less comfort violations since the sampled-based method was more conservative towards comfort. Another method relying on Gaussian error distributions also achieved similar energy performance but violated more comfort constraints than the discrete method.

In these works (Ricardez-Sandoval, 2012; Sanchez-Sanchez and Ricardez-Sandoval, 2013; Bahakim and Ricardez-Sandoval, 2014), the authors present methods to make the optimization results more robust to uncertainties depending on the risk threshold of the control designer. These parameters can be tuned depending on the type of building: hospital vs. warehouse.

2.3.8 Data-Driven Models and Reinforcement Learning

The last approach to model-based predictive controls is to model the system solely on sensor data. For data-driven models, the advantage is that very little work needs to be put in to define the model. Sensor data is used to train the models. The disadvantage is that it needs a lot of high quality and diverse data to learn the behaviour of the system. There is no guarantee of good performance in cases not observed in the training set; the model may not extrapolate very well.

Yan et al. (2017) have trained on Gaussian process regression models to predict the energy use of a building. The GP regression also gives the certainty ranges on the outputs. This can be useful for fault detection and diagnostics. When comparing the model to the building

energy use, if the measured falls outside the certainty boundaries, it can signify a fault. The authors have implemented the models and training process and have made it available online[7]. Rastogi et al. (2017) have also used GP regression models to emulate a higher fidelity simulation engine to speed up analysis.

Afram et al. (2017) review artificial neural network based MPC approaches. The models were trained using various calibration metrics and at various levels – system and subsystem. They showed that the methodology works quite well for many cases. Zhao and Magoulès (2012) also includes ANN models in their study with similar conclusions. Smarra et al. (2018) have used random trees and random forests to model a building and apply MPC to reduce energy consumption.

Reinforcement learning (RL) has received tremendous attention lately after having defeated the world's strongest Go player[8] trained purely by self-play (Silver et al., 2017) and performing at a professional level in an imperfect information game of Dota 2 (OpenAI, 2018) and Grandmaster level in Starcraft 2 (The-AlphaStar-Team, 2019). Contrary to IBM's Deep Blue chess program, these methods are not domain specific and the training methods can be generally applied to any problem that can be formulated as a Markov decision process – with care, this assumption can be relaxed. In a nutshell, an RL agent interacts with its environment to come up with a policy – what action to take when in a certain state – to maximize its sum of future discounted rewards. There exist many learning schemes and high-quality implementations are made available freely online through OpenAI Baselines (Dhariwal et al., 2017), Tensorforce (Schaarschmidt et al., 2017), and others. There has been successful application of RL agents learning on imperfect simulation systems. Simulators cannot reproduce all the details of reality, so OpenAI et al. (2018) have instead trained a 24 degrees of freedom robot hand in a simulation environment where they randomize many of the parameters and the resulting RL agent becomes robust to this reality gap. The work relies on concepts of learning inverse dynamics models (Christiano et al., 2016), domain randomization and

[7]https://harvardcgbc.org/cgbc-launches-online-gaussian-processes-forecasting-tool-to-analyze-building-energy-consumption/

[8]Lee Sedol has now retired due to the frustration of not being able to defeat AlphaGo https://www.forbes.com/sites/aswinpranam/2019/11/29/why-the-retirement-of-lee-se-dol-former-go-champion-is-a-sign-of-things-to-come/#6b4fa4fa3887

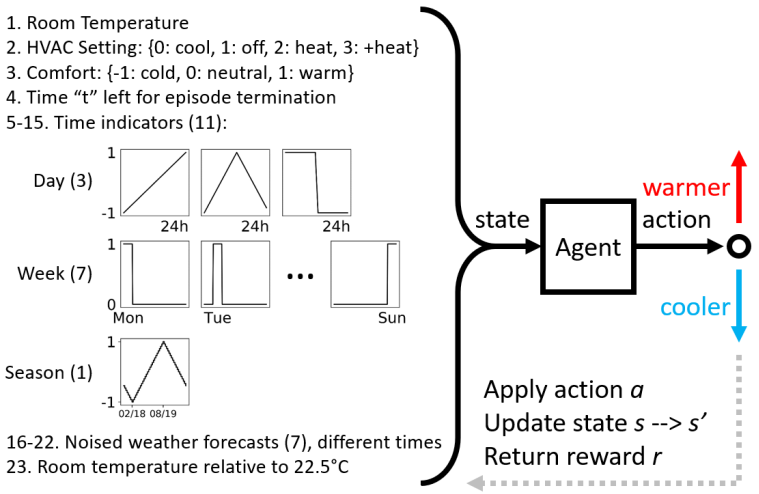

Figure 2.2: States included for reinforcement learning agent to decide from simplified actions. Feedback loop of returning updated states and reward (Dermardiros et al., 2019).

adversarial training (Pinto et al., 2016, 2017).

RL has been applied to the building controls domain by adjusting the space thermostat setting by making comfort fuzzy (Yamaguchi et al., 2015), a continuous temperature value (Nagy et al., 2018), we have applied it on a simplified RC-network based building environment (Dermardiros et al., 2019) where the RL agent sees certain states and applies actions similar to what a person would desire, see Figure 2.2 , or using a full-simulation engine like EnergyPlus (Moriyama et al., 2018). However, RL methods require the agents to learn the environment and the optimal policy which leads to requiring a lot of data in the form of experience. Both MPC and RL are based on dynamic programming (Bertsekas, 1995) and at their limits converge to the same solution, however, MPC has the advantage of having an explicit model of the building which can be troubleshooted separately from the controls. Model-based RL approaches where the model is a grey-box model also exist (Kamthe and Deisenroth, 2017; Sanchez-Gonzalez et al., 2018).

Compared to MPC, RL methods map a state to an action whereas MPC methods take in the current state plus certain predictions as an input to a model and relying on an optimization technique determine the actions. Once trained, an RL agent will perform faster than an MPC scheme and with a smaller software footprint; however, training the agent to be robust remains an open research question. The difference is that MPC solves the full optimization

for the given timestep but does so for a convex case; RL approximates the optimization using value-iteration and approaches the optimal after many episodes. RL relies on a reward function and hard constraints are usually softened into the reward function. MPC can retain hard constraints, which could be softened using a slack variable or softened also into the cost function. In practice, once RL has converged, it requires a single pass to compute the control profile, whereas MPC must calculate the optimal control profile; therefore RL is faster; however, since RL utilized function approximations – neural networks –, their stability is not fully proven theoretically. The combination of the two approaches is at a preliminary stage but shows great promise. In this thesis, the focus is on using MPC.

2.4 Financial Bottom-Line

Although MPC has many advantages over conventional controls, it still is met by resistance from the industry.

The report by WGBC (2013) reviews the costs and benefits of green buildings for developers, investors and occupants. It reports cost figures from various sources analyzing what is the premium to build green and if the resulting benefits are worthwhile. They report that "[over] 85% of total workplace costs [are] spent on salaries and benefits, compared to less than 10% on rent and 1% on energy." On a monetary front, since the cost of energy is two orders of magnitude lesser than salaries, in no way can an energy reduction measure be justified if it affects employee productivity. Looking at it the other way, with 1% of the total operating cost of the workplace, we can have a positive impact on the larger 85% through the increase of comfort leading to increased performance and productivity[9]. The report also lists many studies linking improved occupancy comfort leading to increased productivity. Knowing occupants' preferences and their likely schedules can also be used for pre-conditioning a space and to sequence the HVAC system's operation to reduce costs.

[9]Which is the main theme of IEA EBC Annex 79 - Occupant-Centric Building Design and Operation `http://annex79.iea-ebc.org/` which continues the work following IEA EBC Annex 66 - Simulation and Definition of Occupant Behaviour in Buildings

2.5 Summary

MPC was able to replicate many known heuristics automatically suggesting that an optimization-based approach can replace specialized and sub-optimal engineered control sequences. By relying on sensitivity analysis, the number of inputs can be reduced, thus reducing the cost of data collection and make the models robust to over-fitting. Sensor data derived models based on supervised machine learning approaches are scalable with the computational capacity of the future – models can be physics-free or have physics-based domain knowledge introduced. Uncertainty consideration will make results robust to change and have minima that are insensitive to perturbation and be stable. Uncertainty can also describe the codependency of parameters. The prediction horizon length can be a function of the physical behaviour of the system, be it related to its time constant and type of zone or occupancy. The financial benefits of MPC is briefly introduced since although HVAC energy consumption represents a small portion of the overall operational cost, it does have a significant effect on occupant comfort and productivity.

Works reported in this chapter have described the success and benefits of MPC for controlling a building. The literature review identified the following research areas: (i) what is the current practice and the need to explain and promote MPC to practitioners in building controls since there is a lack of real-world examples outside of academic endeavours, the need to develop off-the-shelf equipment able to interface optimization techniques within the context of building operation, (ii) approaches to modelling the system and its dynamics broken down into a spectrum of having purely data-driven models (black-box) towards physics-based models (white-box); possibility of using a hybrid approach where certain phenomena are modelled with a grey-box model and more stochastic phenomena with stochastic and/or black-box models; approaches to modelling the exogenous inputs, (iii) methods of calibrating and/or training the model based on data, a discussion about metrics to minimize, (iv) simplifications to consider whether it be on the modelling side through reduced-order models, or on the system side through relying on hierarchical approaches and/or breaking down into modes of operation through clustering or based on domain expertise or a calendar schedule, (v) the importance of considering uncertainties and how to better consider them

for operational robustness, (vi) approaches to solve optimal controls from relying on different types of models and using different approaches: convex optimization or meta-heuristic methods; in certain cases, various cases are solved offline and this data is used to train a simpler model that can be deployed online with minimal loss of performance; reinforcement learning agents can be trained offline as well – called *off-policy*, and (vii) there is a strong financial incentive to make spaces more comfortable for occupants to improve productivity. The important and interesting conclusion is that all these points can be further explored independently and each would benefit from one another.

2.6 Overview of Research Plan

The literature identified suitable paths for simplified methodologies of applying MPC into a wider market starting from high performance buildings with on-site renewable energy generation.

The research plan is to begin with analyzing the current behaviour of the library and how it compares to a national average. This analysis can spawn suggestions and guidelines for future designs of NetZEBs, but, more importantly, serves as a modelling data pre-processing step to filter and process raw information using domain expertise.

Although the literature covers a wide gamut of modelling approaches including neural networks, here, simplified modelling approaches will be used. Simpler models have fewer degrees of freedom and therefore would theoretically require less data to calibrate and a simpler model tends to be more interpretable. Models of different order will be compared where detail is added to capture the behaviour of more complex HVAC systems. A study on how much data is required will determine the trade-off between having a model quick vs having an accurate model in deployment.

A common approach to time series modelling is using autoregressive models. This approach will be compared to the simplified modelling approach to see whether a physics-free approach converges to the same parameters or whether the physics-based co-dependencies have an impact.

To train models, literature suggests that no metric is rightfully superior to any other

metric and so its selection depends on the modeller. Here, we will rely on the commonly used metrics – based on ASHRAE Guideline 14 – MSE, NMBE and CV(RMSE). However, we would need to modify them to cover multiple future timesteps. As a modification, an exponentially decayed weighing term will be added to emphasize nearer-term predictions. Since models are multi-zonal, the prediction errors can be also weighted based on a relative importance, *e.g.* relative volume of the space, relative comfort impact of the system. Both aforementioned weighings will be compared.

To obtain robust predictions, literature recommends training multiple models and rely on an ensemble of predictions. The multiple models can be different based on it being trained on: (i) randomized initialization, (ii) different dataset, (iii) using a different importance weighing or prediction horizon, (iv) different model architecture, (v) different loss metrics, and/or (vi) different optimization methods. The reasoning is that each model can predict certain instances differently and by having an ensemble of models, a more informative prediction can be obtained. Here, we will test these approaches but keep an ensemble through the optimization method – Markov chain Monte Carlo.

Past MPC studies applied to building were done using white-, grey- and black-box approaches and either considered uncertain exogenous forecasts or, unrealistically, used perfect forecasts. In this thesis, the exogenous inputs will be approached to be realistic and what would be obtainable in a real case.

The MPC framework is general and generic. Certain works relied on genetic algorithms to solve the optimization problem whereas others used convex optimization or approximations of convex optimization to solve the dynamic program. Convex optimization solvers are very fast and have convergence guarantees. This thesis will rely on convex optimization: convex cost functions, models and constraints.

The cost functions to minimize tend to be specific to the modellers end goal. They would need to be more flexible. We instead will start with the common approach of minimizing energy and/or power and then move towards a general approach of having the building net consumption match a utility-imposed demand profile. This is a more abstracted method since the profile can be designed to mimic the energy minimization problem or other but can also be used to minimize grid interaction – by setting the profile to 0 – or track a dynamic

price scheme. This sort of profile tracking approach is seen more in robotics literature and practice.

To alleviate the uncertainties in the model and forecasts, a sample-based iterative method will be used. For a given timestep, the optimization is ran multiple times by randomizing the model instance and sampling exogenous inputs; the optimal profile is obtained for these samples and is averaged. Next, this approach is repeated but the control profile is constraint to not be too different than the control profile of the previous iteration. This will be repeated for a number of iterations and the norm between control profiles from one iteration to the next will be further constraint. This approach is reminiscent to iterative methods used in non-convex optimization.

As a final step, the control profile obtained from the sampled MPC approach can be compared to the actual operation of the building. As a future work, to have a gradual shift from current operations to optimal operations, a distance metric measuring the difference between these two can be used to constrain the optimal controls from not being very different than current practice. This will assure a safer operation, will allow a controlled level of exploration which will allow the collection of novel data to refine the model, and will allow the building operator to build confidence and intuition on how the optimal controller is working. This approach is reminiscent on trust-region bounded reinforcement learning methods and is left as a future work.

2.6.1 Objectives of PhD Thesis

To accomplish the research plan, several objectives are identified:

1. **Analyze the performance of the Varennes NetZEB and offer improvements.**
    - Perform an exploratory data analysis: find trends and correlations,
    - Compare operation to common and best practices,
    - Suggest improvements and guidelines for future buildings for the operation of the mechanical, lighting and building-integrated photovoltaic/thermal systems.
2. **Design low-order models for control purposes.**

- Given above analysis, approach needed to best obtain a low-order model, added detail to correspond to system input, not about adding precision,
- Augment calibration metrics for model long-term stability,
- Use calibration and optimization approach that does not assume parameter independence; distribution on parameters,
- Compare and contrast fits based on amount of data used, period of data and end application of the model.

3. **Develop a noised MPC framework using various input models and cost functions.**

   - Build models for estimating future energy consumption, ambient temperature, solar radiation, and photovoltaic generation,
   - Generate noised model instances based on model parameter distributions,
   - Design various cost functions including (i) reducing energy, (ii) reducing peak demand, (iii) tracking a desired profile while considering or not the renewable energy production; and assure optimization remains convex,
   - Run optimization sampling over parameters and noised exogenous inputs; iterate for a given timestep while constraining the optimal control profile towards robust operation,
   - Analyze results and demonstrate its performance,
   - Modular approach in essence and extendable towards the general case.

The approach presented in this thesis is general but applied to a low-rise institutional building that is operated based on a schedule. It can be extended to other schedule-driven buildings and future work can expand to occupancy-driven spaces and residential buildings. The Varennes library case study, introduced in the next chapter, includes renewable energy generation, ground-source heat pumps, occupancy-driven ventilation and radiant hydronic slabs for space conditioning. Although the library is a net-zero energy building (NetZEB), the focus is more about the interactions among renewable production, energy storage, on-site consumption and the grid interaction.

Chapter 3

Energy Performance, Comfort and Lessons Learned from a NetZEB

This chapter is based on a published article[1]. The article includes the overall post-inauguration performance of the building. Some details have been omitted for the sake of brevity and focus.

3.1 Overview

The Varennes library will be the central case-study in this thesis. It is an institutional building designed for net-zero annual energy balance – see Figure 3.1 for overall images, Figure 3.2 for a cross-sectional schematic and Table 3.1 for an overview of the building's architectural, mechanical and electrical systems. Although the library is a net-zero energy building (NetZEB), the focus is about the interactions between renewable production, energy storage, on-site consumption and the grid interaction. The building behaves like a nano-grid. The analysis in this section is to understand how the building is operating, how it can be improved in its design and in its operation which will guide future construction and improve the current building stock. It is presented before the modelling chapter since the analysis and understanding of the system will drive the modelling methodology. For other buildings,

[1]Dermardiros, V., Athienitis, A. K., & Bucking, S. 2019. Energy Performance, Comfort and Lessons Learned from an Institutional Building Designed for Net-Zero Energy, ASHRAE Transactions, 125, Part 1.

a similar approach of exploration and understanding must be performed before modelling to assure the model matches the system. Raw logged quantities have to be transformed and this requires awareness of how the various systems interact and the causal direction of information.

The following section introduces the building and the design intent. Section 3.3 analyzes the energy consumption and its end-use breakdown whereas section 3.4 focuses on the energy production and the net energy balance. Section 3.5 illustrates a cold sunny day highlighting the need for optimal controls to dampen the effect of grid interaction. For completeness, in the Appendix, section A.1 covers the lighting, section A.2 covers the natural ventilation system, section A.3 reproduces key findings from a previous study (Dermardiros et al., 2017) about controlling the hydronic radiant slab system in conjunction to the air system, section A.4 demonstrates that the current operation is causing a seasonal imbalance of heat transfer between the library and the ground, and section A.5 details the building-integrated photovoltaic and thermal (BIPV/T) system with a simplified linear modelling methodology for the electrical component.

3.2 Introduction

The city of Varennes is an off-island suburb of Montreal (latitude 45°N). With its growing population, the city needed a new library to replace its aging one. From 2010 to 2011, a team consisting of municipal representatives, CanmetENERGY-Varennes researchers, Concordia University academics and industry partners was formed and adopted an integrated design process through several design charettes. Since the beginning, the objective was to make the library the first net-zero energy institutional building in Canada with a building-integrated solar system. Two key concepts determined the overall shape of the building and the integration of the technologies:

1. The design team estimated the annual energy consumption to be around 70 kWh/m^{2}yr, resulting in an energy consumption of 147,000 kWh per year. To reach *site energy* net-zero (Torcellini et al., 2006) with solar electricity generated by a PV system optimally tilted and oriented due South, a 110-120 kW system would be required. This capacity

Figure 3.1: Varennes library tagged images. [1] Entrance, south-west view; [2] North facade; [3] South facade; [4] 2nd floor facing West; [5] 2nd floor, middle section, facing South; [6] Ground floor facing South; [7-8] Mechanical room; [9] South facade; [10] Inauguration, from left to right: Dr. Konstantinos (Costa) Kapsis, Dr. Andreas K. Athienitis, Major Martin Damphousse, Vasken Dermardiros and Rémi Dumoulin. (A) Forced convected BIPV and BIPV/T area; (B) Naturally convected BIPV portion (out of view); (C) West facade, vine supports; (D) 2-car charging station; (E) Skylights on northern roof; (F) Fixed exterior louvers, solar shading; (G) Geothermal boreholes; (H) Ceiling fans; (I) Motorized windows; (J) Displacement ventilation integrated to bookshelves/stacks; (K) Underfloor ventilation diffuser; (L) Hydronic radiant slab; (M) Geothermal heat pumps; (N) BIPV/T heat into AHU; (O) AHU.

would require a roof area of 700 to 800 m^2 to generate close to 1200 kWh/yr per kW installed based on well established solar potential maps from National Resources Canada (NRCan) and measured data (Athienitis and O'Brien, 2015).

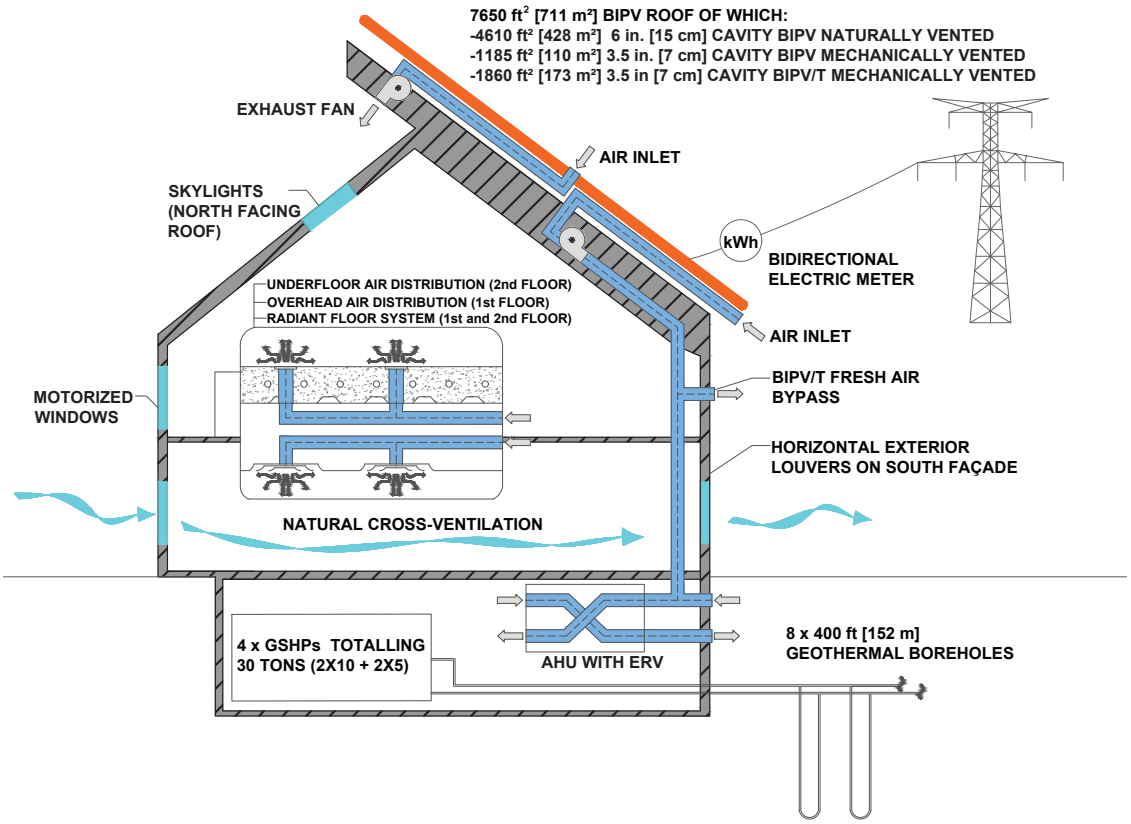

Figure 3.2: Varennes library schematic courtesy of Dumoulin (2019).

2. The depth of the building would have to be 6 to 10 m to promote deep daylight penetration (Athienitis and O'Brien, 2015) and night free-cooling through motorized windows on opposite facades.

The early design charettes (15) served to develop a common vision for the net-zero energy building and to implement it into a practical design for the local climate. The SNEBRN group aimed to educate the architects and engineers – selected after a competition organized by the municipality – on new energy efficiency and solar technologies. Through better integration of the different building subsystems, system components would function more efficiently and therefore can be sized smaller. The secondary objectives of this project were for Varennes to transfer acquired knowledge to the building design sector, convince other municipalities to adopt the integrated design process method, reduce the perception of high-performance having a higher life-cycle cost, and to educate and showcase to the public the library's various net-zero energy enabling technologies, particularly their integration.

Table 3.1: Varennes library features.

Architectural	
Site	Varennes, Quebec, Canada
ASHRAE Climate Zone	6
Net Floor Area, m^2, [ft^2]	2100 [22600]
Width/Depth, m	55.3/17.1
Roof tilt, °	37
Window type, S	Double-glazed argon low-e wood-frame
Window type, N/E/W/skylight	Triple-glazed argon low-e wood-frame
WWR, S/N/E/W, %	30/10/20/30
Shading, S, fixed louvers	165 mm wide, 20°tilted toward window 250 mm c/c, 100 mm from glass
U-value, window, S, W/m^2K	2.56
SHGC, window, S	0.58
U-value, window, N/E/W/skylight	1.82
SHGC, window, N/E/W/skylight	0.47
R-value, wall, m^2K/W	5.1
R-value, roof, m^2K/W	8.4
Mechanical	
Main system, type	Centralized DOAS modulated based on CO_2
Main system, features	GSHP, ERV, solar thermal recovery
Distribution system, 1st floor	4-pipe fan coil, overhead diffuser
Distribution system, 2nd floor	4-pipe fan coil, UFAD, displacement diffuser
Distribution system, S/E/W perimeter	Radiant slab, 125 mm thick, heat+cool
Cathedral area, 2nd floor	Ceiling fans
Natural ventilation	Motorized windows
BIPV/T area, m^2, [# units]	173 [66]
BIPV/T maximum air volume, L/s [cfm]	1140 [2420]
Domestic water	Low-flow fixtures
Electrical	
On-site PV, nominal capacity, DC kWp	110.5
PV panel, unit capacity [W] and # units	260, 425
Inverter capacity, kW [kW/unit, # units]	100 [10, 10]
Lighting, typical type, controls	T8 fluorescent, 1-2 tube luminaires, DALI system
LPD, W/m^2 [W/ft^2]	7.64 [0.71]
Other features	EV charging station (2 cars), no coffee machines, no vending machines, no refrigerated water fountains

The now-built library has on-site renewables utilizing a 110.5 kWp building-integrated photovoltaic (BIPV) system where heat is also recovered from a section of the array and used to pre-heat the fresh air intake. The building's many architectural and mechanical features

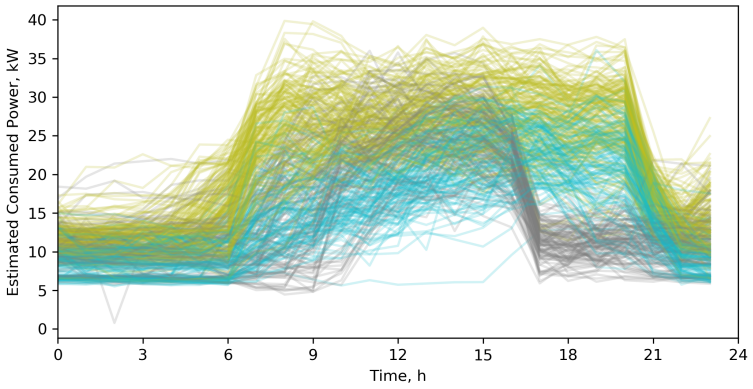

Figure 3.3: Daily consumption data with clustering applied. Each colour represents the day's cluster assignment.

were integrally designed to achieve the net-zero energy target with several key decisions made at the early design stage. During the first year after inauguration, an operational energy use intensity (EUI) of 78.1 kWh/m^{2}yr was achieved and has since been reduced to 70.0 kWh/m^{2}yr. Considering renewables production, the net-EUI was 14.5 kWh/m^{2}yr. This is a 95% EUI reduction over the national institutional average (NRCan, 2016).

The library was inaugurated on May 16$^{\text{th}}$, 2016, achieved LEED Gold certification, won an Award of Excellence 2014 in Real Estate for Innovation from the Urban Development Institute of Quebec (Macogep, 2014) and won an Award of Excellence from the Association of Consulting Engineering Companies of Canada (ACEC, 2016).

The following sections break down the energy consumption, analyze the energy production and their interaction. The final section demonstrates how better controls can alleviate the mismatch.

3.3 Energy Consumption and End-Use Breakdown

To get a better understanding on how the library is operated, we plot the daily electrical consumption since September 2017 – prior data was corrupted. Figure 3.3 shows two patterns: (1) days where the consumption drops at 9 PM and (2) days where the consumption drops at 6 PM. Applying a k-means clustering algorithm, available from the Scikit-learn Python

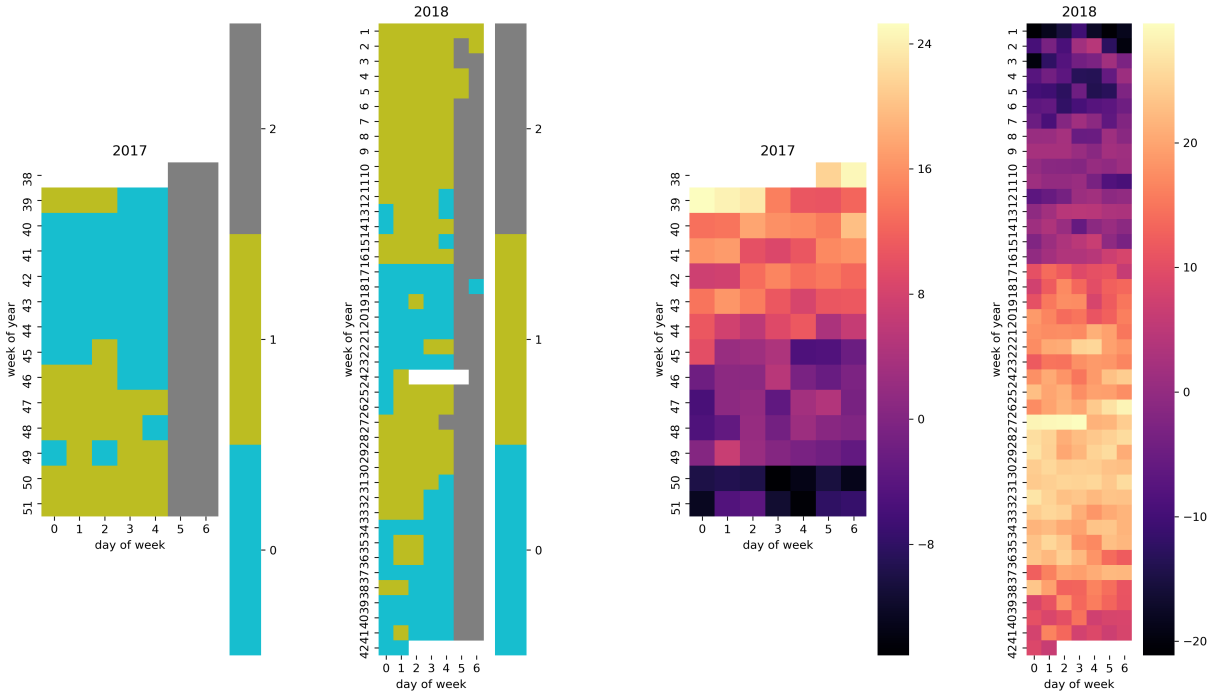

(a) Consumption day cluster assignments.

(b) Average exterior temperature.

Figure 3.4: Calendar heatmaps.

package (Pedregosa et al., 2011), the data is separated into 3 typical days. The consumption at each hour of the day would represent the dimension of the point ($\mathbb{R}^{24}$), and k-means would attempt to group points that are close together – it is a centroid-based method. The hypothesis is that there would be 3 days to represent weekends and weekdays with either high consumption or low consumption depending if it is the shoulder season or not.

To validate this hypothesis, the next step of the exploratory analysis is to observe the cluster assignments to the average exterior temperature. Figure 3.4, shows these side-by-side and the hypothesis does not seem to be agreeable. The hypothesis of there existing 3 clusters can be simplified to only 2. Alternatively, a non-parametric clustering approach, such as a Gaussian Mixture Model or DBSCAN, can be used.

The largest part of electrical consumption is due to space conditioning, see Table 3.2. Starting with the heating load, we plot the heating power as a function of the temperature

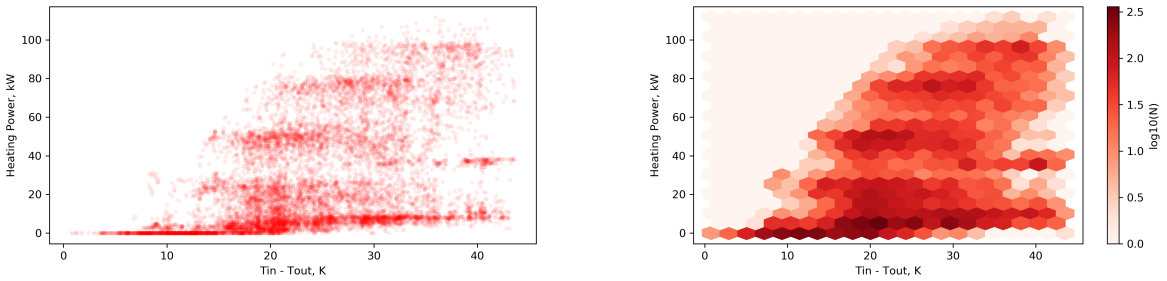

(a) 15-minute data scatter plot.

(b) 15-minute data logarithmically-scaled binned.

Figure 3.5: Heating power vs. indoor-outdoor temperature differential.

difference between inside and outside, and also for clarity, the same points are binned in a logarithmic scale, see Figure 3.5. A trend of increasing power can be observed as the difference gets larger in the data show for 15-minutes intervals, however showing a large spread. Looking at the heat pumps, we have observed a cycling behaviour. The scroll compressors in the heat pumps cannot be modulated and the heat pumps work in cycles and in stages. By resampling the data into 1-hour intervals, we suspect the heating power to be smoother. The stages can be observed in the figure: notice the flat portions at approximately {22, 40, 50, 80, 100} kW. The discrete behaviour of the heat pumps must be later considered in the MPC formulation. The heat pumps use the ground as a thermal source and remain efficient even at very cold temperatures; the coefficient of performance (COP) of the heat pumps were calculated to be close to 5 in heating mode.

The energy breakdown is shown in Table 3.2 between June 1st, 2016 and May 31st, 2017. During a portion of that period, although individual luminaires are addressable and dimmable, lighting was running on a fixed schedule and at full intensity. The lighting power has since been reduced through dimming. Fan and pump power take a significant portion due to the radiant slab systems requiring circulation pumps and the fan coil units having each their own fans. The *other* category includes plug loads such as computers, book check-out counter, etc. From the beginning, the energy design team had decided to exclude energy intensive equipment such as refrigerated vending machines, water fountains and coffee makers.

Table 3.2: End-use breakdown and energy use intensity (EUI). Data from August 2015 to August 2016: first year of operation.

Category	Energy, kWh [% of total]
Consumption	166,490
Lights	49,950 [30%]
Heating/Cooling	44,950 [27%]
Pumps	33,300 [20%]
Fans	33,300 [20%]
Other	4990 [3%]
Production	134,070 [80%]
Difference	32,420 [20%]

3.4 Energy Production

The library has a 110.5 kWp roof-mounted building-integrated photovoltaic (BIPV) array. From the total 711 m^2 [425 panels] PV area, 428 m^2 [258 panels] is naturally vented through a 150 mm [6"] air gap between the PV panels and metal roofing. The remaining 280 m^2 [167 panels] is fan-assisted and vented through a narrower 70 mm [2.8"] air gap. The air flow behind the panels serves to reduce overheating and to increase production efficiency. From a 173 m^2 [66 panels] portion of the forced air area, heat from the PV panels is recovered through the outdoor air flowing in the cavity under the panels which is used as fresh air; this airflow to the fresh air intake is controlled through variable speed fans during the heating season, see Figure 3.2 – this system is known as BIPV/thermal (BIPV/T) as it produces useful heat in addition to electricity. See Appendix section A.5 for more details.

A net daily energy balance is shown in Figure 3.6. This figure demonstrates when the library is net-consuming versus net-producing. In winter and summer, the building consumes approximately 400 kWh daily, whereas during the shoulder seasons, it exports around 200 kWh daily. Taking the same period used in the end-use breakdown (June 1st, 2016 to May 31st, 2017), we plot in Figure 3.7 the load duration curve. This figure shows the hourly net power demand sorted from net-consuming to net-producing. By intercepting the curve with the x-axis, the number of hours where the library is net-consuming can be determined. For the given period, 6784 hours [77%] are net-consuming or net-importing and the rest, 1976 hours [23%], are net-producing or net-exporting.

Excess electricity is sold to the grid and the library is compensated up to 50 kW as per

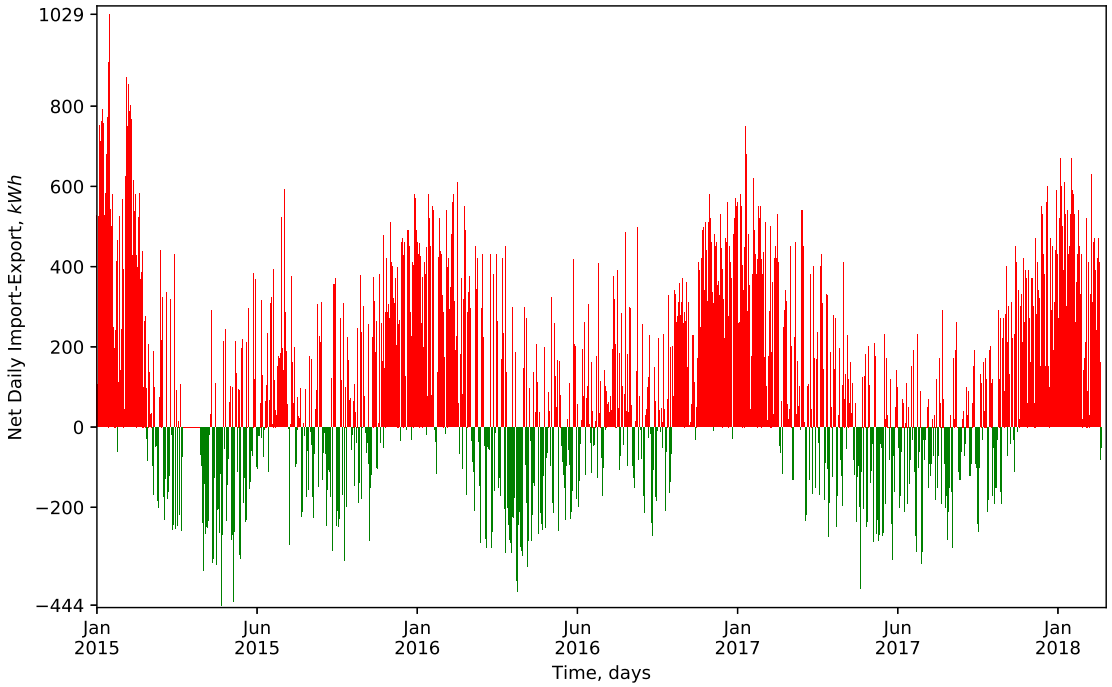

Figure 3.6: Net Daily Electrical Energy Balance. Positive, red, is net-importing and negative, green, net-exporting.

the agreement with the utility. As can be seen from Figure 3.7, by intercepting the curve with -50 kW and integrating the area between the curve and the intercept line, we determine that 642 kWh of energy was exported *pro gratis*. There are no batteries installed and therefore the library is incentivized to consume its electricity on-site and/or to sell its electricity to clients having plugged their electric vehicles to the library's charging station. What is missing from the load duration curve is the sense of time: the highest net consumption happens in the winter evening whereas the highest net production is during solar noon during the shoulder seasons. Besides, the heating and cooling loads are not balanced and the long-term effects of this on the ground would need to be analyzed, see Appendix section A.4. Another type of visualization would be warranted to express the shorter-term fluctuations and assess the need and the control strategy for shorter term thermal and/or electrical storage solutions.

3.5 Grid Interaction on a Cold Sunny Winter Day

The definition of net-zero energy corresponds to a span of a 1-year window. The peak export and peak import are months apart for the library. Shorter term needs exist where peak daily production and consumption are hours apart.

Focusing on a cold sunny winter day, Figure 3.8 shows the energy consumption and production throughout the day. Since the library is open to clients at night, there is a need for heating. Could the overproduction of electricity during noon be better utilized to reduce the need for heating at night? The library does not have electrical batteries but features a hydronic radiant slab system which can be likened to a thermal battery. By overheating the radiant slab during noon, the residual heat can be used throughout the night thus maximizing the consumption of renewable energy on-site and minimizing the grid interaction.

A preliminary study has been conducted in Dermardiros et al. (2017) to better balance

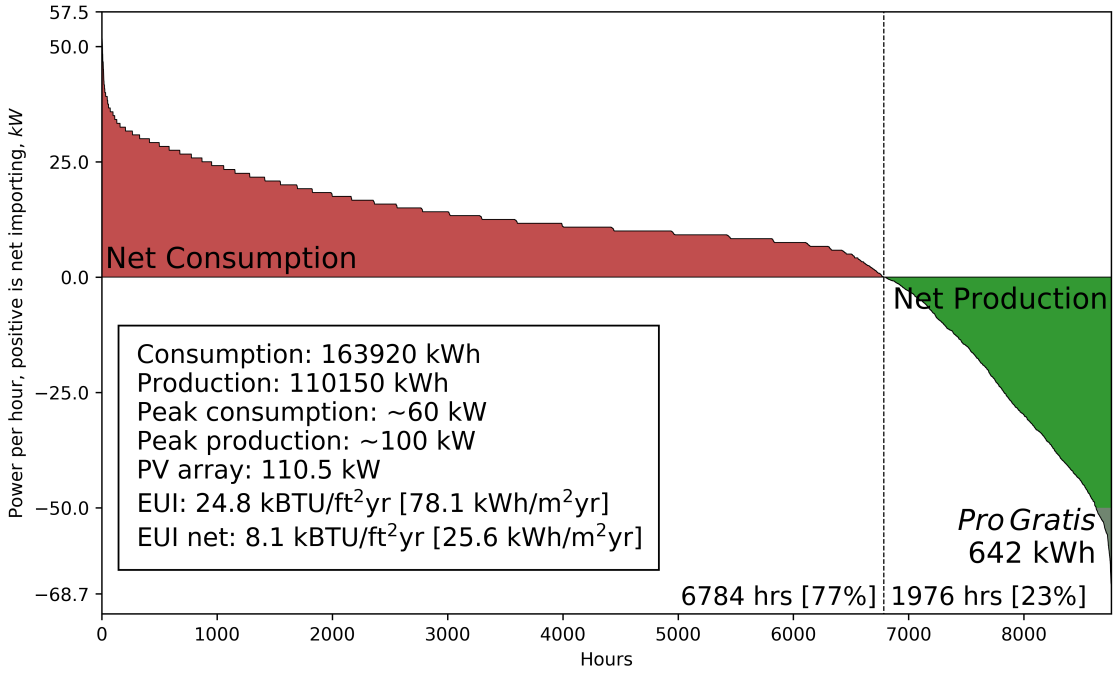

Figure 3.7: Electrical load duration curve: Data from June 1st, 2016 to May 31st, 2017, first year after inauguration. Maximum net import (consumption) occurs during heating season around 7-9 PM; maximum net export (production) occurs during shoulder season around solar noon.

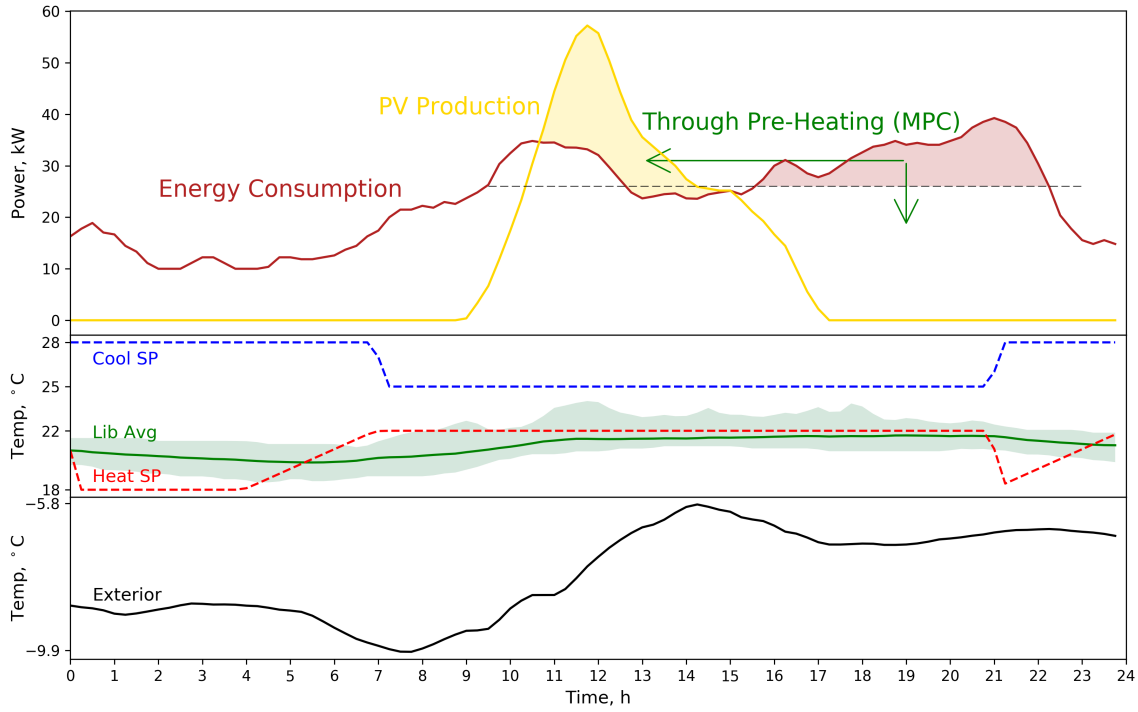

Figure 3.8: Cold winter day illustrating where evening heating requirements could be covered by noon PV overproduction.

the daily fluctuations of heat between the radiant slab and the air within the building. The study's results confirmed that 50% the peak HVAC demand can potentially be reduced in the morning through optimal controls – details reproduced in the Appendix section A.3. The study assumed perfect information on exogenous inputs and did not consider the renewable electricity production. The radiant model slab was detailed and this approach cannot be easily generalizable. Going forward, a higher-level approach is considered.

3.6 Conclusion

The library is a strong case-study in this thesis because of a combination of features: (1) on-site renewable energy generation with heat recovery for fresh air pre-heat, (2) passive solar design: window selection and sizing, concrete slab thermal buffer, overall geometry, (3) highly instrumented, (4) demand-driven ventilation, partially underfloor displacement ventilation, (5) radiant slab-based heating and cooling, primary system for space condition-

ing, (6) motorized windows for natural cross-ventilation, (7) operated on a schedule which minimizes occupancy-related uncertainties, and (8) proactive and receptive building operators.

The building acts as a its own nano-grid and represents the buildings to come. By being able to model and control this building, methods proposed can be expanded to cover more conventional roof-top prepackaged unit based buildings, buildings operating on schedules and buildings that have on-site renewables and storage. This also opens opportunities to participate in demand response and dynamic tariff programs. The following chapter builds on top of the analysis to derive low-order models suitable for controls.

Chapter 4

Establishing Low-Order Models for Building Power and Thermal State Forecasting

4.1 Overview

This chapter presents a methodology to derive reduced order models to properly estate and to forecast the thermal behaviour and energy demand of buildings. To this aim, a state-space modelling approach with physics-based and physics-free parameterization is applied by using model training with common metrics extended for long-term predictions. The methodology also involves physical simplifications, necessary to break down the larger dynamic of the building system into a smaller sub-systems, and model order reduction techniques. The idea behind this approach is to provide a predictive model, calibrated on real data to obtain a high level of accuracy, to be used for developing energy flexibility and advanced management strategies for the next generation of buildings where intermittent renewable energy sources will play a major role. To prove the effectiveness of the proposed methodology and of the developed approach, data from a net-zero energy library, a solar net-zero energy institutional public building located in Varennes, Quebec, Canada, are used. The chapter provides a basic description of the models, data collection methods and controllable points. The developed models are trained in various cases to analyze how the optimal parameter weights change

with time, and to observe the influence and magnitude of inputs on the model outputs. Three different orders of models compartmentalizing the HVAC components differently and for specific practical end uses are presented.

The following section introduces the need for model-based predictive controls (MPC) as buildings will become key participants in utility regularization with the increase of renewable energy sources. Section 4.3 details the methodology for building the low-order models, transforming the raw collected data, proposing calibration metrics and finally establishing 3 low-order models characterizing the different HVAC systems within the library. Finally, sections 4.4 and 4.5 offer discussions on the modelling methodology, compares fit results to what is obtained from reading the plans and offers conclusions about how to extend and expand the methodology to other schedule-driven buildings such as buildings with roof-top units representing a large number of all commercial and retail buildings in North America.

4.2 Introduction

As more decentralized renewable energy sources are introduced onto the grid to make the utility power mix cleaner (Bucking et al., 2016), utility level load balancing is becoming an issue. Photovoltaics can potentially create local generation peaks where the grid may not be able to absorb this production if not directly consumed. Wind turbines rely on wind which fluctuates. Thus regulation can occur on the utility side through modulating power plants or using large scale storage solutions, or on the consumption side through incentives and links with intelligent systems and thermostats. Intelligent buildings and homes can aid the utility by relying on energy flexible concepts such as optimally controlling their thermal and/or electrical storage systems (Denholm and Hand, 2011; Jensen et al., 2017; Morales et al., 2014; Aduda et al., 2016; Reynders et al., 2017).

In this framework, commercial and institutional buildings can be considered as demonstration sites to implement efficiency improvement initiatives and flexibility measures and strategies to optimally manage the energy fluxes within the building and between the building and the grid (Buonomano et al., 2016). Demonstration projects on high energy performance commercial and institutional buildings provide relevant examples and practical experience

increasing knowledge and social acceptance of energy issues and actions. These buildings have potential to adopt flexibility strategies, by optimizing the operation of integrated energy technologies (Ma et al., 2017) with the aim to reduce their pressure on the energy grid (Mlecnik, 2018). The future of the grid is tending to be a transactional grid where energy and information will be exchanged among buildings in an open market, going from a larger community towards the micro- and nano-grid. The nano-grid can be as simple as a single building with its on-site renewable energy production and storage solution.

Most large commercial and institutional building constructions contain significant thermal mass in the form of exposed concrete, thermal and/or electrical storage solutions, and large slow-responding systems where P/PI are inadequate (Afram and Janabi-Sharifi, 2014; Candanedo et al., 2011; Athienitis et al., 1990). A model-based predictive control system can be used to better utilize the thermal/electrical storage and the algorithm can also be used to discover optimized supervisory controls depending on the requirements of the building owner/client. MPC technology requires a model describing the system dynamics with acceptable accuracy to drive control decisions which traditionally involved huge costs for modelling, data collection, expert monitoring and deployment and was cost-prohibitive for medium-sized buildings (Shaikh et al., 2014). The objective of this chapter is to develop a control-oriented model to be used in MPC by using collected data. This model would be transformed into absolute quantities which are building agnostic and used to calibrate and train linear predictive models. Different low-order models with extended metrics to train them are derived to drive high-level MPC controls with significant level of accuracy. A key objective of the work is to evaluate the control models applicability as a function of operating and weather conditions of the controlled building. To this aim, physics-based and physics-free parametrization in a state-space representation will be tested to compare and contrast their performance in forecasting. Engineering time must be minimized to make MPC cost-effective and so generalized approaches are preferred. Models with physical significance are expected to maintain sensible performance during extreme conditions where black-box models tend to fail in extrapolation.

Collected data are gathered at the Varennes library, the first institutional net-zero energy building in Canada located just off Montreal in the city of Varennes, Quebec (Dermardiros

et al., 2019). The building acts as a nano-grid with its on-site photovoltaic (PV) generation and has a thermal energy storage solution as part of its structure. There is no electrical storage system on-site, but can be considered for a future add-on. The work presented here can be transferable to other buildings running on a schedule since the library is first conditioned based on the time of day and then based on occupancy. A preliminary study from the authors proposes an optimization-based MPC strategy on the radiant slab for a single thermal zone of a nearly zero energy building, the Varennes library, located in Varennes, Quebec, Canada (Dermardiros et al., 2017), also see Appendix section A.3.

This chapter focuses on the development of a low-order model that is to be used in an optimized controls framework, namely MPC. The literature suggests low-order models are sufficient for supervisory-level applications. The method herein is to first approach the building top-down and develop the order of models as a function of the systems present and whether there is a time lag component within the system – such as the case of heating being applied into a radiant slab system which then gradually releases its energy towards the space directly above. Collected data is transformed into heat flows and multi-zone temperatures aggregated towards a weighted average of corresponding zones. By applying these transformations, the modelling approach can be extended to any other building operating on a schedule – vs being occupant-driven, and thus stochastic. The end goal being controls, the models need to be stable over time. Common calibration metrics are extended for longer prediction horizons and can optionally be weighted to put importance on nearer term forecasts and/or have varying weighting for each thermal node. Models are trained using a nonlinear least squares method and refined through a Monte Carlo based approach to break the assumption of variables being independent. A visualization is developed to better analyze the behaviour of the model. As a parametric study, models are formulated to either include physics-based co-dependencies or to be physics-free equivalent to a first-order in time autoregressive model. Various lengths of training data are used to train the models to analyze the impact on prediction accuracy and uncertainty in parameter weights. Neural-network-based models are not considered since the data set is insufficient in length to adequately train them.

The chapter is developed as follows: section 4.3.1 details the 3 developed models; section 4.3.2 explains the data transformations applied; section 4.3.3 defines the training and

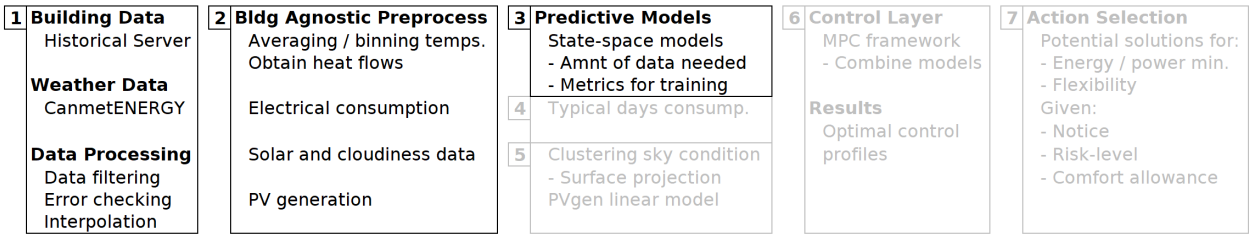

Figure 4.1: Control-oriented modelling for MPC: dark text in this chapter.

testing sets; the training metrics and explains the visualization developed to better assess this fit; section 4.3.4 defines the modelling framework and is represented in a state-space formulation; sections 4.3.5, 4.3.6 and 4.3.7 detail and analyze the fits for the 1st, 2nd and 3rd-order models respectively; and this paper ends with a discussion and conclusion on how to extend the work to other cases and buildings.

4.3 Materials and Methods

The methodology proposed herein, see Figure 4.1, is about obtaining data from the building's BAS or other sources and then process it to obtain building agnostic data: temperature and heat flow. A causal analysis is demonstrated to validate the interdependence and influence of variables on each other in Appendix section B.1. The temperature and heat flow data are used to fit various control-oriented models suitable for MPC. Models are fit using least-squares followed by a Markov chain Monte Carlo (MCMC) posterior estimation to obtain the uncertainty in the parameters. The model and model fits are thoroughly analyzed and visualization methods are proposed to assure their applicability. Metrics for model fits are proposed that can be tuned to obtain model behaviours giving importance to certain zones or also weighing the prediction accuracy of the present more than the distant future. In the following chapter, the final model will be used in an MPC framework to minimize various cost functions.

4.3.1 Building Models

The first step of the proposed methodology is to derive grey-box resistance-capacitance (RC) models of varying order of detail to be used for control aims. Specifically, several building models are developed to predict the indoor air temperature of the building under investigation. The first model is a RC network where all building capacitances are lumped together in a single node with one effective capacitance. This model is used to determine the overall time constant (τ) of the building and to predict how much total heating or cooling would be required in the next hours or day. The second RC network model splits the massive capacitance from the massless one, *i.e.* indoor air, relying on two thermal nodes. The third model further splits the building in two thermal zones, with and without active heating elements. Finally, an equivalent auto-regressive model with exogenous parameters (ARX) in a state-space representation of the same order in time and space is presented for comparison, without assuming any physical co-dependencies, *i.e.* physics-free model. It is worth noticing that care must be taken when selecting the model regressors, especially for training a model with non-representative inputs: either ones that have no correlation with the output or ones that will lead to over-fitting the model. A problematic regressor in the case of a building operating on a schedule would be a time indicator regressor. Here, the model would fit the interior temperature to the time of day instead of what truly affects the temperature.

All models refer to a building heated and cooled through several HVAC components, central and local, which must be regulated to control its indoor air temperature. As a function of the order of detail of the grey-box model, different temperatures are identified. To characterize the derived models and to perform the parameter identification through measurements, the Varennes Library is considered as real case study building detailed in the previous chapter.

The hydronic radiant slab is the primary source of space conditioning in the south, east and west perimeter zones, see Figure 4.2. The current controls for the radiant slab function based on two operational modes: heating or cooling. If the zone is in cooling mode, no heating can be supplied to that zone and vice-versa. There are opportunities to reduce the overall energy consumption of a zone with radiant slabs by either pre-heating or pre-cooling in anticipation of a future load, such as occupancy or solar gains.

Figure 4.2: Varennes library plan highlighting areas supplementarily served by a hydronic radiant slab circuit.

4.3.2 Data Transformation

At the library, all the control points and variables are archived. Certain variables act as intermediate variables used by different control programs to operate the various systems and subsystems. Certain points are logging checks, *e.g.* there are points that monitor contact switches that confirm if a damper is fully opened and only after this confirmation is a fan allowed to operate. To model the thermal and electrical behaviour of a building, many of these points are either unnecessary or will need to be processed into other quantities, such as massflow rate or heat.

In this chapter, the interest remains to study the behaviour of the building on a higher

level and so certain low-level logged quantities will need to be aggregated or transformed. Aggregation can be in the form of averaging the temperature of spaces weighted by the floor area covered by that sensor. Transformation can be taking a pump state and its designed flow rate, the properties of the circulating fluid and the temperature difference between inlet and outlet to calculate the amount of heat transferred within that thermal circuit. By applying these transformations, building specific quantities are mapped to absolute quantities – such as temperature and heat – that are building agnostic. The work following this transformation is general and transferable.

According to the available systems and subsystem to operate, as well as to the grey-box models, different parameters and input are taken into account. General model inputs (not learned parameters), including weather data and measured temperatures, alternatively used in each RC model, are described below; units are given in round parentheses and in which model order they are used in square brackets.

GHI (W/m^2) [1,2,3] global horizontal irradiance obtained from CanmetENERGY-Varennes – research centre located in Varennes, 8 km from the library.

$\mathbf{T_{ext}}$ (°C) [1,2,3] is the exterior temperature measured on-site.

All the HVAC output (terminal fan coil units, DOAS AHU coil, convectors and radiant slab), internal and solar gains are networked to the air node. The HVAC output and other gains are split among the air and slab nodes in the second and third order grey-box models. Differently, the third model further splits the building in two thermal zones to separate the zones with and without the presence of a radiant slab system (*i.e.* one zone is relative to the floor without a radiant slab and one above a radiant slab located along the south, east and west perimeter). Accordingly, different node temperatures and inputs are identified. Their interdependence and causal effects are further analyzed in the Appendix section B.1 and is used to develop the models in the following sections.

$\mathbf{T_{air}}$ (°C) [1,2] is the average library temperature as used by the central system.

$\mathbf{T_{air\ north}}$ (°C) [3] area weighted average of air temperatures **not** above a radiant slab.

$\mathbf{T_{air\ south}}$ (°C) [3] area weighted average of air temperature above a radiant slab which are along the south, east and west perimeter.

$\mathbf{Q_{total}}$ (W) [1] is the total heat transferred to the library as per the energy balance at the heat-pump – which provides heat/cooling to the DOAS AHU, the radiant slabs and fan coil units. Since the library is in 100% heating mode, we can be sure that the overall heat balance calculation is valid; in a mixed mode, the fluid temperature differential shows the net heat transfer. $Q_{total} = [\dot{m}c_p(T_{supply} - T_{return})]_{water-glycol\ mix}$

$\mathbf{Q_{slab}}$ (W) [2,3] portion of total heat transferred to the slab. The radiant slab is a constant flow on/off system. There are 11 zones with radiant slabs. The designed flowrates were obtained from the mechanical drawings; flowrates for the fancoil units and AHU were also on the plans. Trendlogs from the library indicate when a slab is in use. $Q_{slab} = [\dot{m}c_p(T_{slab,in} - T_{slab,out})]_{water-glycol\ mix}$

$\mathbf{Q_{air}}$ (W) [2] portion of total heat transferred to the library but not the slab.

$\mathbf{Q_{air\ north}}$ (W) [3] area weighted Q_{air} where weight represents the portion of the library **not** covered by the radiant systems over the total area.

$\mathbf{Q_{air\ south}}$ (W) [3] area weighted Q_{air} where weight represents the portion of the library covered by the radiant systems over the total area.

$\mathbf{Cons_{ø\ HVAC}}$ (W) [1,2,3] is the electrical power consumed at the library not including the HVAC system. Power consumed by HVAC equipment equals to Q_{total}/COP_{system} where the COP is the system level coefficient of performance accounting for the fans and pumps and the actual heat-pump compressor. It is calculated to be approximately 4.5 for heating and 4 for cooling since the source is a ground loop.

4.3.3 Calibrating and Training a Model

Training and Testing Data Sets Two successive weeks starting in February (19 to March 5, 2018) are chosen to test the model fit. To train the model, data proceeding this date is used for varying lengths. Winter weeks are used since it represents the most challenging case

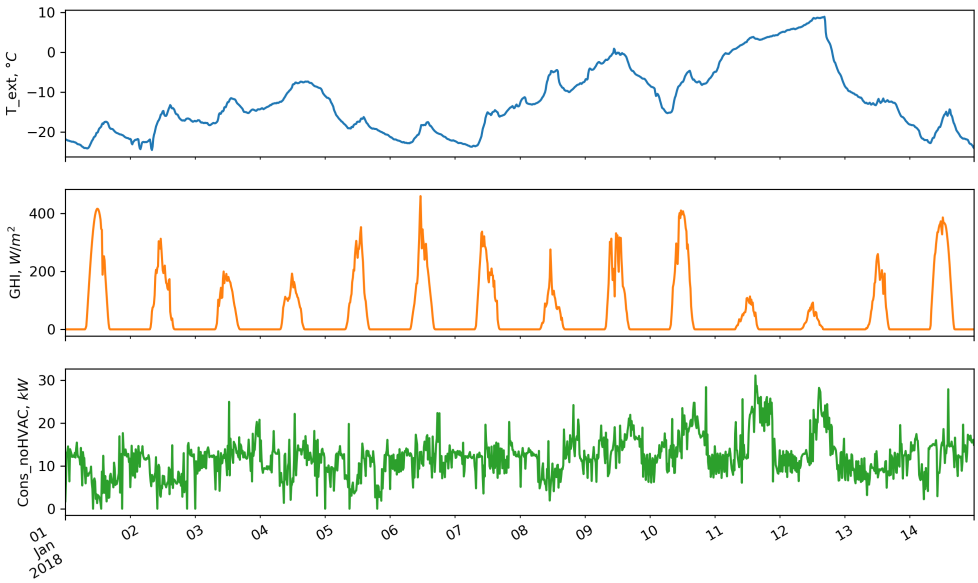

Figure 4.3: Exogenous model inputs: exterior temperature and global horizontal irradiance (GHI). Training range: January 1 to February 18, 2018; testing range: February 19 to March 5, 2018; plotted range: January 1 to 14, 2018.

for both the building and the utility. The exogenous inputs include the exterior temperature and global horizontal irradiance (GHI) and are shown in Figure 4.3 for the first two weeks of the year. The rest of the period has temperatures near -10°C and solar radiation peaks slowly increasing.

Training Metric Žáčeková et al. (2011); Prívara et al. (2012) have used a mean squared error over a prediction horizon as a metric to minimize to train simple models for MPC. We have extended their metric to include an exponential decaying term to give lesser importance to further predictions, see Equation 4.1. Similarly, ASHRAE's preferred NMBE and CV(RMSE) metrics from Guideline 14 (ASHRAE, 2002) have been extended for a prediction horizon – resulting in the extended NMBE (extNMBE) and extended CV(RMSE) (extCVRMSE) metrics respectively, see Equations 4.2 and 4.3. The decaying term, δ_j, which can be tuned, through β, to emphasize the importance of nearer term predictions over pre-

dictions towards the end of the prediction horizon is given in Equation 4.4.

$$extMSE_{zone} = \frac{\sum_{j=1}^{ph} \delta_j \sum_{k=1}^{nt} [T(k+j) - \hat{T}(k+j)]^2}{nt \sum_{j=1}^{ph} \delta_j} \tag{4.1}$$

$$extNMBE_{zone} = \frac{\sum_{j=1}^{ph} \delta_j \sum_{k=1}^{nt} [T(k+j) - \hat{T}(k+j)]}{\sum_{j=1}^{ph} \delta_j \sum_{k=1}^{nt} T(k+j)} \tag{4.2}$$

$$extCV(RMSE)_{zone} = \frac{100\sqrt{extMSE}}{\bar{T}} \tag{4.3}$$

$$\delta(t = j, \beta) = e^{-\beta j} \tag{4.4}$$

Optimizer The resulting calibration problem is solved using the Python `lmfit` package[1] (Newville et al., 2016) using the Levenberg-Marquardt algorithm for nonlinear least squares minimization (Levenberg, 1944; Marquardt, 1963). The results are then used as priors to obtain the maximum likelihood via a MCMC sampling method using the `emcee` package[2] (Foreman-Mackey et al., 2013). A MCMC method samples from the parameter priors to then estimate their posterior probability distribution which explains the uncertainty of the parameters without having to assume independence. The parameters are initialized randomly. Having performed successive training runs, the initialization does not affect the converged values. All parameters are constraint to be non-negative with the physical parameters bound to sensible ranges according to the information obtained from the architectural plans.

Timestep For a physics-based formulation, the timestep is an explicit parameter in the state-space representation. By resampling the data for longer timesteps, the fitting process can be eased. The fitted variables represent physical properties of the building and are – generally – time-invariant. However, certain minute effects are smoothed and their corresponding parameters can become erroneously misfit.

[1] `https://github.com/lmfit/lmfit-py`

[2] `https://github.com/dfm/emcee/`

Visualization of Fit The goal of modelling is to choose a model that can predict the behaviour of the system for multiple timesteps forward with minimal loss of accuracy and without diverging behaviour. The models will be used in model-based predictive controls where, given a starting point, the dynamic programming objective is to minimize a cost within a prediction horizon – multiple timesteps. Although only the first optimal action will be taken from the optimal action profile, the optimization needs to be solved on a longer timestep to minimize the cost on the long term.

To access the quality of the model, we have developed a visualization, see Figure {4.4}, to plot the recursive rollout of the model: starting for a timestep, the model uses measured future weather and recorded actions to predict the subsequent thermal states recursively. Each rollout is plotted in sequential colour whereas the measured data – or ground truth – is drawn in black. A perfect model will have the coloured lines overlapping the black line. We have plotted the rollouts using the actual temperatures and also just the difference relative to the measured data baseline. In the latter, the coloured lines would preferably remain near 0.

Last, the prediction horizon extended metrics, see Equations 4.1, 4.2, 4.3, are shown in the plot for 10 hour rollouts.

4.3.4 Low-Order Model Representation, Simplified Without Hidden States

The RC thermal modelling approach is used to model the physical behaviour of the systems and is represented as a state-space formulation:

$y(t) = x(t+1) = Ax(t) + Bu(t) + Cw(t)$, where:

$y(t)$ model output, which is the same as what goes back in for the following timestep (recursive).

$x(t)$ system variables to track, *e.g.* zone temperature.

$u(t)$ controllable variables, *e.g.* heating/cooling stages, fan, damper position, or other.

$w(t)$ exogenous inputs, *e.g.* weather and time indicators.

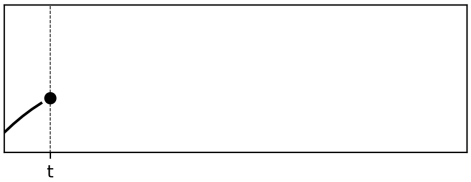

(a) Given the current time, the model needs to forecast for a prediction horizon of length n.

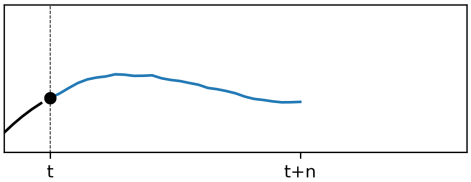

(b) Using the exogenous input forecasts, the model predicts the temperature until time $t+n$ shown with the blue line.

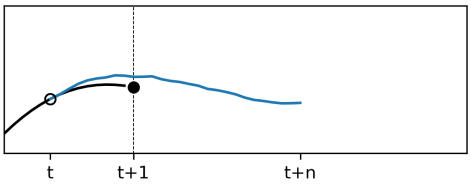

(c) Time advances by one step. The actual temperature at $t+1$ is below the predicted temperature done in the previous timestep. The model appears to over-predict the temperature on near term.

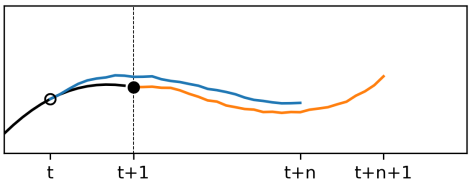

(d) The same model is now fed with the (possibly) updated exogenous input forecasts and predicts the temperature for another n timesteps starting from the actual temperature at $t+1$ shown with the orange line.

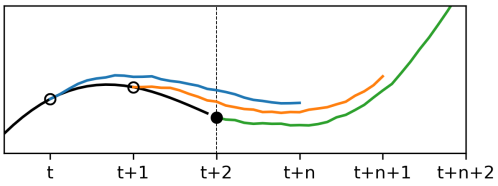

(e) The process is repeated for every time step. A good model's prediction must remain close to the measured data or ground truth (black line) and not diverge on far predictions.

Figure 4.4: Visualization of fit explanation and example.

A, B, C state and input matrices.

The library is conditioned with an air system and a radiant slab where the radiant system is only present within a portion of the building. The models would need to distinguish between zones with the radiant system and zones without. Since the models and later proposed optimal controls are applied at a supervisory level, the zones can be combined. Finally, since the library is very well insulated – see section 3.1 Table 3.1 – and the walls are

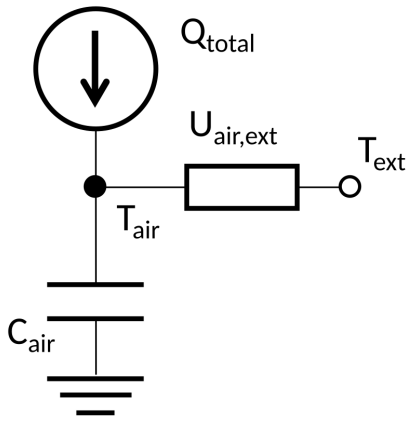

Figure 4.5: 1st-order grey-box model architecture for the Varennes library. Heat inputs include all sources combined which can include solar and internal gains.

not made of massive elements, all the thermal capacitance can be assumed to be inside the building in the form of the books, stacks, furniture and the concrete slab.

Three model orders are presented: (1) 1st-order model lumps both air and radiant systems together, (2) 2nd-order model separates the air and radiant systems but not the zones with and without radiant slab, and (3) 3rd-order model separates the systems and the zones. The 1st-order model could be used in shoulder seasons to optimally use free-cooling since the HVAC system would be shut down. The 2nd-order model can also be used to control the window operation in free-cooling but also have the capacity to better utilize passive solar gains. The 3rd-order model is the simplest model that represents the HVAC system with fidelity and is used in the next chapter. A higher-order model could be designed to separate the floors but since both floors are operated the same way and their arrangements including window sizes and bookshelves are similar, we stopped at the 3rd-order. Having this simplified approach with more emphasis on data pre-processing would allow the methodology herein to be applied to other buildings.

4.3.5 1st-Order Model

Beginning from the simplest case of taking an overall approximation of the whole library, we can draw an equivalent thermal RC circuit in Figure 4.5 with state and input matrices detailed in the Appendix section B.2.1.

Training The models are trained on collected data from January 1st to February 18, 2018, and validated on data following until March 5. As an initial test, a range from 1 to 7 weeks of training data was used to fit a model. The extended mean squared error (extMSE, see Equation 4.1) is used as the cost function. Two decaying factors and two lengths of prediction horizons to train on are used. The parametric run results are showing in Table 4.1. Using 1 week of data, we obtain a model with the least amount of bias in the test set (extNMBE). This model captures the short-term trends well but would not be stable in its parameters. Among the 7 weeks, training the model on 3 weeks seems optimal with parameter values equalling the results from 2 and 4 weeks of data. Using 7 weeks of data seems to be too much for a low-order model where the model tries to fit on past behaviours which are no longer applicable to future predictions. By extending to a longer prediction horizon, the model parameters change a little but by including the exponential decay term, the best fits are closer to the 3-week values. All fits resulted in having no correlation between non-HVAC electrical consumption and interior temperature, and were forced to 0 when running the Monte Carlo (MC) posterior estimation.

The obtained parameters for both physics-based (grey) and physics-free (black) approaches are shown in Table 4.2 with their differences. Table 4.1 reports the corresponding fitted effective physical parameters. The largest difference is for the T_{ext} regressor: the physics-free model depends less on the exterior temperature, however this can lead to prediction errors in application. The physics-based approach converged to a better solution in less iterations since it has less free variables and includes physically meaningful co-dependencies.

The MC posterior estimation method begins after first fitting the models using a nonlinear least squares method and using the fits as priors. The MC method does not assume the parameters are centered around a Gaussian distribution, but looking at the results from the MC fits in Figure B.2 in Appendix B.3, we do observe the variables to follow a normal distribution – see subplots in the diagonal. The other subplots show the drawn samples as a parameter vs. parameter scatter plot. Locations of high density are shown with a contour plot; locations of low density are just shown as points.

Table 4.1: 1st-order grey-box model parametric run. Default settings: timestep: 15-min, decay factor: 0, prediction horizon: 6 hours; metrics calculated on test set for a 10 hour horizon.

Train Weeks	1	2	3	4	5
$U_{air,ext}$	1336±6 (0.46%)	1570±5 (0.34%)	1533±5 (0.30%)	1558±4 (0.28%)	1647±4 (0.27%)
C_{air} (*10^6)	563±4 (0.72%)	734±4 (0.54%)	724±3 (0.47%)	750±3 (0.43%)	838±3 (0.41%)
α_{sol}	66.3±1.1 (1.70%)	105.4±1.1 (1.08%)	109.4±1.1 (0.97%)	124.9±1.0 (0.83%)	147.2±1.1 (0.75%)
α_{gains}	0.0	0.0	0.0	0.0	0.0
extMSE	0.11297	0.10389	0.10183	0.10304	0.10606
extNMBE	0.000246	0.001930	0.000621	-0.000349	-0.000396
extCVRMSE	1.5811	1.5162	1.5011	1.5100	1.5320
Train Weeks	6	7	4	4	4
			ph:10	dy:0.2	dy:0.2, ph:10
$U_{air,ext}$	1650±4 (0.25%)	1774±4 (0.25%)	1637±4 (0.24%)	1522±5 (0.31%)	1525±4 (0.23%)
C_{air} (*10^6)	861±3 (0.38%)	1020±4 (0.40%)	814±3 (0.38%)	719±3 (0.44%)	723±2 (0.33%)
α_{sol}	153.8±1.1 (0.72%)	195.1±1.4 (0.70%)	147.4±1.1 (0.73%)	114.9±1.0 (0.88%)	117.0±0.8 (0.66%)
α_{gains}	0.0	0.0	0.0	0.0	0.0
extMSE	0.10777	0.11798	0.10665	0.06582	0.06615
extNMBE	-0.000905	-0.001587	-0.000654	-0.000146	-0.000241
extCVRMSE	1.5442	1.6158	1.5362	1.2069	1.2099

Table 4.2: 1st-order state matrix entries. Metrics calculated on test set for a 10 hour horizon. Settings: timestep: 15-min, decay factor: 0.2, prediction horizon: 6 hours, train data: 4 weeks. The grey-box equivalent column gives the corresponding positional entries in the state-space matrix described in the Array column.

Regressor	Array	Black-box	Grey-box	Δ(Grey-Black)	%Δ	Grey-box equiv.
T_{int}	$a_{1,1}$	0.99773±0.00021	0.99809±0.00001	0.00036	0.	$1 - U_{air,ext}\Delta t/C_{air}$
Q_{total}	$b_{1,1}$	(1.239±0.024)*10^{-6}	1.233*10^{-6}±0	-6*10^{-9}	0.	$\Delta t/C_{air}$
T_{ext}	$c_{1,1}$	0.00111±0.00058	0.00191±0.00001	0.00133	69.6	$U_{air,ext} * \Delta t/C_{air}$
$Cons_{øHVAC}$	$c_{1,2}$	0.	0.	0.0	-	$\alpha_{gains}\Delta t/C_{air}$
GHI	$c_{1,3}$	0.	0.00015±0.000001	-0.00015	-	$\alpha_{sol}\Delta t/C_{air}$
extMSE		0.1099	0.0658	-0.0441	-67.0	
extNMBE		0.00754	-0.00014	-0.00768	5490	
extCVRMSE		1.559	1.207	-0.352	-29.2	

Testing The models are tested on collected data from February 19 to March 5, 2018. A parametric run is tested for varying lengths of training data, two different prediction horizons and two decaying rates. Figure 4.6 shows the resulting metrics. Focusing on the extended MSE, we observe a minimum around the 3-4-week mark, meaning 3 weeks of data is sufficient

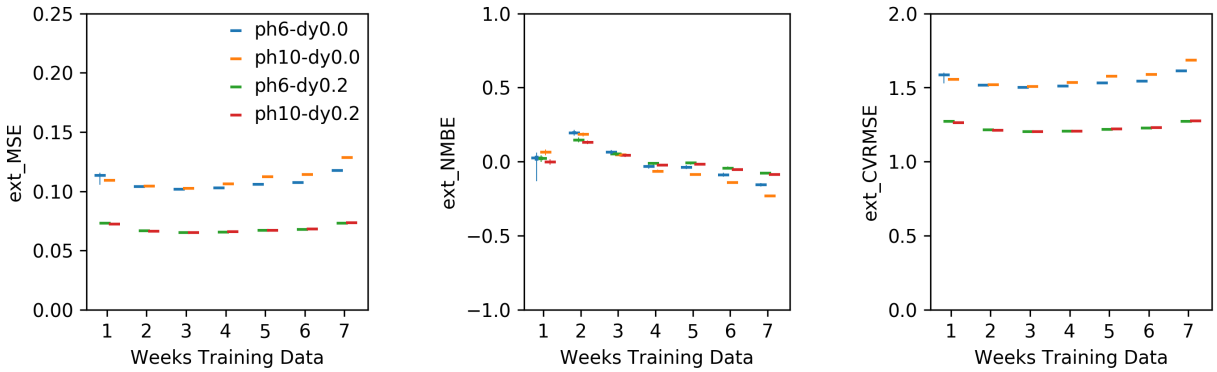

(a) MSE (b) NMBE (c) CV(RMSE)

Figure 4.6: 1st-order grey-box model fit metrics given different weeks of training data; comparing prediction horizon (ph) length and decay (dy) factor. Extended bar is the mean value with the extended thick line showing 1σ range and the extending further thin line showing 2σ range. The metrics show a minimum around the 3-4-week mark.

to predict the thermal behaviour of the building when using a 1st-order model. By using a decay term, the MSE values are decreased since further predictions, which tend to diverge more due to accumulation of errors, have less weight. For the extended NMBE, the trend is lowered with more data but shows a large increase when using 2 weeks of data: given 2 weeks of data, it may be better to train the model on just 1 week and retrain it after obtaining a third week of data. The models fit on one week of data showed the most uncertainty in the resulting metrics and so should be avoided.

Using 4 weeks of data and a small decaying term, we plot both fitted models on the test range in Figure 4.7. In the first chart, we observe the coloured lines following the black measured data line well. Plotting the difference between coloured lines and black, we obtain the baselined chart. The difference seems to oscillate in 12-hour periods which signifies that a higher-order model is warranted. If the resulting pattern was indicative of a white-noise process, then no information is left in the data to extract. Focusing on the physics-free parametrizations, the trends follow the measured data well except that they are always under-predicting the temperature and this is obvious in the baselined plot.

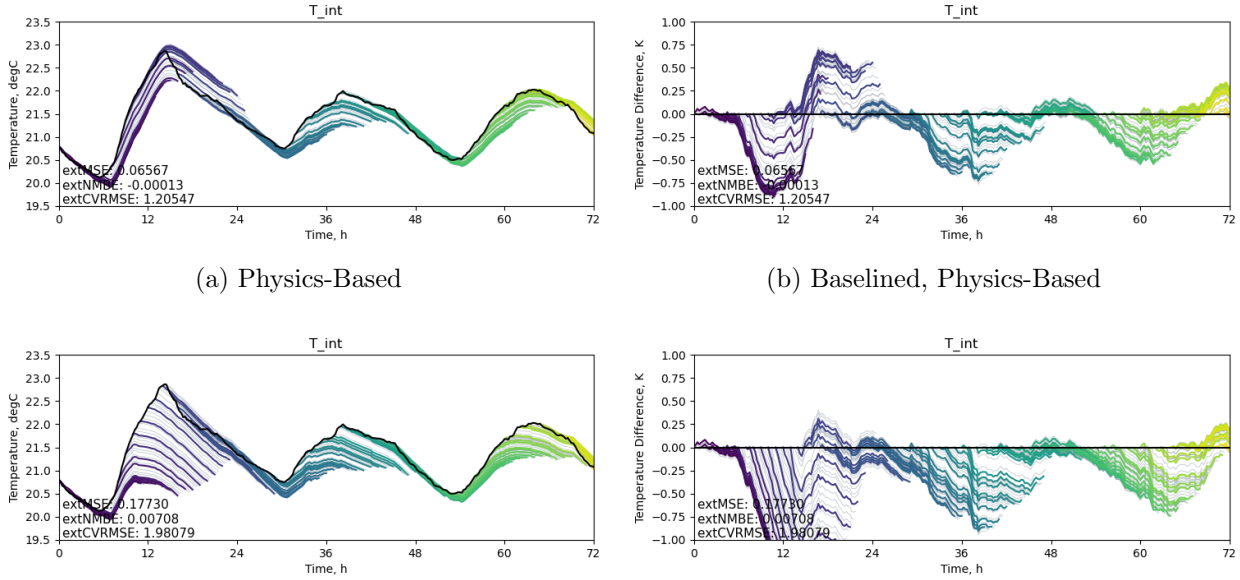

(a) Physics-Based

(b) Baselined, Physics-Based

(c) Physics-Free

(d) Baselined, Physics-Free

Figure 4.7: 1st-order model prediction traces for T_{int}: timestep: 15-min, decay factor: 0.2, prediction horizon: 6 hours, train data: 4 weeks. Each sequentially coloured line represents a rollout at the hour for clarity with thin grey lines for steps in between. For graph interpretation see 4.3.3.

4.3.6 2nd-Order Model

To separate the heat-pump output directed to the slab from the rest which goes towards the air-based system (terminal fan coil units, DOAS AHU coil and convector). The amount of heating or cooling going into the radiant slabs must be determined and removed from the total. The Q_{slab} quantity can be calculated with an energy balance based on the water-glycol solution going into and out of the slab and can be done as a pre-processing step. The 1st-order model is expanded to separate the effects of the two systems, shown in Figure 4.8 with state and input matrices detailed in the Appendix section B.2.2.

Training Here, we introduce an importance weighing factor since the modelling for two zones is using a unified metric. The weighing can be based on area, volume or another importance factor. In this case, a 50/50 and 10/90 percent slab-to-air importance factors are used. Various combination were analyzed but we report two base cases of using a uniform weight

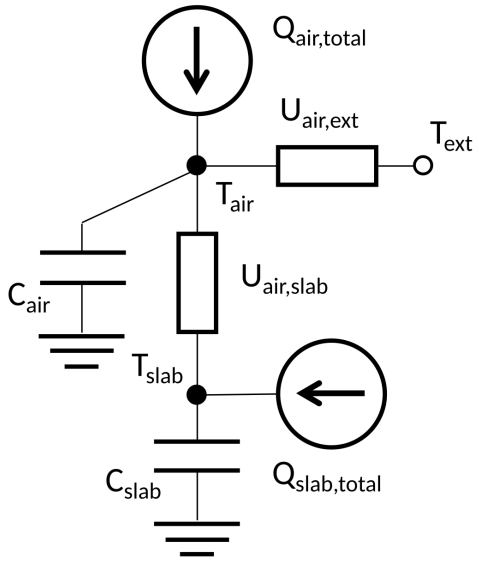

Figure 4.8: 2^{nd}-order grey-box model architecture for the Varennes library. Heat inputs include all sources combined which can include solar and internal gains.

and a more extreme case. The 10/90 puts more emphasis on the air temperature prediction since it has a larger effect on occupant comfort relative to the radiant slab temperature. Table 4.3 shows the effect of this importance factor on the resulting parameter values for the physics-based parametrization. By putting more importance on the room air, the parameters relating to the slab are changed; no significant effect on the air parameters can be observed.

Since the physical properties of a building do not change with time – except if windows are operated –, changing the sampling rate should have no effect on the fitted values; this is done to reduce the time needed for convergence. Table 4.3 shows this fact holds for most parameters except for α_{sol} and C_{slab} for the 10/90 importance factor.

Table 4.4, like in the case of the 1^{st}-order model, shows the comparison of physical and physics-free model parametrizations for a set of specific settings. These settings were chosen because they minimized prediction error. To predict the temperature of the slab or air, the physics-free way comes close to the physics-based model without having explicitly considered the co-dependence of the parameters. This signifies that the method can separate the two systems. The other terms have some discrepancies albeit the overall accuracy appears better for the physics-free approach, however the fitting time was longer but can be reduced using parallelization. The parameters corresponding to the physics-based approach are shown in

Table 4.3: 2nd-order grey-box model parametric run. Default settings: timestep: 15-min, decay factor: 0.2, prediction horizon: 6 hours, train data: 4 weeks; metrics calculated on test set for a 10 hour horizon.

Importance	50/50	50/50	10/90	10/90
Slab/Air		timestep: 1-hour		timestep: 1-hour
$U_{air,slab}$	10'000	10'000	10'000	10'000
C_{slab} (*10^6)	429±4 (0.87%)	432±12 (2.79%)	1524±44 (2.87%)	2126±134 (6.29%)
$U_{air,ext}$	1204±2 (0.18%)	1211±6 (0.52%)	1231±2 (0.15%)	1237±6 (0.47%)
C_{air} (*10^6)	354±1 (0.33%)	339±4 (1.26%)	348±1 (0.30%)	332±4 (1.08%)
α_{sol}	53.1±0.8 (1.54%)	51.0±2.4 (4.73%)	790±25 (3.13%)	768±38 (4.88%)
α_{gains}	0.0	0.0	0.0	0.0
extMSE	0.14876	0.12151	0.11358	0.14362
extNMBE	0.006786	0.005437	0.004368	0.006140
extCVRMSE	1.7973	1.6270	1.5821	1.7786

Table 4.3. The sum of the capacitances from the 2nd-order model is close to the capacitance from the 1st-order model. The conductance towards the exterior is reasonably close as well, signifying that it can be possible to grow the RC network dynamically. The uncertainties of the grey-box approach are not shown because they are negligible.

The MC posterior estimation in Figure B.3 in Appendix B.3 for the 2nd-order model is not as clear-cut as the 1st-order model: some parameters seem to have a bimodal distribution. More samples can be drawn to refine the search, however, this does not improve the result.

Testing The testing set and approach is the same as the 1st-order modelling section except that we are comparing importance indices instead of metric decay rates. Figure 4.9 shows the resulting metrics and does show a minimum around the 3-4-week mark, but it is not as pronounced as the previous section. The extNMBE and extCVRMSE metrics do not have a clear minimum. Thus, obtaining more than a week's data does not improve the accuracy of the model predictions.

Using 4 weeks of data, a small decaying term and a 50/50 importance factor, we plot both fitted models in Figure 4.10. The physics-based models tend to follow the measured data well. The slab temperatures tend to be over-predicted while the air temperatures are under-predicted. No visible trend is observed in the baselined traces; which means the order of the model is sufficient for the data. Looking at the physics-free models, the slab predictions

Table 4.4: 2^{nd}-order state matrix entries. Metrics calculated on test set for a 10 hour horizon. Settings: timestep: 15-min, decay factor: 0.2, prediction horizon: 6 hours, train data: 4 weeks, importance: 50/50. The grey-box equivalent column gives the corresponding positional entries in the state-space matrix described in the Array column.

Regressor	Array	Black-box	Grey-box	Δ(Grey-Black)	%Δ	Grey-box equiv.
Slab						
T_{slab}	$a_{1,1}$	0.9466±0.00760173 (0.80%)	0.9790	0.0323	3.31	$1\text{-}U_{air,slab}*\Delta\ t/C_{slab}$
T_{air}	$a_{1,2}$	0.0539±0.00835137 (15.50%)	0.0210	-0.0328	-156.53	$U_{air,slab}*\Delta\ t/C_{slab}$
Q_{slab}	$b_{1,1}$	$(2.3803\pm0.8757)*10^{-6}$ (36.79%)	$2.002*10^{-6}$	-0.3783E-06	-18.90	$\Delta\ t/C_{slab}$
T_{ext}	$c_{1,1}$	$(0.2488\pm49.745)*10^{-6}$ (199.98%)	N/A	-	-	N/A
$Cons_{øHVAC}$	$c_{1,2}$	0.	N/A	-	-	N/A
GHI	$c_{1,3}$	$(119.40\pm92.507)*10^{-6}$ (77.48%)	0.000239	0.000120	50.04	$\alpha_{sol}*\Delta\ t/C_{slab}$
Air						
T_{slab}	$a_{2,1}$	0.0436±0.0360 (82.75%)	0.0254	-0.0182	-71.68	$U_{air,slab}*\Delta\ t/C_{air}$
T_{air}	$a_{2,2}$	0.9503±0.0385 (4.06%)	0.9715	0.0212	2.18	$1\text{-}U_{air,slab}*\Delta\ t/C_{air}$ $-U_{air,ext}*dt/C_{air}$
Q_{air}	$b_{2,2}$	$(1.8906\pm1.0033)*10^{-6}$ (53.07%)	$2.676*10^{-6}$	0.7854E-06	29.35	$\Delta\ t/C_{air}$
T_{ext}	$c_{2,1}$	$(19.208\pm86.630)*10^{-6}$ (451.02%)	0.00306	0.00304	99.37	$U_{air,ext}*\Delta\ t/C_{air}$
$Cons_{øHVAC}$	$c_{2,2}$	$(0.1099\pm0.1110)*10^{-6}$ (101.00%)	N/A	-	-	$\alpha_{gains}*\Delta\ t/C_{air}$
GHI	$c_{2,3}$	$(240.44\pm34.041)*10^{-6}$ (14.16%)	N/A	-	-	N/A
extMSE		0.13838	0.14876	0.010385	6.98	
extNMBE		0.00660	0.006786	0.000191	2.81	
extCVRMSE		1.59928	1.7973	0.198025	11.02	

follow well the measured data; the air temperature is always under-predicted. For other hyper-parameters, the same behaviour was observed.

4.3.7 3^{rd}-Order Model

The modelling can be further complicated by separating the areas served by the radiant slab and air systems versus simply by the air system which are predominantly in the north zones, see Figure 4.11 with state and input matrices detailed in the Appendix section B.2.3. The 3^{rd}-order model shows three nodes: the area of the library not served by a radiant slab, the area served by a radiant slab and the radiant slab itself. Heat fluxes going into each node are based on the designed flowrates of each circuit and the state of the valves, similarly in approach used for the 2^{nd}-order model. The valves are either open or closed. Solar radiation is considered only on the south nodes. The library is mostly a large open space, and the

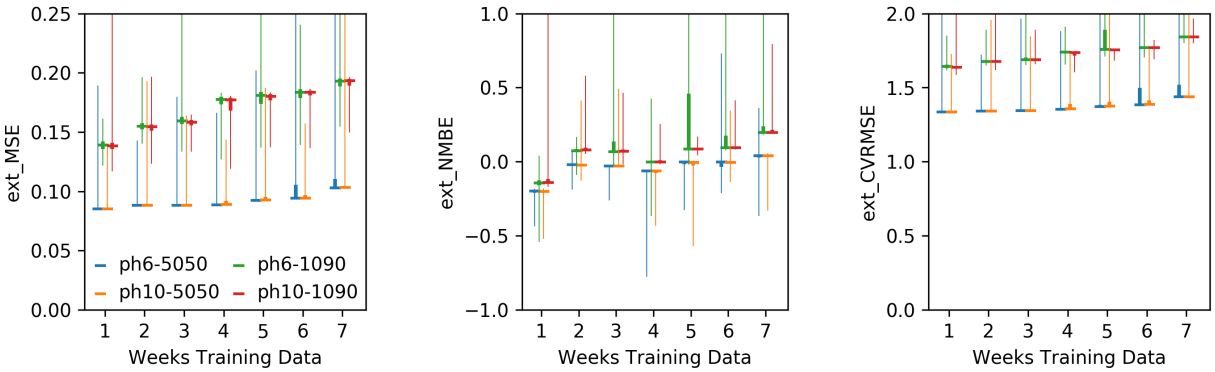

(a) MSE (b) NMBE (c) CV(RMSE)

Figure 4.9: 2nd-order grey-box model fit metrics given different weeks of training data; comparing prediction horizon (ph) length and importance factor. Extended bar is the mean value with the extended thick line showing 1σ range and the extending further thin line showing 2σ range. The metrics show a minimum around the 3-4-week mark.

air flow between sides is represented by a conductance between the two nodes. Physics-free parametrization was not performed for the 3rd-order model since the convergence time was an order of magnitude longer and prediction error was around twice as large compared to the physics-based model.

Training Similar to before, having a 3rd-order model, three weighing factors can be used to merge the metrics from 3 zones. Here, a 33/33/33 and 10/45/45 percent slab-to-$\text{air}_{\text{north}}$-$\text{air}_{\text{south}}$ importance factors are used. The 10/45/45 ratio puts more emphasis on the air temperature predictions relative to the radiant slab temperature and was chosen to approximate the case reported for the 2nd-order model. The importance factors can be chosen depending: on the area served by the system, the capacity devoted to each space, or based on other heuristics. Here, as an example, the importance weight of the slab is reduced since thermal comfort is more attributed to the air temperature. The radiant effects are not large in the library since the slab is not operating at a high temperature. The fit results are shown in Table 4.5. The weighing factor is mostly affecting the slab equivalent capacitance and the air conductance between north and south zones. A fit using summer data from June 18 to July 16, 2018 is included. The model trained on this period is then tested on the following

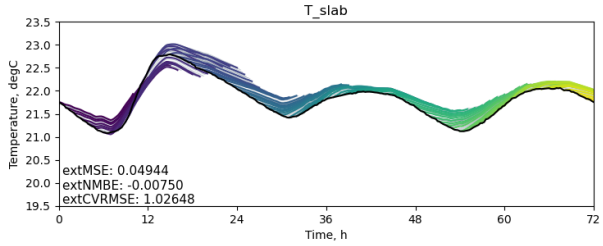

(a) Physics-Based: T_{slab}

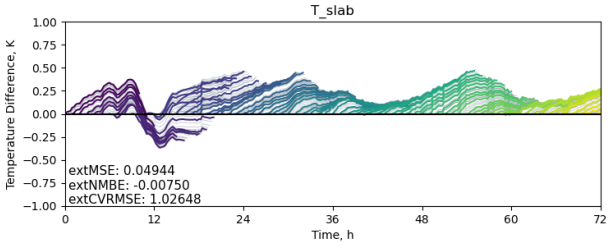

(b) Baselined, Physics-Based: T_{slab}

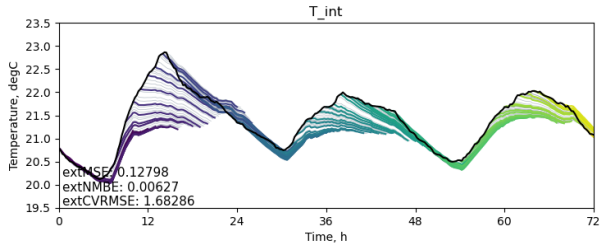

(c) Physics-Based: T_{air}

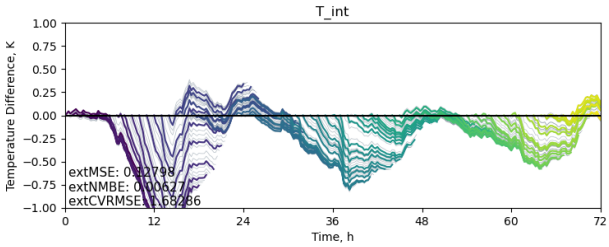

(d) Baselined, Physics-Based: T_{air}

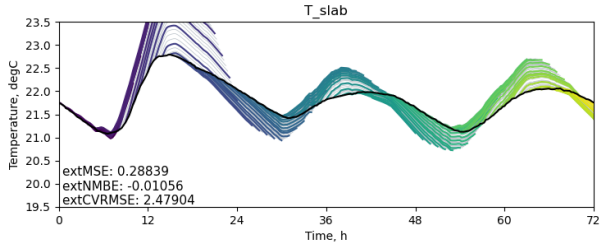

(e) Physics-Free: T_{slab}

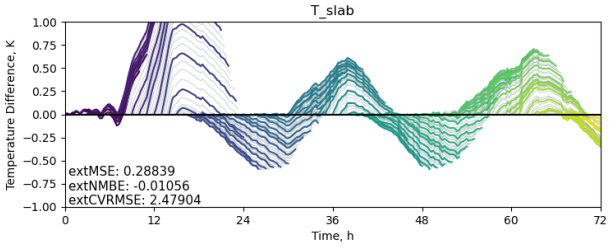

(f) Baselined, Physics-Free: T_{slab}

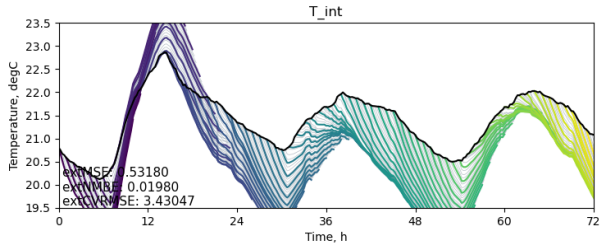

(g) Physics-Free: T_{air}

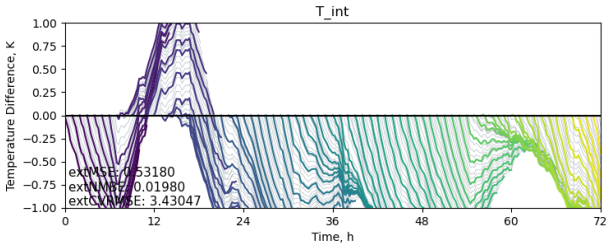

(h) Baselined, Physics-Free: T_{air}

Figure 4.10: 2nd-order model prediction traces for: timestep: 15-min, decay factor: 0.2, prediction horizon: 6 hours, train data: 4 weeks, importance: 50/50. Each sequentially coloured line represents a rollout at the hour for clarity with thin grey lines for steps in between. For graph interpretation see 4.3.3.

two weeks of data. Besides from having a fully-heating or fully-cooling mode, it is difficult to know with certainty which part of the library would be in heating and which in cooling due

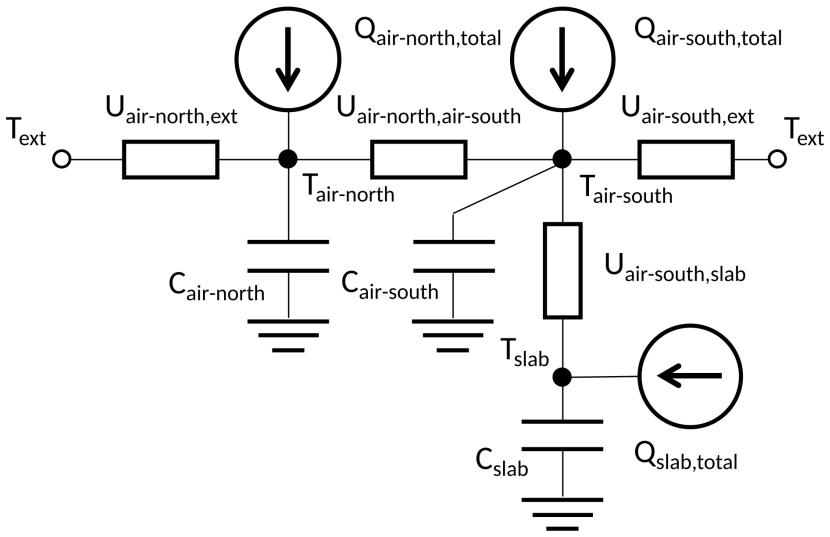

Figure 4.11: 3rd-order grey-box model architecture for the Varennes library. Heat inputs include all sources combined which can include solar and internal gains.

to the lack of flow measurements at the equipment level. Therefore, it is difficult to model the library at a high-level for shoulder seasons.

When comparing the winter and summer parameter fits, the capacitances are very different: the slab capacitance has almost an order of magnitude change and the uncertainty in the variable fits is larger. However, looking at the effect of these uncertainties on the predictions in Figure 4.15, the predicted temperatures are reasonably close to the measured data.

The MC posterior estimation in Figure B.4 in Appendix B.3 for the 3rd-order model shows many parameters following a slight bimodal distribution: there could be local minima in the cost landscape. The sampling is noisier than the previous two runs. A longer sampling is perhaps warranted, however, as previously noted, this would not necessarily improve the final result.

Testing The testing set and approach is the same as the 2nd-order modelling section. Figure 4.12 shows the resulting metrics. No clear minimum can be seen for any of the metrics, therefore obtaining more than a week's data does not improve the accuracy of the model predictions. Unlike the previous two cases, we see a much larger resulting variability in the results. As there are more free variables in the model, minimal fits tend to be uncertain.

Table 4.5: 3rd-order grey-box model parametric run. Default settings: timestep: 15-min, decay factor: 0.2, prediction horizon: 6 hours, 4 weeks of training data; metrics calculated on test set for a 10 hour horizon.

Importance	33/33/33	10/45/45	33/33/33
Slab/AirS/AirN			Summer
C_{slab} (*10^6)	564±50 (8.89%)	868±345 (39.81%)	5451±2493 (45.74%)
$U_{air\text{-}south,slab}$	10'000	10'000	4150±1100 (26.59%)
$U_{air\text{-}south,ext}$	1094±18 (1.64%)	1149±9 (0.75%)	1490±209 (14.02%)
$U_{air\text{-}north,ext}$	462.4±14.5 (3.14%)	438.8±6.7 (1.53%)	971.7±203.0 (20.89%)
$U_{air\text{-}north,air\tilde{}south}$	7447±749 (10.06%)	8893±281 (3.16%)	9880±1142 (11.55%)
$C_{air\text{-}south}$ (*10^6)	185±10 (5.16%)	200±3 (1.43%)	987±221 (22.40%)
$C_{air\text{-}north}$ (*10^6)	272±4 (1.30%)	271±2 (0.90%)	999±172 (17.25%)
α_{sol}	79.7±4.8 (6.05%)	90.0±1.6 (1.80%)	78.2±19.7 (25.13%)
$\alpha_{gains\text{-}south}$	0	0	0
$\alpha_{gains\text{-}north}$	0	0	0
extMSE	0.06725	0.06238	N/A
extNMBE	-0.00054	0.00026	N/A
extCVRMSE	1.20430	1.15557	N/A

Having fitted these models first using `lmfit`, the resulting uncertainties were not nearly as wide as the fits following the MCMC method. The assumption of parameter independence and its fit being normally distributed is shown to be generally not true. RC-based models should be fit or calibrated with linear or other solvers first, and then refined using solvers that do not make those assumptions. By erroneously keeping the independence assumption, it may result in grossly underestimating the uncertainties in the parameter values.

Using 4 weeks of data, a small decaying term and a uniform importance factor, we plot the temperatures in Figure 4.13. All temperatures are reasonably close to the measured data traces. The slab temperature is over-predicted while the air temperatures are under-predicted. Small oscillations can be observed in the baselined plots for the air temperatures signifying that the model can have more terms added to improve fidelity. Keep note that these traces were drawn with the mean parameter fits.

Using the MC sampled parameters, an ensemble of models can be used to draw samples of predictions over various time steps, see Figures 4.14 and 4.15. The predictions are shown in a 95% confidence band – from 2.5% to 97.5%. Similar to the prediction trace plots, a good model would encompass the measured data – represented by the blue line – within the shaded

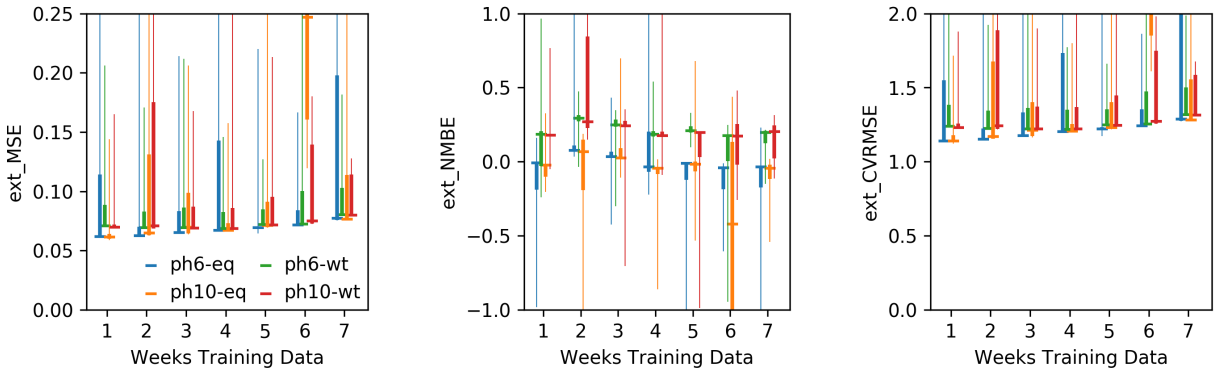

(a) MSE (b) NMBE (c) CV(RMSE)

Figure 4.12: 3rd-order grey-box model fit metrics given different weeks of training data; comparing prediction horizon (ph) length and importace factor (eq=33/33/33, wt=10/45/45). Extended bar is the mean value with the extended thick line showing 1σ range and the extending further thin line showing 2σ range. No clear minimum can be observed for any of the metrics given weeks of data; no conclusion can be drawn about how much data is optimal.

bands. *Baselined* versions are drawn showing the difference of the predictions relative to the measured data. Using this approach, hours where the prediction is most uncertain can be observed. Prediction errors and uncertainties grow most during noon when solar radiation is maximal; thus, complicating the simplified models to account for better solar radiation could be warranted. However, the worst-case prediction – 95% bound for 4 hours forward – is off by 1K, which is very accurate given sensor error is ±0.5K. Compared to winter, the summer fit seems to be more uncertain particularly for the northern zones in the morning. This can be due to the increase of solar radiation during the morning into the library.

4.4 Discussion

Given the selected metrics, the physics-based models with 3-4 weeks of data showed the best accuracy. The interpretation is as follows: 1-week of data will fit the model parameters for the immediate behaviour of the building, however, if the training data includes a holiday or special event, this can skew the parameter fits since the collected data is not representative of the typical behaviour of the system. When taking a much longer period – 8-weeks – the

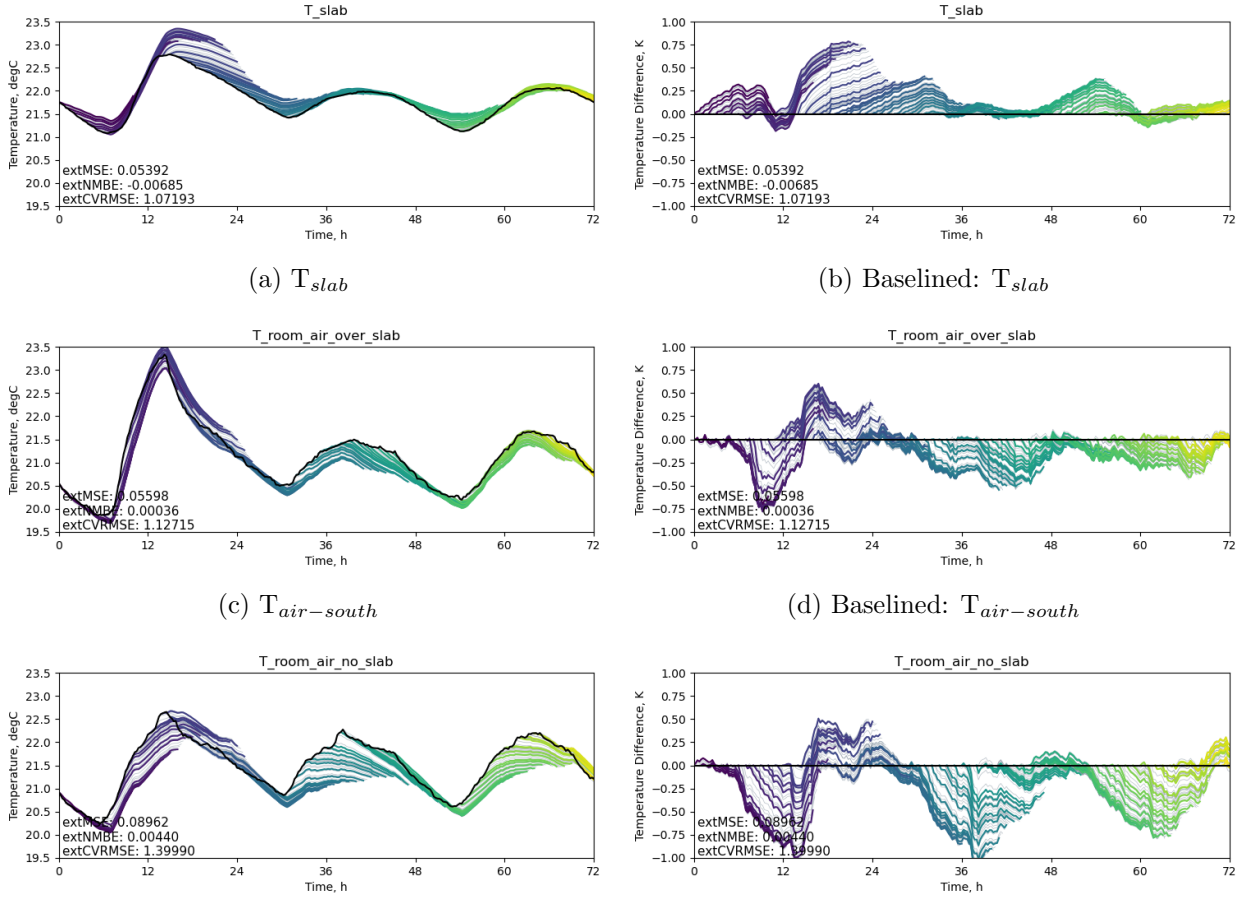

(a) T_{slab} (b) Baselined: T_{slab}

(c) $T_{air-south}$ (d) Baselined: $T_{air-south}$

(e) $T_{air-north}$ (f) Baselined: $T_{air-north}$

Figure 4.13: 3rd-order model prediction physics-based traces for: timestep: 15-min, decay factor: 0.2, prediction horizon: 6 hours, train data: 4 weeks, importance: 33/33/33. Each sequentially coloured line represents a rollout at the hour for clarity with thin grey lines for steps in between. For graph interpretation see 4.3.3.

change of the weather will be averaged; the outside temperature could be warmer than it was 8-weeks ago but the model parameters will be fit using old and possibly stale data. The linear model has a small predictive capacity and cannot fully describe seasonal variation; it must be retrained daily using a sliding window of data. More complex models, *e.g.* deep-recurrent neural network, could capture this behaviour albeit requiring much more data.

The final values of the metrics represent the inaccuracy of the model. These numbers – taking the square-root of the MSE – are below the inaccuracy of the temperature sensors used on site which have a rated range of ±0.5K.

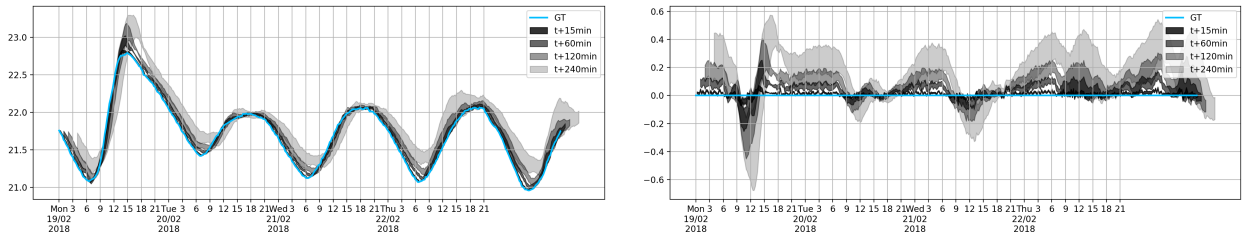

(a) T_{slab}

(b) Baselined: T_{slab}

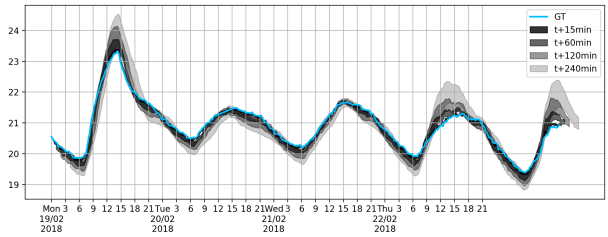

(c) $T_{air-south}$

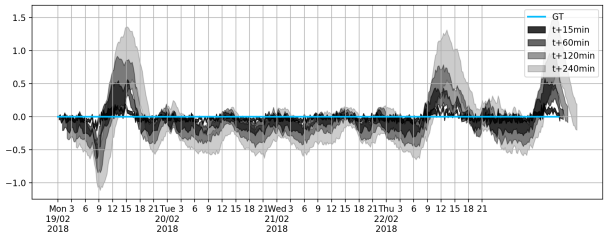

(d) Baselined: $T_{air-south}$

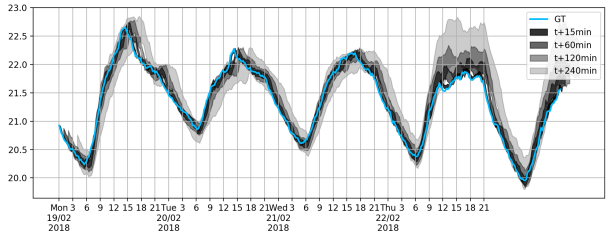

(e) $T_{air-north}$

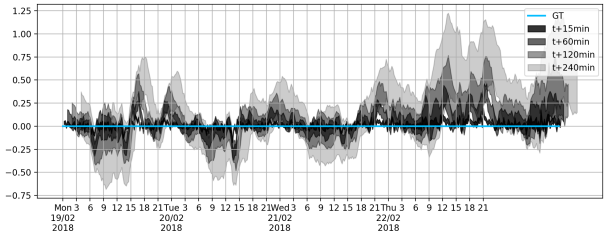

(f) Baselined: $T_{air-north}$

Figure 4.14: 3rd-order ensembled model prediction physics-based traces for winter: timestep: 15-min, decay factor: 0.2, prediction horizon: 6 hours, train data: 4 weeks, importance: 33/33/33. The predictions are shown in a 95% confidence band – from 2.5% to 97.5%.

By applying a data transformation on the raw data to convert values into energy and temperature, the applied methodology is made agnostic to the representing building and can be transferred to other buildings. The model order is chosen to discretize the energy flow within the building to better utilize the systems present, namely to better utilize the radiant slab as a form of thermal storage whereas the air would not be able to hold heat as well.

Through the proposed methodology, model parameters are learned with a random initialization and are not very different given the sampling period and rate: the parameters are representations of physical qualities and are time-invariant. Whether the learned parameters come close to calculated values based on the building architectural, mechanical and struc-

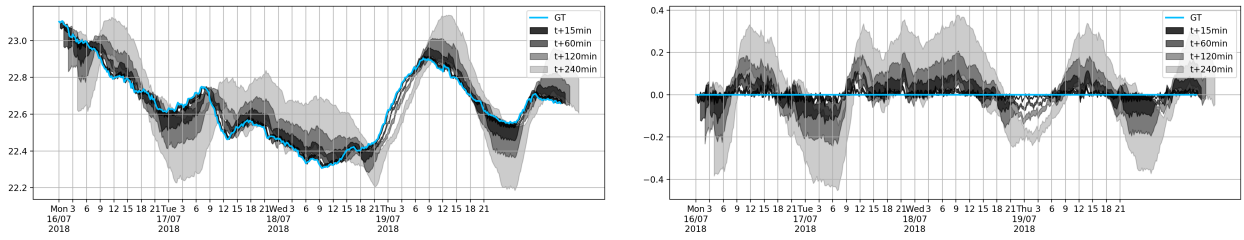

(a) T_{slab}

(b) Baselined: T_{slab}

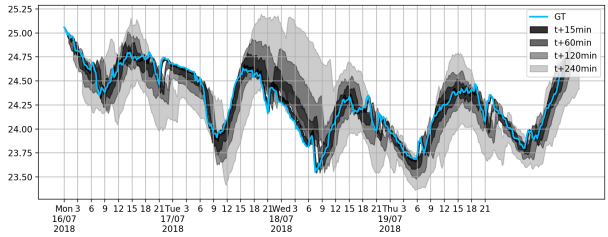

(c) $T_{air-south}$

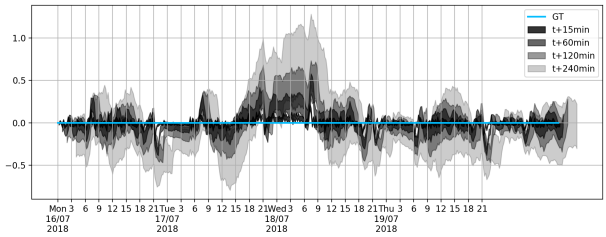

(d) Baselined: $T_{air-south}$

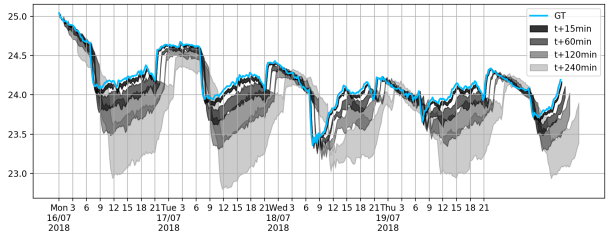

(e) $T_{air-north}$

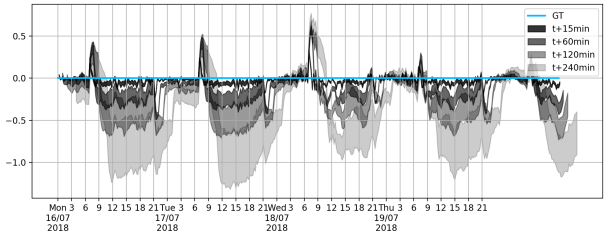

(f) Baselined: $T_{air-north}$

Figure 4.15: 3rd-order ensembled model prediction physics-based traces for summer: timestep: 15-min, decay factor: 0.2, prediction horizon: 6 hours, train data: 4 weeks, importance: 33/33/33. The predictions are shown in a 95% confidence band – from 2.5% to 97.5%.

tural plans is an interesting question which typically cannot be answered due to the lack of complete information. In this case, we had access to the full set of plans and we estimated the building physical parameters in Table 4.6. In addition, the fitted and estimated values are within the same order of magnitude. The estimated total U-value of the building envelope is better than the best fit, this can be due to construction issues or due to air leakage around the windows and doors which was not included in the estimate.

Three different orders of models compartmentalizing the HVAC components differently were presented. The simplest 1st-order model lumps all heat transfer mediums into a single node. This approach would be suitable to quantify the amount of heating or cooling that

Table 4.6: Building characteristics estimated using construction drawings.

Parameter	Unit	Value
C_{slab}	J/K	$268.8*10^6$
C_{air}	J/K	$357.0*10^6$
$U_{air,ext}$	W/K	860

the building would require throughout the day and prepare accordingly. For a finer analysis, to more effectively represent the building's various components, a higher order model is necessary. A 3rd-order model represents the minimal number of nodes required to distinguish the various systems and to enable the ability to forecast the radiant slab separately from the air system. Arguably, the library can be described with 6 nodes – 3 per floor – since the first floor utilized overhead diffusers and the second floor, an underfloor air displacement system. The simpler approach was selected since the second floor also features ceiling fans which are left running throughout winter and thus both floors have a well-mixed air distribution. By first analyzing the system in a building, similar zones can be grouped together and thus result in a simplified model. Given, for example, a 20-floor building, a typical floor approach can be used to model all middle floors together. However, for controls, care must be taken to not control all the middle floors the same way as to avoid generating a peak demand and to utilize diversity and flexibility in operating schedules and actual occupancy.

We had access to all construction plans and logged quantities were used to derive heat flows quantities; which may not always be accessible especially with older buildings where plans are either lost or outdated. With the recent releases of Haystack 4 (Haystack, 2020) and Brick (Balaji et al., 2016; Brick, 2020), building components can be tagged into hierarchical and interdependent systems and more useful quantities – such as energy flow instead of damper positions or fluid entering/exiting temperatures – can be reported to the BAS. Having overall energy flows in a building, the creation of control-oriented models can be greatly simplified and even be done within the end controllers. Ease of model creation can also facilitate automated fault detection and diagnosis, preventative maintenance and help with cost-optimal retrofit projects. Brick also has the advantage that it is specified as a database, can be queried as such.

4.5 Conclusion

Three different orders of models are presented in this chapter with extended metrics to train them. The 3rd-order model is the most informative one to drive high-level MPC controls in the library, however it includes more free parameters and it resulted in fits with the highest levels of uncertainty. The 2nd-order model could be suitable for shoulder seasons as well when operating strictly the radiant slab and pre-cool the slabs in anticipation of solar gains. Finally, the 1st-order model can be used in the shoulder seasons when the windows are opened and the HVAC system – including the radiant slab – are not functioning; it can be used to determine how to operate the windows to maximize night-time free-cooling/flushing without leading to over-cooling the library the next morning. It can also be used to estimate the total quantity of heating or cooling to prepare pre-emptively for the day. As a future work, all 3 models can be used as an ensemble giving a certain model more importance depending on the operative and/or exterior conditions. When the windows are open and the central HVAC is off, the 1st-order model can be prioritized.

The methodology proposed is applied to a building predominantly operating on a schedule. Between predefined times, the building must be operating within a comfortable temperature. In this work, the modelling approach is simplified to cover larger areas; that would signify that this would be used for supervisory-level controls. In a simpler building utilizing rooftop units (RTU) for single zones, the same simplified modelling approach from this work can be directly used for controls – a 1st to 2nd-order model per RTU. A significant portion of commercial and retail buildings in North America are of the slab-on-grade building with an RTU system archetype and operate on schedules. The methodology in this work can be applied directly.

For occupancy-driven buildings, such as individual offices or residential buildings, an occupant model would first need to be learned and then input into a model as proposed here. For more complex buildings with many zones or with systems exhibiting nonlinear behaviour, such as large office towers or grocery stores: the HVAC system and zones can be broken down hierarchically and the non-convexities can be made convex for a given iteration.

The work presented is for the Varennes library which utilizes a photovoltaic array and

ground-source heat pumps. The radiant slab system offers some thermal storage but is not a dedicated solution. The resulting controls tend to overheat the space to utilize excess PV production during the day for the purpose of reducing electrical consumption. Thermal comfort within the space is the limiting factor. Having a dedicated solution will alleviate this limitation.

Depending on the building load profile, there may be a cost-benefit calculation to perform to chose either, or both, a thermal storage solution, such as a water tank, and a battery bank, or alternatively to charge electric vehicles (EV). If stored electricity will be used to drive a heat-pump outside periods of solar availability, it might be more cost-effective to simply heat or cool water in a storage tank and use the stored capacity when needed. Convex models of water tanks can be formulated with finite difference methods and would remain feasible for MPC. Convex models of batteries can be used if electrical storage is more economical. The library features EV charging stations however modelling EVs can be more challenging due to the probabilistic nature of arrival and departure times of EV owners.

The reduced-order models obtained with the proposed approach are used to be applied in an MPC strategy for the control of the indoor air temperature. The model reduction method is an effective tool to design predictive strategies, in which low-order models are preferable with respect to complex and detailed models. A potential application is the simulation of energy demands in districts where buildings will play an active role in the near future. Thus, by having a control-oriented model of the building, dynamic controls can be used that track the price of electricity and minimize operating costs while guaranteeing the comfort of its occupants.

Chapter 5

Sampling-Based Model Predictive Controls

5.1 Overview

This chapter focuses on the potential of a novel methodology to derive low-order grey box models exploited for model predictive controls of the next generation of buildings. To manage the requirements of high-performance buildings and of smart grids, the developed control strategies includes multiple optimization objectives: minimize operational cost, minimize peak demand following a notice by the utility, track a net consumption profile to maximize self-consumption of renewable energy production or to aid the grid toward energy flexibility. With the aim to validate the MPC performance, the proposed approach is applied to the first solar net-zero energy institutional building of Canada, situated in Varennes, Quebec. This building, a library, features a hydronic radiant slab system which delivers heating and cooling into most spaces along with an air system responsible to bring fresh air to the space and offer supplemental conditioning. Since the methodology in this chapter is developed for a complex case, the radiant slab may be turned off to represent a more conventional building relying purely on an air system. The simulated cases are for bounding conditions to clearly showcase the advantages of the proposed MPC approach over conventional strategies applied on the calibrated model, as studied in the previous chapter. Results show how aggressive or risky the controller can be is a function of the building owner's request with guarantees on a

pre-set level of performance.

The following section introduces the needs and advantages of the proposed method. Section 5.3 details the methodology used to combine exogenous input models with the building thermal model. Section 5.4 gives the model-based predictive control (MPC) general and generic formulation, followed by various cost functions and their results. Section 5.5 pushes the approach further taking the fully-noised and sample-based approach to solve the profile-tracking cost function that can be defined as promoting energy flexibility. Finally, sections 5.6 and 5.7 discusses the results and offers key conclusions spawned from this method.

5.2 Introduction

Unlike conventional approaches, MPC has the advantage to make the control intent explicit and dynamic able to utilize future information to optimally operate a building. However, it is not yet widely applied. There is a need for a more robust-to-uncertainties approach where the level of risk can be selected: worst-case would be too conservative. Uncertainties are from predictions – exogenous inputs: weather, occupancy –, model structure/simplifications and model trained parameters. The use of advanced controls as MPC will be crucial for the next generation of buildings that will need to be *energy flexible* considered as the "ability to adapt the energy profile without jeopardizing technical and comfort constraints" (Aduda et al., 2016; Reynders et al., 2018). In addition, grids will tend to be transactional, and energy and information will be exchanged among buildings in an open market which translates to a paramount need for dynamic and connected control schemes. The MPC cost function can track a desired load profile set by the utility to assure its reliability, while the building operator would be compensated through incentives.

In this framework, this chapter runs sample-based MPC to determine how to operate energy systems under uncertainty while guaranteeing a certain level of performance. The modelling is divided into 5 parts: (1) building thermal model, (2) plug load and lighting power, (3) ambient temperature noised model, (4) photovoltaic power generation, (5) solar cloudiness model. These parts make a flexible framework and come together to generate the control sequences to be applied. The overall proposed process is summarized in Figure 5.1.

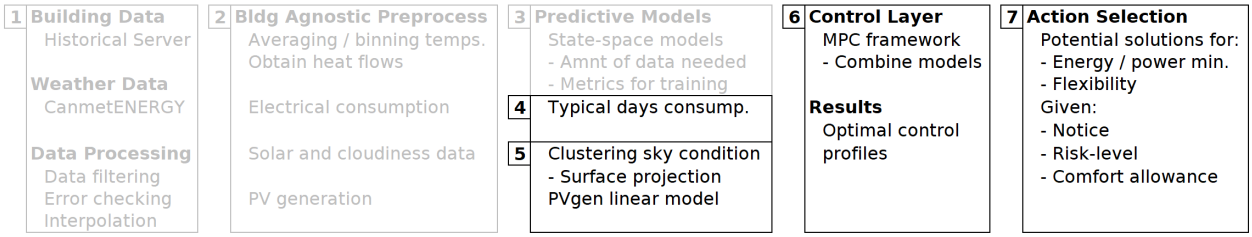

Figure 5.1: Control-oriented modelling for MPC: dark text in this chapter.

The MPC performance is demonstrated by conducting a case study analysis applied to the Varennes library to show the advantages of the proposed MPC approach over conventional strategies. In particular, through the proposed case study analysis, we show the robustness of the controller as a function of the requested level of performance of the building. Specifically, an MPC for floor heating slab systems in response to dynamic electricity prices is modelled with the aim to shift peak power demands and provide energy flexibility. The MPC controller is implemented in the Python simulation platform and its reliability, its thermal and energy performance are tested.

Following the literature review presented in chapter 2 section 2.3, to further the state-of-the-art in convex optimization based MPC utilizing convex physics-based grey-box models, the contribution herein is the development of a robust iterative sample-based MPC approach that does not assume distributions on the noise. An ensemble approach is used for the building modelling and the various inputs to the models are modelled producing probable consumption and production profiles. A winter season is analyzed for a net-zero energy library located in Varennes, near Montreal, Canada. The winter season is used because it represents the most strenuous period for the utility given the climate is very cold and there is a low solar availability and therefore peaking gas production plants may need to be used to meet demand thus increasing greenhouse gas emissions.

5.3 Materials and Methods

An MPC for floor heating slab systems in response to dynamic electricity prices is modelled. The aim of the controller is to shift peak power demands and provide energy flexibility.

The Python programming language is considered to implement the MPC controller and to test its reliability as well as its thermal and energy performance. A control-oriented grey-box dynamic thermal model for the building, including the radiant slab, the HVAC and the renewable energy systems, is developed. This section includes a detailed description of the proposed 3rd-order grey-box thermal model developed to capture the thermal dynamics of the system, the uncertainties and noise, as well as of the MPC formulation. A state-space representation is considered to formulate convex and easily-solved optimization problems, and to add white noise to obtain a more realistic stochastic model that will include uncertainties. These are subdivided in two categories, (i) epistemic uncertainty: model related uncertainties due to structure and parameter weights, (ii) aleatoric uncertainty: exogenous inputs including exterior ambient temperature, solar radiation and occupant-driven consumption.

5.3.1 Prediction of Exogenous Inputs

Building Loads The investigated building is the Varennes library, an institutional building designed for net-zero annual energy balance, represented in Figure 5.2. The solar building produces electricity from a 110.5 kWp building-integrated photovoltaic thermal (BIPV/T) system (Candanedo, 2010; Athienitis and O'Brien, 2015), also see Appendix section A.5. The building is also equipped with a ground-source heat-pump (GSHP). Measurements from 1st-year after inauguration operational observations are considered to characterize the model and to perform its parameter identification, as reported in Dermardiros et al. (2019), also see section 3.3.

As an initial step, the total electrical consumption of the building is split into two parts: one from components that the control algorithm influences and one relative to uncontrolled devices. The plug loads and lighting are driven by occupancy and the library operation schedule. As mentioned, the building is heated and cooled through several HVAC components – central and local – regulated to control its indoor air temperature. The HVAC system is driven by the ambient conditions, operation schedule and, finally, on occupancy via CO_2-based demand-driven fresh-air ventilation.

The uncontrollable loads need to be predicted to determine the future electrical consumption of the building. The consumption due to the HVAC component can be obtained

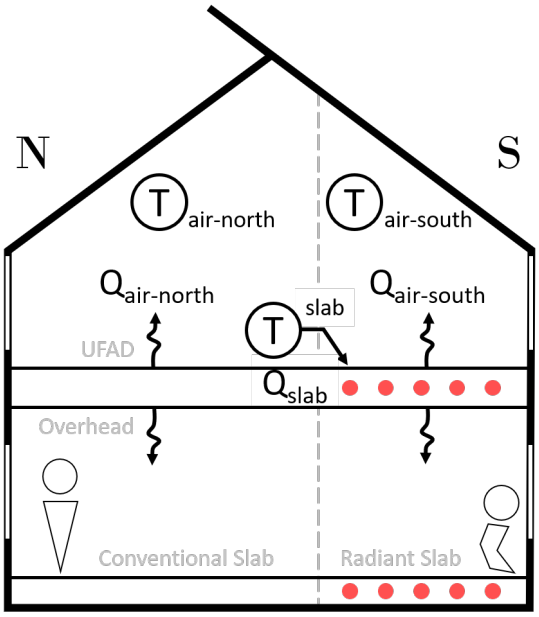

Figure 5.2: Simplified schematic cross-section of the Varennes library equivalent to the thermal network circuit.

via $\text{Cons}_{\text{ø HVAC}} = \text{Cons}_{\text{total}} - \frac{Q_{total}}{COP_{system}}$ and the remainder is contributed by the plug loads and lighting. Since subsystem metering is not available, these categories cannot be further distinguished. A system-level coefficient of performance (COP) of 4 for cooling and 4.5 for heating is considered for the operation of GSHP, circulation pumps and fans.

Removing the consumption of the HVAC component from the total one should eliminate weather-related dependencies, except for the lights. Lighting might be on longer during the winter and/or there should be more plug loads during exam periods given students tend to study in libraries. The electrical consumption can be clustered using the k-means algorithm to discover whether typical days can be obtained: shoulder seasons – spring and fall – weekdays, non-shoulder weekdays and weekends/holidays. In this case, the k-means algorithm groups similar points together where a point is in $\mathbb{R}^{96}$ representing 24-hour data in 15-minute timesteps. However, clustering did not clearly separate the data. A second option is to group the data based on the day of the week since the library operates on a weekly schedule and some similarity between each day are expected, as shown in Figure 5.3. Considering that there are only passive infrared occupancy detection sensors in the library, the number of guests is unknown. Thus, to visually inspect if the electrical consumption follows

occupancy, the Google Popular Times API (Google, 2020) was considered to obtain a relative occupancy rate when the library is open to the public. By having better occupancy data, enhanced occupancy prediction models can be utilized shifting from operating the building using a fixed schedule towards an occupant-driven operation enabling higher savings and improving comfort.

The consumption predictions are used in the MPC formulation to minimize grid interaction. Note that for a given day, a consumption profile is sampled for that day. Alternatively, a sample can be generated by taking an averaged profile and noising the full profile based on the variance from the data.

Exterior Ambient Temperature Forecast Noised Model Weather data is obtained from the local airport – Pierre-Eliot Trudeau, IATA: YUL, ICAO: CYUL – which publishes forecasts for the next 168 hours three times a day: morning, noon and evening (of Canada, 2015; SWOB-ML, 2020). It is processed to obtain a model representing the uncertainty in the data and can be used in a sampling-based setting – details in Appendix section B.5.

Photovoltaic Power Generation The PV AC generation is calculated from the projected unit solar radiation onto the PV arrays according to geometric correlations (Duffie et al., 2020) – details in the Appendix section B.4. To do so, solar radiation data were obtained from CanmetENERGY-Varennes located 8 km away from the library for 2018 in 5-minute intervals to match the building's electrical data collection rate. The model was trained for every month, obtaining a good match as shown in Table 5.1 and in Figure 5.4. The best-fit parameter in January (0.0544) differs the most and is due to a malfunction resulting in a total loss of production for a few days. This approach can also be useful for a simplified fault detection strategy. Note that this part remains separated from energy model, but it is input in the optimization.

Solar Radiation Cloudiness Sampling Solar radiation prediction is very difficult. Instead of trying to predict what will *really* happen, the idea is to use what *could* happen and that for certain types of days. Specifically, the bounding cases are simple that they have little variance: fully overcast and perfectly clear days. In between the two cases highly depends on

Table 5.1: Linear PV AC production model best-fit parameters per month.

Month	Parameter
JAN	0.0544
FEB	0.0800
MAR	0.0898
APR	0.0864
MAY	0.0844
JUN	0.0814
JUL	0.0801
AUG	0.0806
SEP	0.0831
OCT	0.0834

cloud movements and is highly variable. In application, only the class of day would need to be predicted. Solar radiation data were collected in 5-minute intervals for 2018 with details of the approach in the Appendix section B.6. As an example, solar radiation daily profiles for the three types of days are given in Figure 5.5.

5.3.2 Building Thermal Model

The investigated library building is split in 2 thermal zones, the first one refers to the area served by both the radiant slab and the air system whereas the second one refers to the area only served by the air system. A 3rd-order minimal RC thermal model that represents the overall library is developed with a sketch of the thermal network reported in Figure 4.11, see section 4.3.7. The thermal nodes represent: (1) the radiant slab that is present on the southern perimeter of the building, (2) the air of the thermal zone above this slab, and (3) the air of the thermal zone without radiant slab.

5.4 Model-Based Predictive Control

5.4.1 Formulation

In this section, the system and input prediction models are brought together into a MPC formulation. A general MPC framework is described in Equation 5.1: a loss function is to be minimized over a prediction horizon, subjected to various constraints where some describe

the dynamics of the system to control while others define limits and boundary conditions.

$$
\begin{aligned}
J = \min_{u^0,\ldots,u^{N-1}} \; & \sum_{k=0}^{N-1} l_k(x^k, u^k, w^k) \\
\text{subject to } & h_i(x^k, u^k, w^k) = 0, i \in \{1, \ldots, m\}, \text{ equality constraints} \\
& g_j(x^k, u^k, w^k) \geq 0, j \in \{1, \ldots, n\}, \text{ inequality constraints} \\
& x^0 = x, \text{ current state} \\
& x^{k+1} = f(x^k, u^k, w^k) = Ax^k + Bu^k + Cw^k, \text{ system dynamics}
\end{aligned}
\tag{5.1}
$$

Where,

x^k system variables track the system dynamics,

u^k control variables which can be manipulated in order to improve the building performance,

w^k exogenous inputs representing time series that can be observed but cannot be controlled, such as weather,

$l(x, u, w)$ loss or cost function which could be to minimize the utility cost, or the grid interaction, or some other cost,

$h(x, u, w) = 0$ equality constraints; here, the system dynamics of the system (next-step interior temperature) is given by the trained model, and,

$g(x, u, w) \geq 0$ inequality constraints, here, the inequality constraints are the boundaries of the problem: can include the capacity of the heating system, toggling limitations to reduce wear, the comfortable temperature range, an allowance for discomfort, etc.

Having a model and the MPC formulation, the cost function $l(x, u, w)$ can be tuned to minimize other likely cost functions: operation cost,

$$
J = \min_{Q^0,\ldots,Q^{N-1}} \; \sum_{k=0}^{N-1} c^k Q^k_{total}, \; c : \text{relative heating cost} \tag{5.2}
$$

peak demand following a notice by the utility,

$$
J = \min_{Q^0,\ldots,Q^{N-1}} \; \sum_{k=0}^{N-1} (c^k Q^k_{total}) + \|\mathbf{Q_{total}}\|_\infty \tag{5.3}
$$

track a net consumption profile to maximize self-consumption of renewable energy production or to maximize aid to regulate grid's overall demand – energy flexibility,

$$J = \min_{Q^0,\ldots,Q^{N-1}} \left\| \frac{cQ_{total}}{\mathrm{COP}_{\text{heating system}}} + E_{\text{plug loads}} - \text{profile}_{\text{desired}} \right\|_{norm} \tag{5.4}$$

where PV generation can also be included,

$$J = \min_{Q^0,\ldots,Q^{N-1}} \left\| \frac{cQ_{total}}{\mathrm{COP}_{\text{heating system}}} + E_{\text{plug loads}} - \text{profile}_{\text{desired}} - \text{PVgen} \right\|_{norm} \tag{5.5}$$

and where the norm can be norm-1 or norm-2 where the profile divergence would be either penalized linearly or quadratically.

The constraints are common and summarized:

$$\begin{aligned}
&\text{subject to } \underline{T} - s_{\text{comfort}} \leq T \leq \overline{T} + s_{\text{comfort}}, \text{ no comfort slack for } T_{\text{slab}} \\
&\quad \underline{Q}_{\text{total}} \leq Q_{\text{total}} = Q_{\text{air}} + Q_{\text{slab}} \leq \overline{Q}_{\text{total}} \\
&\quad [\underline{Q} \leq Q \leq \overline{Q}]_{\text{air, slab}} \\
&\quad x^0 = x \\
&\quad x^{k+1} = Ax^k + Bu^k + Cw^k, k \in \{0, \ldots, N-1\} \\
&\quad \frac{\Delta t \sum s_{\text{comfort}}}{3600} \leq s_{\text{comfort budget}} \\
&\quad s_{\text{comfort}} \geq 0 \\
&\quad \frac{Q_{total}}{\mathrm{COP}_{\text{heating system}}} + E_{\text{plug loads}} \leq E_{\max} \\
&\quad \text{PVgen} = \alpha_{\text{projected2PVpower}} \mathrm{I}_{\text{proj}}
\end{aligned} \tag{5.6}$$

Where,

Q thermal power,

E electrical power,

$PV_{\mathbf{gen}}$ photovoltaic power generation, force to zero for MPC to not consider generation,

$\mathbf{profile}_{\mathbf{desired}}$ desired electrical power profile to track, a profile of 0 would minimize grid interaction,

$\underline{v}$ **and** $\overline{v}$ lower and upper limit of variable v,

$s_{\mathbf{comfort}}$ slack variable for comfort, used to allow optimization problem to be feasible if initial temperature is outside allowed limits,

$s_{\mathbf{comfort\ budget}}$ slack variable for comfort budget,

$\alpha_{\mathbf{projected2PVpower}}$ best-fit parameter to convert projected solar radiation into AC electrical power output – see Table 5.1, and,

$\mathbf{I_{proj}}$ solar radiation normal projection onto the PV array.

5.4.2 Solver

The MPC framework is programmed in `cvxpy` (Diamond and Boyd, 2016) in Python and solved using the `ECOS` solver (Domahidi et al., 2013) using default settings on an x86-64bit-based Linux machine with an Intel Atom processor to emulate a low-power edge device. In the most difficult case, the full noised iteration would complete in less than 5 minutes for a 12-hour prediction horizon for the 3$^{\text{rd}}$-order model.

5.4.3 Energy and Power

Energy results are reported for a sample cold (μ: -13°C) sunny weekday, January 26, 2018, and the MPC performs optimization starting midnight with a 24-hour prediction horizon. The cost function to be minimized is the operation cost – Equation 5.2 – which corresponds to the minimization of the energy demand. Perfect forecast information is used and a comfort budget of 0.5°C is allowed per library zone. The addition of this slack variable reduces the risk of having an infeasible optimization problem when the state conditions are not favourable.

Results in Figure 5.6a refer to the north thermal zone without radiant slab – Air no Radiant – being heated starting at 5AM until around 7:30AM after which the south thermal zone with radiant slab – Air over Radiant – is heated. The temperature profile follows a linear ramp without being explicitly programmed to do so. Heating is also applied towards the end of the day for the south zone. The slab is not utilized. It is worth noticing that the MPC algorithm supplies just enough heat to the north zone throughout the day to maintain its temperature exactly at the heating setpoint. The dashed lines show how the

building was operated on that day following conventional reactive controls. Compared to MPC, regular controls consume 821 kWh of energy for HVAC during the full day, whereas the MPC approach consumes 630 kWh. Since power is not penalized, the optimal control tends to turn on aggressively early and late in the day.

To consider a case of a morning peak in a time-of-use tariff structure, the energy cost between 6 to 9AM is increased by a factor of 5. Results in Figure 5.6b shows the north side to start being heated immediately until heating is completely shut off at 6AM. The over-heated space can then free float during the peak period and remain within the comfort boundaries. The south zone is gradually heated and a small amount of heating is used during the peak period. This pre-heating and system staging strategy has emerged through the minimization of the operational cost. To obtain this behaviour in conventional controls, control algorithms would need to be designed, tested and implemented heuristically and the results would not be as perfect. Compared to the uniform pricing case, this case consumes 670 kWh. If additionally there is an evening peak from 4 to 8PM, the evening behaviour is affected by a slight pre-heat but not as aggressive as in the morning since the library closes at 9PM – see Figure 5.6c. This case consumes 815 kWh of energy.

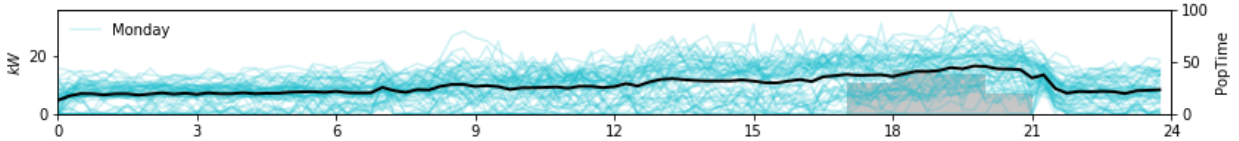

(a) Monday

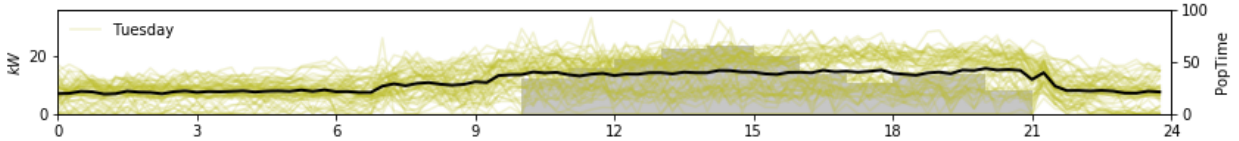

(b) Tuesday

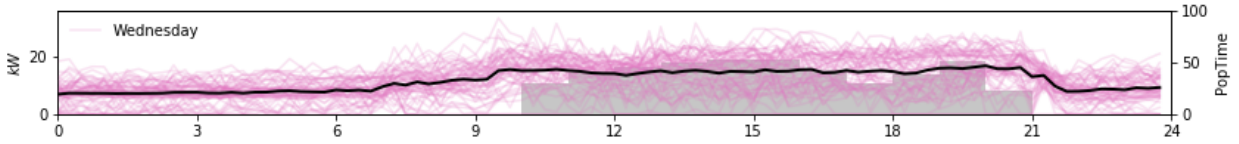

(c) Wednesday

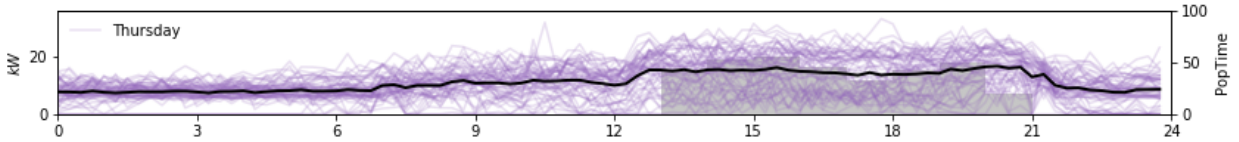

(d) Thursday

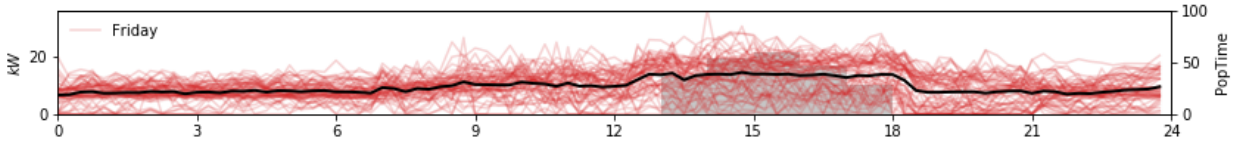

(e) Friday

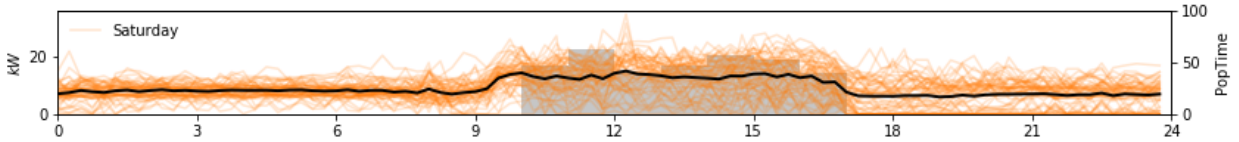

(f) Saturday

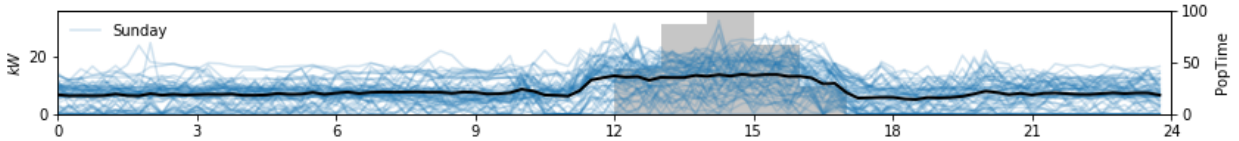

(g) Sunday

Figure 5.3: Electrical consumption without HVAC per day of week with Google Popular Times overlayed on secondary axis.

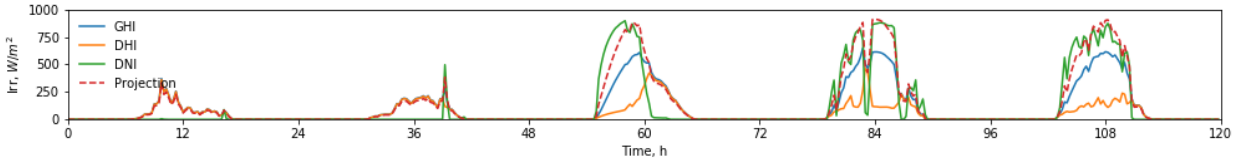

(a) Solar radiation and projection

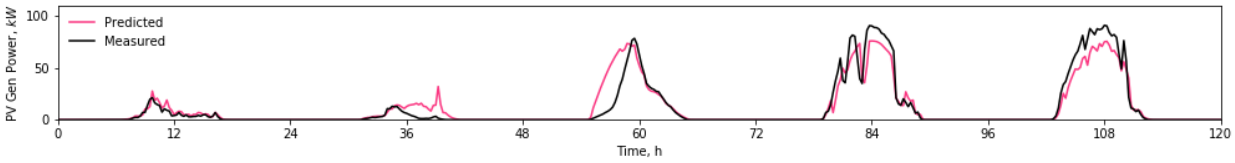

(b) Photovoltaic power generation: predicted and measured

Figure 5.4: Linear PV AC production model using projected solar radiation data.

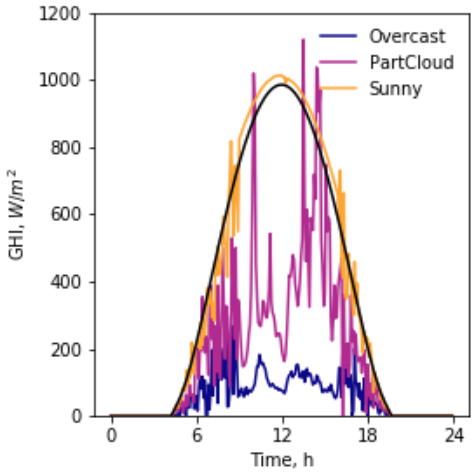

Figure 5.5: Sample of three types of days and base clear day profile in black.

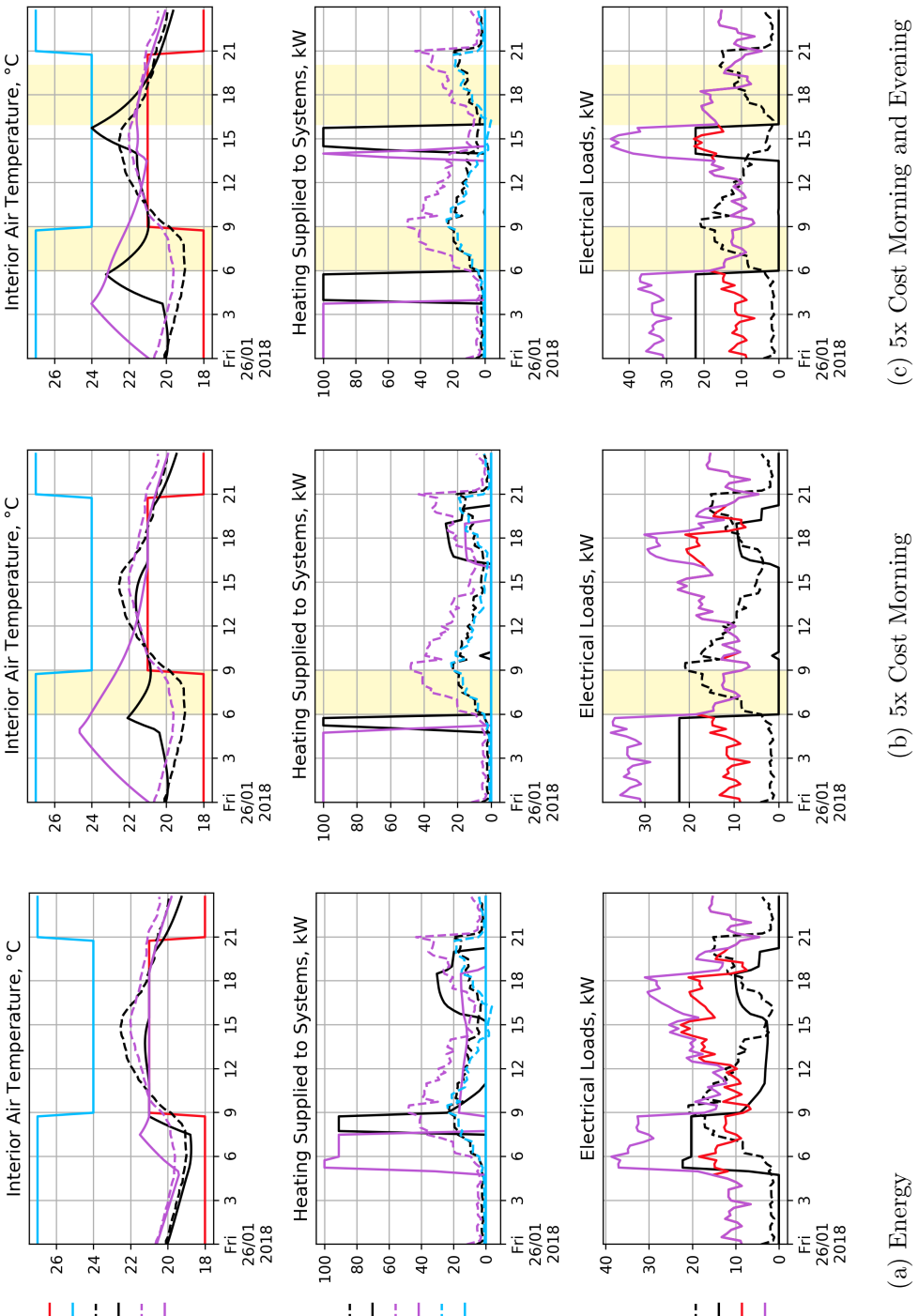

(a) Energy (b) 5x Cost Morning (c) 5x Cost Morning and Evening

Figure 5.6: Energy and power minimization.

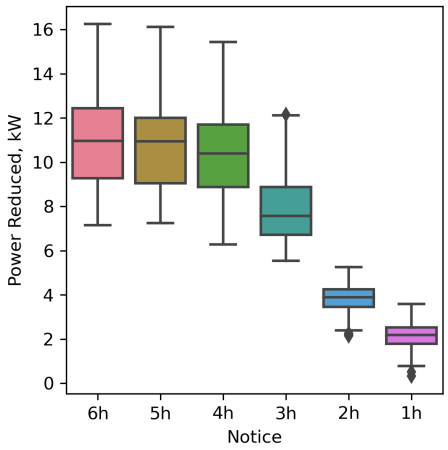

Figure 5.7: Electrical power demand reduction achieved in the morning peak period given notice to the building. A notice of 4 hours and more yields maximal reduction in morning power demand. 100-sample per notice runs for Friday January 26, 2018 – sunny.

5.4.4 Peak Power Reduction Given a Notice

However, the utility may not always promptly share when the electricity price is increased: it may simply give a short notice. To simulate this case, we ran the above cost function but starting at a different time in the night. The measured condition at that time was used as the initial value in the MPC problem. The amount of peak power reduction given the hour of notice is shown in Figure 5.7 for a case where all exogenous inputs are noised, including the weather, solar radiation and consumption. As more notice is given, the more the peak can be reduced. Given more than 4-hour notice marginally improves the results; a minimum of 3 hours is desired. From this box and whisker plot, we can state that a certain peak power demand can be reduced for a certain percentage of the time, *e.g.* if a 3-hour notice is given, around 7 kW of power can be saved 75% of the time (see box end – 25^{th} quantile) and at worst, a saving of just below 6 kW (see whisker end – minimum value). Overall, for this building, the full benefits of demand response can be achieved if at least a 5-hour notice is given; 89% for a 4-hour notice; 61% for a 3-hour notice; and very little benefits for shorter notices without compromising comfort.

5.4.5 Profile Tracking

To test the energy flexibility of the building, we will minimize the norm of the difference between the overall electrical energy consumption of the building – HVAC and non-HVAC combined – and a demand profile, see Equation 5.4. As an example, a sinusoidal demand profile is used that peaks at noon with a mean of 20 kW, an amplitude of 5 kW and a period of 2 per day, see Figure 5.8a. The room temperatures stay within the comfort bounds and the HVAC equipment is cycled so that the total electrical consumption approaches the desired profile – see bottom subplot. In a dynamic pricing event, the demand profile may look similar to the simulated profile with curtailment events around noon and demand response in the mornings and evenings. A low price of electricity near midnight can be translated in a higher demand profile to track. The sine wave can be interpreted as an approximation of an inverted duck curve.

Considering the renewable energy production following Equation 5.5, the total net electrical consumption does not perfectly match the profile during the day, see Figure 5.8b. The HVAC system maximum capacity is reached at approximately 100 kW thermal representing a 28.5 kW electrical load. The spaces and slab are heated much more than needed and the residual heat may reduce the morning start-up energy required for the following day. Any excess power during noon must be exported to the grid and is credited for up to 50 kW according to the current agreement.

In a more basic case, to limit the grid interaction of the library and to promote self-consumption, the demand profile can be set to 0 kW throughout. Figure 5.8c shows the result where the room temperatures are brought to their upper limits and the heat pump is operating at full capacity as soon as there is solar availability. Instead of exporting excess electricity to the grid, the MPC solution heats the library to reduce the evening heating demand.

This approach is sensitive to the following predictions: exterior temperature which drives the heating demand, solar availability which drives the renewable energy production, and occupancy plug loads which drive consumption. Instead of using idealistic and perfect predictions, a noised and sample-driven approach is employed in the following subsection.

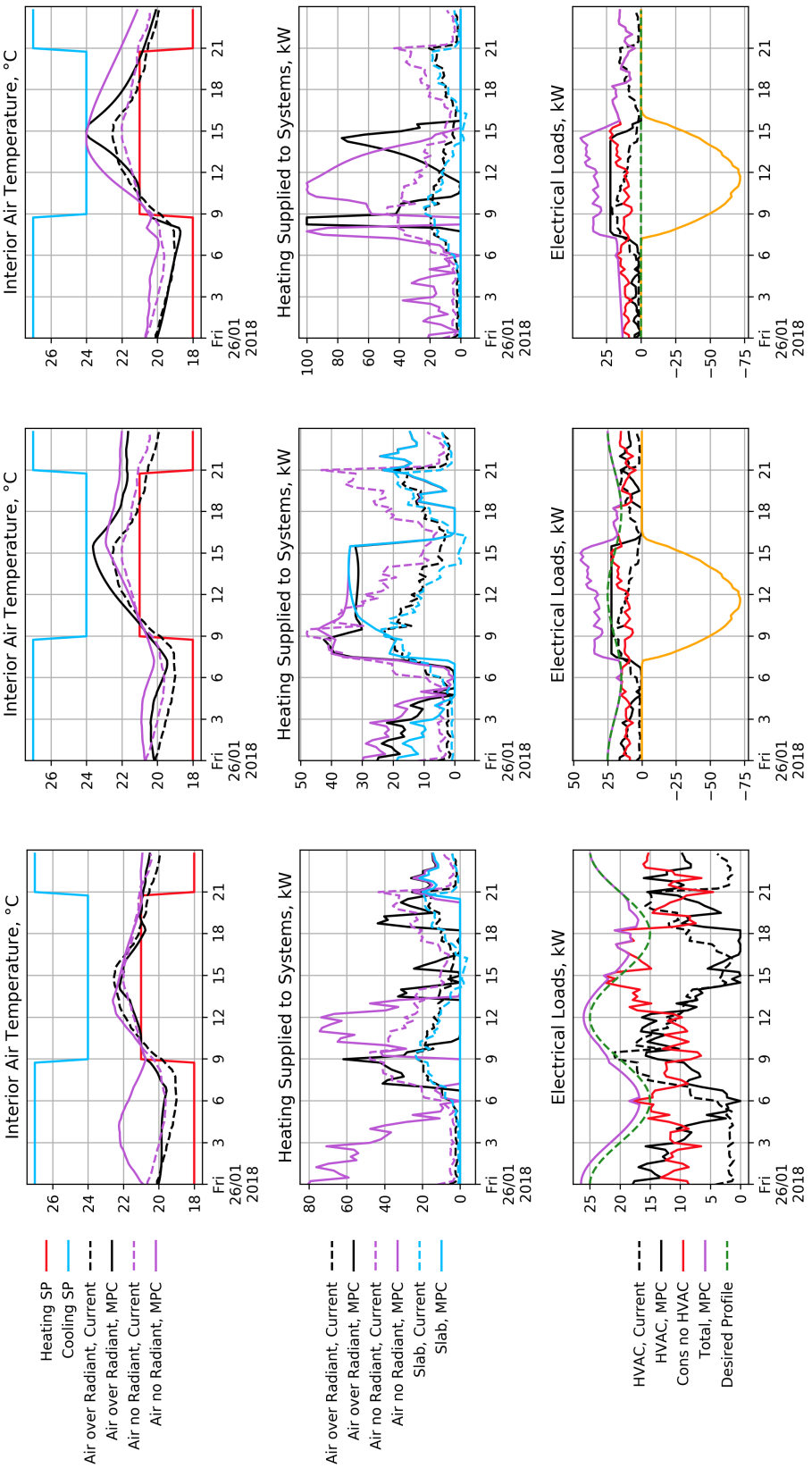

(a) Flexible Profile (b) Flexible Profile with PV (c) Self-Consumption

Figure 5.8: Profile tracking.

5.5 Noised MPC

In this section, we consider four alternatives to the self-consumption cost function: for the HVAC system to consider the photovoltaic production or not, and to either use norm-1 or norm-2 on the cost function.

Fully-noised exogenous inputs and model parameters are used. The noised MPC problem is solved using an iterative sample-based approach. During an initial *burn-in* period, the action profiles between iterations are independent. After this period, the action profiles are averaged, and weighted exponentially based on recency, see Equation 5.7. To assure stability, the norm of the difference between action profiles of a current and past iteration are bounded. For the thermal comfort budget, it is restricted to its final value during the burn-in period. After which, it is set to a large value and decayed with the number of iterations, see Equation 5.8. The thermal comfort budget is a slack variable for comfort: it provides some flexibility in operation and is used to allow the optimization problem to be feasible if initial temperature is outside allowed limits. The bounds are restricted with the number of iterations to obtain a robust profile. Once the number of runs is exhausted, the actions within the control horizon is applied.

A robust MPC result would maintain the temperature of the air a little above the setpoint temperatures given the effect of exterior temperature on the space. If the temperature is too close to the setpoint, a sudden drop of exterior temperature can lead to discomfort. When the controls have converged, they are applied to the best-fit model of the building using the recorded exogenous inputs to simulate the behaviour of the actions and the resulting space temperatures.

$$\begin{aligned} \left\| u^k - u^{k-1} \right\|_2 &\leq \gamma^k \alpha_{\text{dist}} \\ u^k &= \frac{\sum_{i=0}^{k-1} w_i u^i}{\sum_{i=0}^{k-1} w_i} \end{aligned} \tag{5.7}$$

$$s_{\text{comfort budget}} = \begin{cases} s_{\text{min comfort budget}}, \text{if } k \leq \text{burn-in period.} \\ \min(s_{\text{min comfort budget}}, \gamma^k s_{\text{initial comfort budget}}), \quad \text{otherwise.} \end{cases} \tag{5.8}$$

Where,

u^k weighted control variables at iteration k,

γ relaxation factor,

$\alpha_{\mathbf{dist}}$ allowed distance in norm-2 of control variables,

w weight, and,

s slack variable for comfort budget or minimum comfort budget.

This approach is demonstrated for the week starting on January 22$^{\text{th}}$, 2018, optimizing on a 12-hour prediction horizon and applying controls on a 15-minute control horizon. A total of 50 samples are drawn from which 20 are for the burn-in period. After the burn-in period, the comfort slack variable and action profile difference norm bounds are decayed per iteration until a lower limit. In the following section, results for the winter period are reported. Figure 5.9 shows the sampled exogenous inputs starting from 6AM and extending for 12 hours. The prediction horizon is 12 hours and the extra hours are shown to better understand the evolution and divergence of the exogenous inputs as predictions are extended.

Although the MPC is run starting midnight, we show the results for 8:45 and 9:00PM for brevity in Figure 5.10. Here, the convergence of the action profiles and their respective temperature profiles are plotted. Pale lines in pink show the burn-in samples whereas the black lines represent the samples afterwards going from pale to dark for the later iterations. The blue line represents the action profile taken in the previous control horizon and the red line represents the action profile to be taken. If the blue and red lines remain close to each other, the final action profile from the previous iteration has been shown to be stable for two control horizons so the algorithm is considered sufficiently robust. The inverse signifies that the arrival of new information requires the action profile to change for the building operation to remain optimal. This situation has been observed when moving from 8:45 to 9:00PM since the prediction horizon is 12 hours, the controls at 9:00PM see the setpoint change at 9:00AM the following day. This information affects not only the immediate actions around 9:00AM but also actions prior resulting in a linear ramp setpoint profile. The optimal control profile from 8:45PM is relatively flat comparatively, showcasing the advantage of predictive

controls over their reactive counterparts and how the linear ramp was discovered through optimization.

The final result of the power consumption, production and the corresponding temperature progression is shown in Figure 5.11. The control profiles and time progressed as would be in a real application. In this figure, the temperature are tending to be between the heating and cooling setpoints for the south zone but closer to the higher limit during noon. This is due to the MPC favouring over-heating the space to consume more energy during noon when production is increased exporting less to the grid while remaining closer to the lower limit during the morning and evening. For the north zone, the space temperature remains warm throughout. During days with less sun – shown by a decrease in solar PV production – the temperatures are closer to the lower bound since there is no excessive production to warrant overheating a space. The setpoints seem to be violated at the opening and closing hours, but it is in fact the comfort slack variable being fully utilized, and so comfort is attained for the full simulated period for all cases.

Heating is applied to all 3 thermal nodes to minimize grid interaction. The radiant slab's temperature does not seem to fluctuate greatly. It is likely that the collected data does not span the whole range of operation so it is therefore difficult to get an accurate calibration to model the slab. A stronger excitation would be needed to properly characterize the slab. A similar excitation can also be beneficial for refining the other parameters. By applying MPC to a building, its operation changes and the collected data distribution shifts and widens. The new data would be used to enhance the accuracy of the building power and thermal state estimation, which in turn would improve the results from the MPC algorithm.

5.5.1 Current Operation and MPC

One of the key challenges in this type of study is comparing a proposed control strategy or policy with what is currently being used, or base case. The building model, regardless of the type used, is calibrated based on available data. The data is *generated* following a prior control strategy and although can be abundant, it needs to cover a larger domain space, in other words, to have more variance. If the building has always operated a certain way, how can we assure that the MPC policy will lead to the calculated savings? One method

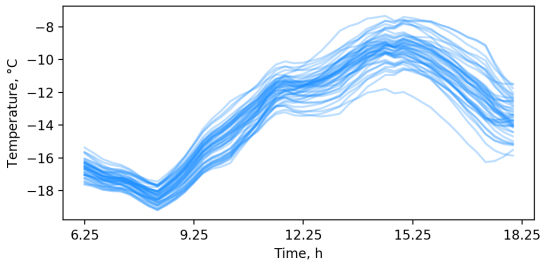

(a) Exterior temperature

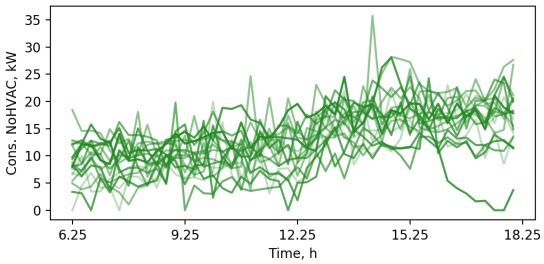

(b) Electricity consumption without HVAC

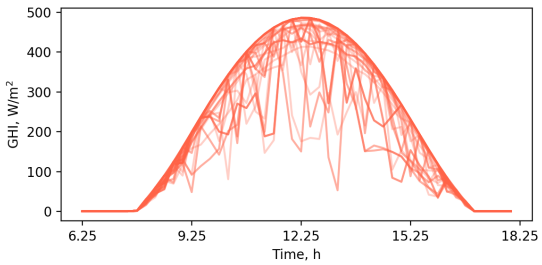

(c) Global horizontal irradiance

Figure 5.9: Noised exogenous model inputs, from 6AM to 6PM, 50 samples.

would be to compare the distribution of actions taken by both approaches and calculate the Wasserstein distance (W_D) between the two, see Figure 5.12. This distance metric shows the minimal amount of area required to move to turn one distribution into the other. In this case, it represents how much energy needs to be displaced to match one strategy to another. An analysis window of one week is used to get a more representative comparison since MPC may act earlier and is consuming more energy during high solar gain periods to minimize grid interaction. A large value signifies that how we are operating the building is vastly different than the conventional controls. Running an MPC algorithm while bounding this metric would allow the control policy to be gradually shifted from current operations towards optimal operations; it would also limit how much the model would tend to extrapolate. This, however, remains an approach to explore in a future work. The results show that the north zone is under utilized in the existing operation. Temperature distributions are shown for the analysis period in Figure 5.13 and show a bimodal distribution where the peaks represent the minimal unoccupied and occupied setpoint temperatures, thus the MPC algorithm tends towards the limits to best minimize energy use.

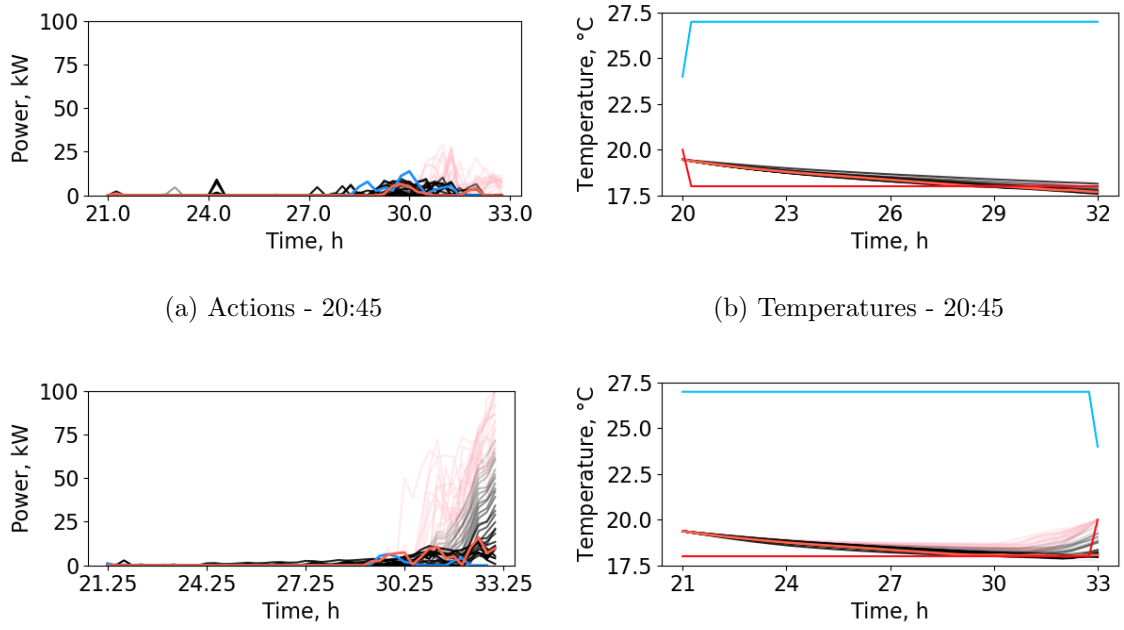

(a) Actions - 20:45

(b) Temperatures - 20:45

(c) Actions - 21:00

(d) Temperatures - 21:00

Figure 5.10: South zone air over radiant slab action profile iterations and resulting temperatures, day 2 of January 22, 2018 week. Upper blue and lower red lines are the comfort limits, pink lines are the burn-in profiles, black lines are the iterated profiles, bright red line is the converged profile and light blue line is the previous timestep's converged profile.

The analysis was repeated to cover the winter season starting January 1st, 2018 – solar data was not available prior to this date and would lead to an incomplete analysis. The strategies are compared and summarized in Figures 5.14 for profile tracking for the two norms as well as with or without the HVAC considering renewable generation. MPC can reduce the consumption of the building and, although it uses more power, it is not billed for it – the utility rate charges for power above 50 kW. Net consumption bar charts are shown in Figures 5.15 where it can be seen that the strategy not considering renewable production does not fully utilize this generation: in cases with PV, the power consumption is increased during full production to limit grid interaction and improve self-consumption shown by a decrease in the net consumption chart.

Overall, the proposed MPC strategies can reduce the energy consumption by 10-12% globally for the winter period without modifying or learning occupancy profiles. We anticipate

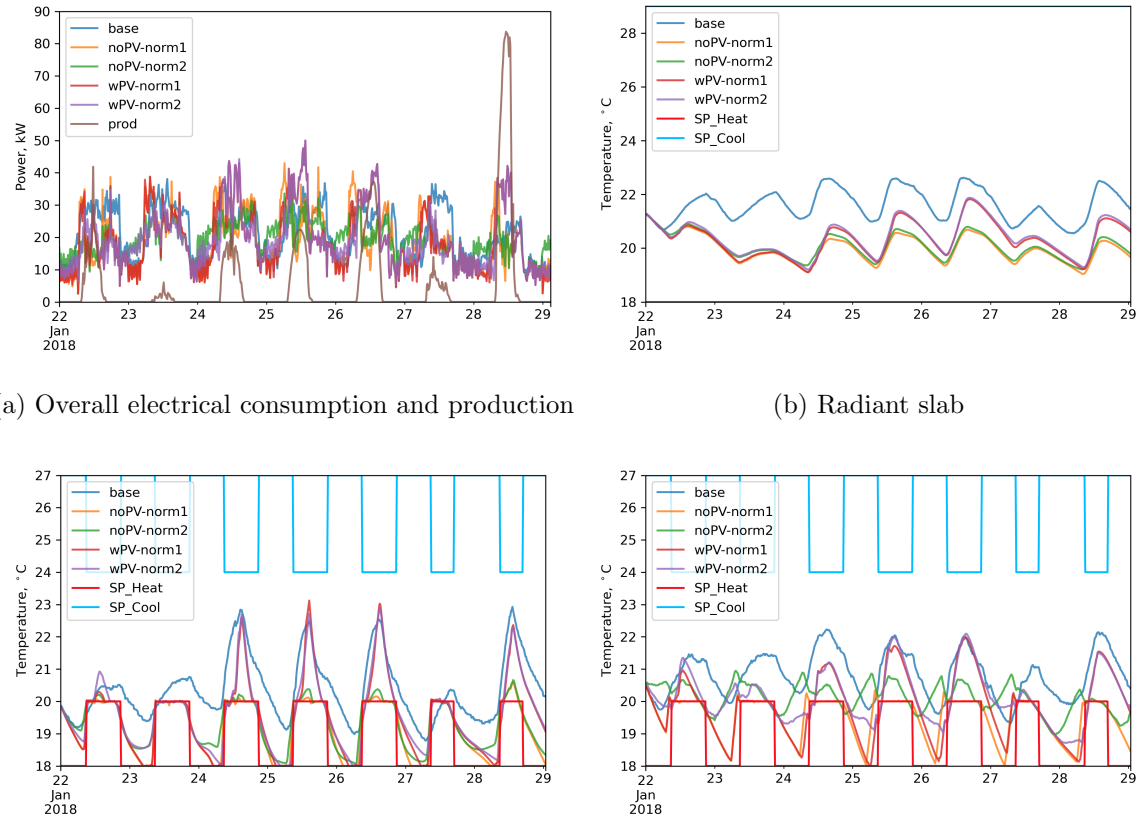

(a) Overall electrical consumption and production

(b) Radiant slab

(c) South zone air over radiant slab

(d) North zone air

Figure 5.11: Resulting power and temperatures given day progression over a week for a 15-minute control horizon and 12h prediction horizon.

greater savings if lighting would also be controlled. Additionally, varying the profile will vary the behaviour. For demand response, the profile can be altered to penalize grid import during this event. Conversely, for curtailment events, the profile can be modified to penalize grid export and incentivize import.

5.6 Discussion

By applying a sampled-based approach, we need not assume a distribution on the uncertainties of the inputs. Using an iterative method of action convergence does help with robustness but work is required to quantify and provide bounds. A true robust strategy would need to optimize over all uncertain instances for a sample-based approach or over the

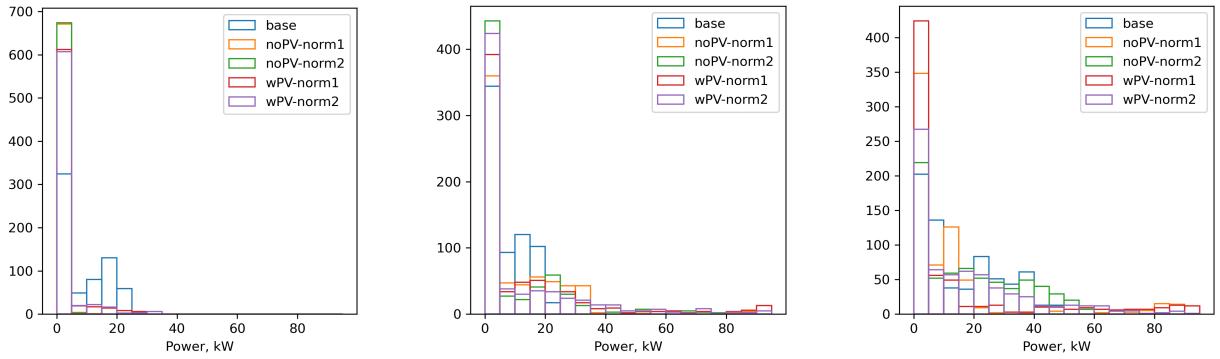

(a) Radiant slab $W_D : 7889, 7991, 6610, 6707\ kWh$

(b) South zone air over radiant slab $W_D : 7372, 5975, 8307, 7557\ kWh$

(c) North zone air $W_D : 11077, 4002, 11892, 4027\ kWh$

Figure 5.12: Heating power distribution for analysis period week of 22 January 2018: current operation and MPC. Wasserstein distances given in legend order compared to the base case.

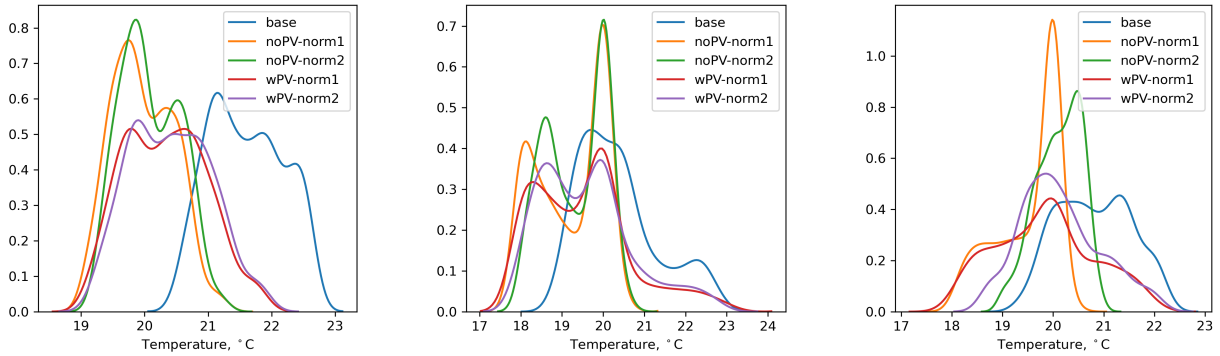

(a) Radiant slab

(b) South zone air over radiant slab

(c) North zone air

Figure 5.13: Temperature distribution for analysis period week of 22 January 2018: current operation and MPC.

distributions which leads to an explosion in the number of equations in the optimization. The resulting will likely be infeasible or certain strong assumptions would need to be made on the distributions. For a practical application in buildings, the proposed method would be sufficient and advantageous over conventional approaches. Finally, comfort was maintained by enforcing a setpoint profile and a small comfort budget slack variable.

A limitation here is that the model is at a system level and not at the component level.

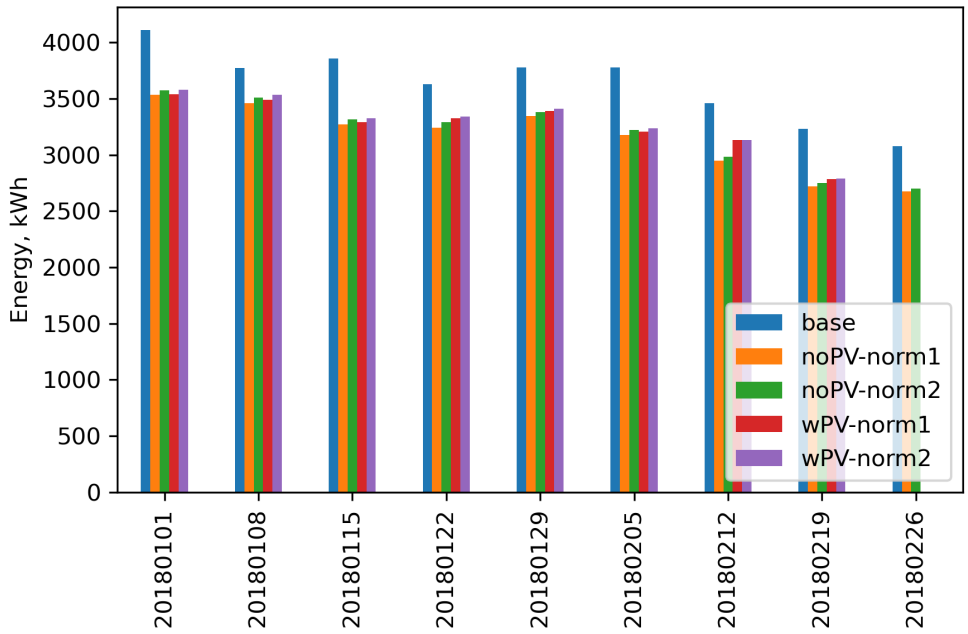

(a) Energy

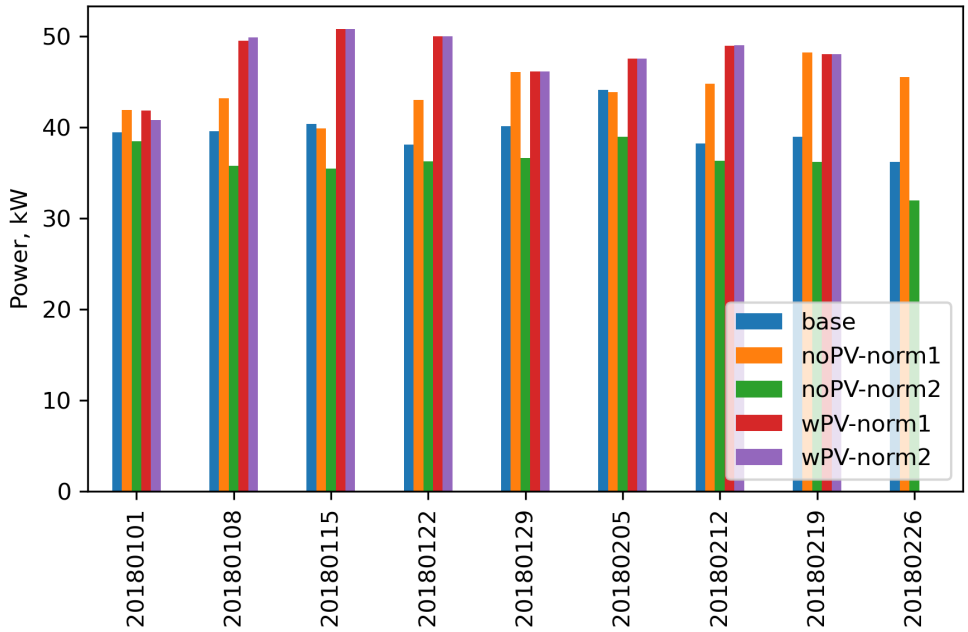

(b) Power

Figure 5.14: Weekly consumption where HVAC considers renewable production or not using norm-1 and 2.

The actions output would need to be translated to supply water temperature setpoints or

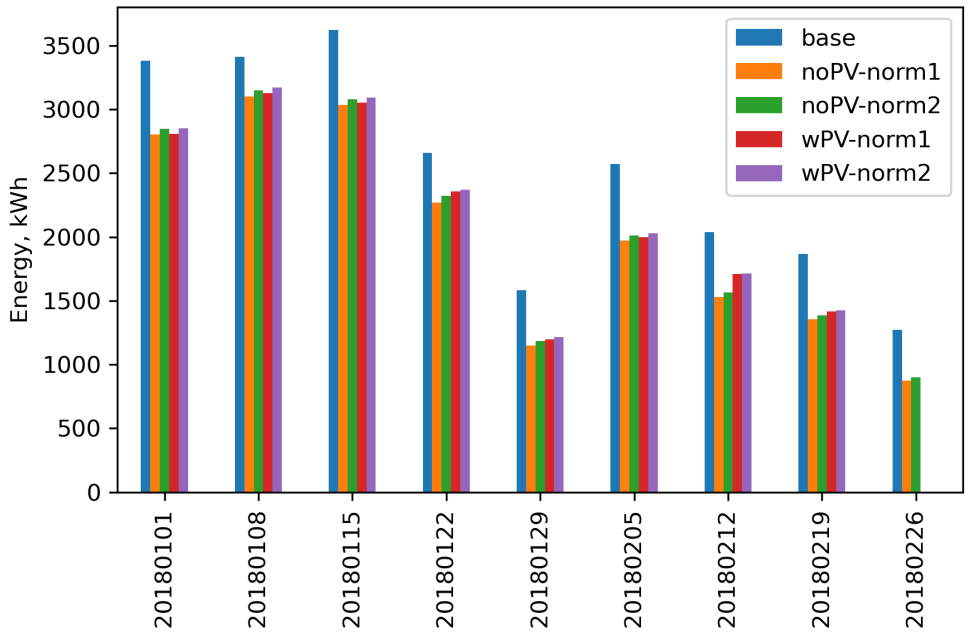

(a) Energy

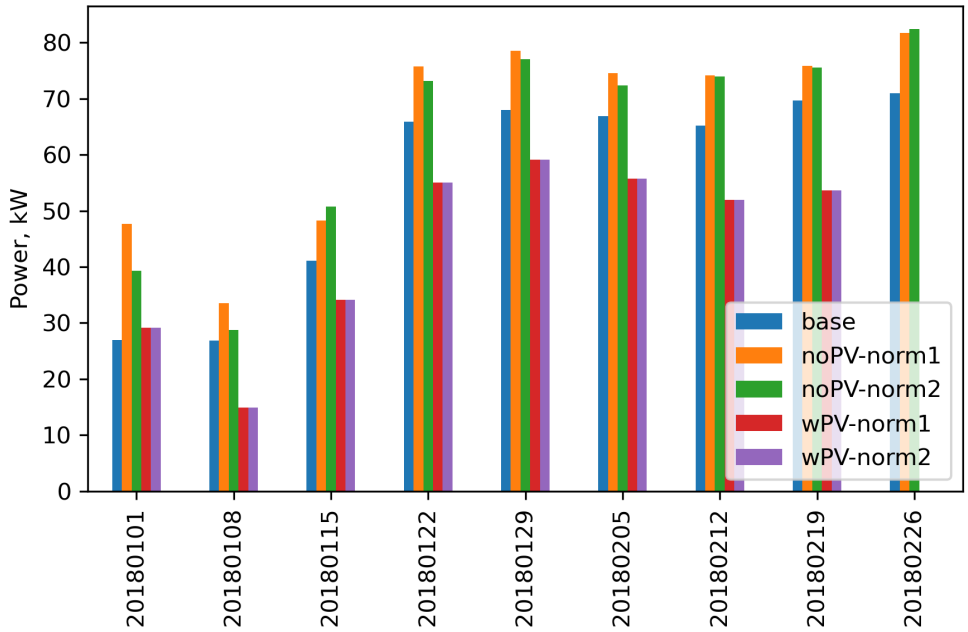

(b) Power

Figure 5.15: Weekly net consumption minus production where HVAC considers renewable production or not using norm-1 and 2.

other. The end components would use the water as needed since the MPC does not consider pump, fan, valve or damper operation. Should the components and their PI/PID controllers be in the MPC loop? This would result in a non-convex optimization. The MPC formulation matches the data collection timestep of 15 mins but controllers are running at much faster rates of multiple scans per second. A hierarchical approach can be used where the MPC algorithm decides the water loop temperatures, operational limits or budgets. It may also be used to update the K_P, K_I and K_D gains on the PI/PID controllers as a macro adjustment.

A bounding weather period is used in the case study. If savings can be achieved for these days and season, savings can be achieved for the rest of the year. To get accurate numbers, a higher fidelity virtual building should be used to truly compare a rule-based reactive approach to MPC (Blum et al., 2019). The high-level modelling can be broken down to the zone level. The state-space modelling and MPC approach can be used as-is and the solution should converge within reasonable delay on a modern computer.

The methodology proposed is applied to a building predominantly operating on a schedule. Between predefined times, the building must be set to a comfortable temperature range. The modelling approach is simplified to cover larger areas; in this work, that would signify that this would be used for supervisory-level controls, whereas in a simpler building utilizing rooftop units (RTU) for single zones, the modelling approach can be directly used for controls. A significant portion of commercial and retail buildings in North America are of the slab-on-grade building with RTU archetype and operate on schedules onto which the methodology in this thesis can be applied directly. This approach could be adapted and applied to control a hot water tank or a battery system in a light-weight residential building. Since wood-framed homes do not carry significant thermal mass, predictive controls would not show great benefits. In a much larger community setting with a shared thermal loop, this method can be adapted however the model and exogenous inputs would need to be selected according to what is most influential. In all cases, the time scale can be adjust to reflect the time constant of the system.

For occupancy-driven buildings, such as individual offices or residential buildings, an occupant model would first need to be learned and then input into a state-space model as proposed here. For more complex buildings with many zones or with systems exhibiting

nonlinear behaviour, such as large office towers or grocery stores, the problem can be broken down hierarchically and/or the non-convexities made convex for a given iteration.

The work presented is for the Varennes library which utilizes a photovoltaic array and ground-source heat pumps. The radiant slab system offers some thermal storage but is not a dedicated solution. The resulting controls tend to over heat the space to utilize excess PV production during the day to then reduce electrical consumption. Thermal comfort within the space is the limiting factor and having a dedicated solution will alleviate this limitation.

Depending on the building load profile, there may be a cost-benefit calculation to perform to chose either a thermal storage solution, such as a water tank, a battery bank, or alternatively to charge electric vehicles (EV) or a combination thereof. If the stored electricity will be used to drive a heat-pump outside periods of solar availability, it might be more cost-effective to simply heat or cool water in a storage tank and use the stored capacity when needed. Convex models of water tanks can be formulated with finite difference methods and would remain feasible for MPC. Convex models of batteries can be used if electrical storage is more economical.

There is a constraint on the slab surface temperature and more flexibility can be achieved using dedicated electrical or thermal storage solutions. For the period between January to August 2018, we have performed an analysis for the current operation of the building to size a battery. In winter for the months of January to March, the battery should output 35 kW to satisfy 95% of the cases; 15 kW for 50% of the cases. During the months of June to August, a 26 kW system would satisfy 95% of the cases in summer. The battery should be sized to be around 250 kWh for the building to be 50% grid-independent and 530 kWh for 95% grid independent. A battery system with those specification would not be cost-efficient given the cost of electricity, even if a portion of the power is sometimes exported without compensation.

The alternative would be to store thermal energy instead of electrical by running the heat pumps during solar availability. The HVAC contributes to 35% of the total consumption of the building; therefore, around 35% of the battery would be used to drive the heat pumps for heating and cooling. For the case of 50% grid independence, that would result in 87.5 kWh. By using a design ΔT of 40K, keeping the glycol heat transfer fluid properties of the library

and assuming an average COP of 4, this would require a very large 7700 litre tank volume which would work as a dug-in tank. An alternative would be to rely on phase-change materials or high temperature brick thermal storage solutions. EVs are another option, but modelling a electric vehicles can be more challenging due to the probabilistic nature of arrival and departure times of EV owners.

5.7 Conclusion

This chapter describes ways of applying a noised MPC algorithm to optimize the operation of a NetZEB. The building features a hydronic radiant slab system along with an air system and on-site renewable energy sources. Since the methodology is developed for a complex case, certain systems can be effectively turned off to represent a conventional building.

The methodologies for modelling the exterior temperature forecast noise, the solar radiation noise given predicted cloudiness, a method to sample the building electrical consumption net of HVAC and a state-space model used in a model-based predictive control framework are detailed. Multiple cost functions are given for several uses: energy reduction, peak reduction via an increased cost of energy during a period, analysis of peak reduction given a notice from the utility, a flexible profile to alternate the consumption of the building with and without considering the renewable energy production. Given the comfort budget, it was observed that the temperatures were maintained between the desired boundaries within the enforced tolerances. Lastly, given all uncertainties, a method is given to select an action profile that would attempt to be robust to the exogenous input uncertainties. These uncertainties are not assumed to be normal. The model parameter weights can also be noised by fitting the model with different data and having a range for all the parameters. The system-level coefficient of performance of the HVAC system can also be fine-tuned to be variable depending on the ground temperature, however, our measurements do not show a large enough variation to justify further analysis. If the heat-pumps were air-sourced, this analysis should be done since a strong correlation does exist.

This study was for the winter season where the operable windows must remain shut. For the shoulder seasons and summer, windows can be operated to allow for free cooling strate-

gies. The model would need to include this information since operable windows effectively reduce the effective thermal resistance of the enclosure due to infiltration. Given the state of the windows, the set of model parameters describing the system would be used within the MPC formulation. To choose the optimal window operating schedule, a branching-based optimization would need to be used and remains as a future work.

The methodology proposed is applied to a building predominantly operating on a schedule. Between predefined times, the building must be set to a comfortable temperature. The modelling approach is simplified to cover larger areas. Therefore this methodology would be used for supervisory-level controls.

In this work, the price of electricity is assumed to remain fixed. In a dynamic market, like in a transactive micro-grid, the cost of electricity will be a function of grid availability in both directions. A good strategy will buy electricity when cheap and sell when expensive, whereas an optimal strategy will anticipate the price – and by extension what the rest of the grid will be doing – and act accordingly. The MPC formulation for flexibility herein will attempt to minimize the norm of the net electricity consumption vs. the desired profile. In a dynamic market, this profile alters continuously and the MPC formulation will track it.

The final assumption is that the approach is applied to a calibrated model and not to the actual library. Applying it to the library would require coordinating with the controls company to develop an edge device that can run all the modelling and optimization scripts on one end and be able to push BACnet commands on the other. This would require a substantial resource investment for hardware, software and cloud-based solution development. As planned future work, this methodology may alternatively be applied to a digital twin model developed in EnergyPlus, Modellica or another white-box modelling software.

Lastly, a physics-based model is a causal model and its structure allows for extrapolation, whereas a black-box model is usually a statistical model which tends to fail in extrapolation. Here, extrapolation can be seen as applying actions that go away from the conventional controls. In this work, we rely on the Wasserstein distance to assess how different the controls are. For a future work, this metric can be input as a constraint where the optimal controls will tend to stay within a trusted region and as data is collected, this region would expand and shift gradually.

Chapter 6

Conclusion and Directions for Future Work

Most buildings today are controlled based on schedules and setpoints. The schedules state when the building is occupied or unoccupied. When the building switches mode, the heating or cooling starts to bring the temperature towards comfort. The amount of heating or cooling provided into a space is proportional to the difference between the current and desired temperatures. When the operation mode is switched from unoccupied to occupied, suddenly, this difference becomes significant and the heaters or coolers are turned on at full-capacity causing a surge in power. To reduce this peak, better conventional controls soften this using a ramp.

Many other such rules are written by expert operators to improve the efficiency of buildings. These heuristics are static and need to be updated with time. Most rules seldom make use of weather and occupancy forecasts, nor do they make use of the building's thermal mass, electrical and thermal storage solutions, nor track dynamic electricity pricing. Hiring an expensive controls technician to improve the commissioning of the building does not guarantee continuous savings since static rules need to be updated regularly.

HVAC control systems must be adaptive. The building structure is usually designed to last 100 years. Offices are remodelled closer to every 8 to 10 years, sometimes less. With new tenants come new demands. The original design may not always be accommodating and updates to the system is necessary and can be costly if it needs to be done by an engineering

firm. An adaptive system would learn the new occupancy and guarantee comfort in real-time.

As of this writing, we are in a pandemic. We are experiencing a shift of conventional office work into more flexible agreements. The need for adaptive systems have become essential to minimize the cost burden of operating buildings assuming full capacity when this will no longer ever be the case. The addition of IoT sensors backed by advanced analytics, modelling and artificial intelligence is necessary.

A challenge that lies to aid adaptive methods is to make discovery of the building mapping and systems hierarchy. A solution would be to rely on a standardized tagging or naming ontology like Haystack 4[1] (Haystack, 2020) and Brick[2] (Balaji et al., 2016; Brick, 2020). Being able to automatically map a building without requiring sifting through construction plans will greatly aid in the widespread adoption of optimal controls in buildings. Incorporating virtual meter information, such as heat flux into a space, or effective COP of a chiller, within smart BACnet objects will simplify modelling and automated fault-detection. Lastly, current day controllers are designed to be robust for low-level applications and they simply do not possess the computational power or memory to perform optimization and advanced analysis; thus more powerful systems or cloud-connected edge devices are necessary to carry out the computation.

The utility is transforming. End users are turning from passive consumers to prosumers and playing an active role by injecting energy from distributed renewable energy sources such as solar panels installed on the roof or from on-site batteries. The utility is becoming a transactive market. Future work will need to address how buildings would operate on a dynamic grid to, besides providing for its occupants and owners, can play an active role in grid regulation. Research to enable a cluster of intelligent buildings to provide ancillary services to redress utility load ramps and valleys reducing the reliance on polluting gas-turbine peaking plants and their associated maintenance costs, and to assure a robust operation and a clean environment for the generations to come.

The International Energy Agency's (IEA) Energy in Buildings and Communities (EBC) Program put forth a new research annex called "Annex 81 - Data-Driven Smart Buildings"[3]

[1] `https://www.project-haystack.org/`

[2] `https://brickschema.org/`

[3] `https://annex81.iea-ebc.org/`

where the end goal is to derive software to ease the development of control-oriented models to be applied in buildings. The annex covers methods of data collection using low-cost techniques, derive models, derive control applications, and drive the adoption rate through case studies, business model propositions, and result dissemination. The objective is also to provide case studies for Brick and to combine it with standardized building controls languages. Validation work is also conducted to have a standardized framework to compare various approaches – including proposing energy modelling as a data science Kaggle challenge[4] (unpublished work), see chapter 2. Collaboration in this Annex is planned and would allow the proposed methods in this thesis to be applied to many other similar type buildings. Additionally, the Varennes library would be a Canadian case study building to test Haystack and Brick ontologies with the standardized controls language.

By using a model-based predictive control method, we can *explicitly* state what we want to maximize (comfort) and minimize (cost, greenhouse gas emissions) and what are the limits to respect (equipment use, cycling). Rule-based methods are *implicit* in their intent offering no guarantees in performance without being fine-tuned continuously.

In this thesis, the objective was to demonstrate a methodology of optimally controlling a NetZEB to reduce its grid interaction under uncertainty. The approach taken was to use a model-based predictive control framework which requires a model of the system being controlled. The focus in this thesis is to analyze the behaviour of the building at the utility and plant level and see how it compares to other buildings of the same archetype according to Canadian and American national statistics.

A linear time-invariant resistance-capacitance network was designed, calibrated on collected data, validated and used. Reducing the number of inputs is reported to improve the accuracy of models. Here, the collected trendlogs from the building automation system (BAS) is transformed to physical quantities using domain expertise: heat flux, area-weighted temperatures, and so on, which are agnostic to the building. Grey-box models of different orders were reported to have worked better for certain applications over black-box approaches. Here, 3 different orders are designed that capture different phenomena. Higher order models can be used to increase accuracy but they tend to result in higher uncertainties because of

[4] `https://www.kaggle.com/c/ashrae-energy-prediction`

having more degrees of freedom.

Linear and nonlinear model fitting algorithms assume parameters to be independent and typically to follow a Gaussian distribution. These assumptions guarantee high performance. However, in building science, the effective conductance of a wall is not independent of the effective capacitance of the building and cannot be dealt separately. In this work, a fitting algorithm is used to determine the model parameters which are then used as priors to be refined using a Monte-Carlo posterior estimation method. Although the model architecture was simplified, distributions over the parameters were used to emulate an ensemble. For comparison, a physics-free approach of the same order was used and we showed that the addition of physics greatly improved the accuracy of the models.

Exogenous inputs were also modelled. Services providing weather forecasts do not give their uncertainty ranges and literature only supplied sparse values. These ranges had to be estimated based on collected data by comparing predictions with what eventually occurred. These distributions serve to add noise to future ambient temperature predictions to obtain control sequences robust to uncertainties in these forecasts. Solar cloudiness was also modelled based on a clustering-based approach where the raw radiation data was normalized according to a clear-sky model. We determined that 3 cloudiness groups was sufficient to have a realistic case which represented: clear sky, partially overcast and fully overcast conditions. In an application, the sky type would need to be forecast for the day and this model would be sampled to obtain likely solar radiation profiles. Lastly, for the electrical consumption of the building not including the HVAC system, we simply sample a historic profile based on the day of the week.

Optimization literature prefers models and constraints to be convex to assure quick and reliable convergence to a minima and provide guarantees on the primal problem via the dual. Cost functions of MPC can be tuned to the end use ideally as long as it is convex. Many papers have minimized energy or operating costs. In Quebec, the operating cost also includes the price of the peak energy demand[5] which can be represented as a 1-norm on the

[5]Buildings are charged for their maximum power occurring in a 15-minute window for the given month – for Hydro-Québec. Electrical plans are continuously changing and the reader is encouraged to read and understand their local utility plans.

energy within a prediction horizon, which is convex. The cost can be extended to describe energy flexibility and grid interactions – a sum of convex functions is convex. Both model and exogenous input are sampled and the MPC problem is solved multiple times where the optimal control profile is converged towards a robust optimal iteratively.

System modelling, exogenous input modelling, the MPC cost function and constraints were derived for the Varennes library case study however remain general and generic for most any other case. The profile-tracking cost function – see Equations 5.4 and 5.5 in section 5.4 – is very flexible and allows the desired profile to be set by the utility. Other cost functions were also demonstrated as well as the case of determining the minimal notice required for the building to react to a demand response signal. The MPC formulations showed a reduce energy and power demand while promoting self-consumption of the on-site renewable PV power production. The contributions herein include the methodology, proposed metrics and visualizations, general MPC cost functions and how to approach MPC using a sampling-based method.

Salient research using reinforcement learning (RL) is being published and shows great potential to be applied in building operation. We have used it in a previous study (Dermardiros et al., 2019) but found that certain constraints had to be softened and included in the reward/cost function. This makes the problem multi-objective where electrical cost must be weighted against the other constraints. In MPC, constraints need not be softened into the cost function; if needed, they can be softened using a slack variable. Thus, the cost function can remain strictly as dollars or energy.

As future work, there are many avenues left to explore. In chapter 4, we determined that 3-4 weeks of training data was sufficient to train a model. In an application, automatically calibrating the model as new data is collected or if the model accuracy drops below a threshold. To mirror the system one-to-one, we would match the order of the model to the number of zones. In this case, we would be constructing a virtual twin of the building and would need to include the states and flowrate of the pumps and fancoil states and would result in a high-fidelity model where saving estimates would be more accurate.

The digital twin method can be applied for other buildings that were designed using BIM where the architectural, mechanical and electrical details can be extracted and parsed into a

simplified model. Tagging and describing the HVAC system using Brick could also be used to simplify the application of MPC or other advanced control methods, such as RL.

RL can be applied to the Varennes library too. RL is stochastic by design and would implicitly learn the various uncertainties, however it requires many samples to converge onto an acceptable control policy. The digital twin can serve as a virtual environment to train such a model. A future work can consider using RL with safety bounds and a rollout policy method (Gamble and Gao, 2018) which seems to be at the intersection of MPC and RL.

Since typical controllers installed in buildings do not contain strong processors, an edge device would be required to pass cloud-calculated optimal profiles to the BAS. The design and use of this sort of device remains a boutique application. A local computer able to communicate with the controllers, for example using BACnet, is an alternative option for clients not wanting to open their building network to the Internet and potentially be at risk of cyber-attacks.

Alternatively to a computer sending control profiles to each controller, various cases can be solved offline and these solutions can be simplified into decision trees – if-then-else logic perhaps with a clustering pre-process step – which can be run directly on BAS controllers. Here, the computer would update the weights and parameters on the controllers from time to time. This would be the simplest approach that would not interfere with the controllers' internal logic.

Lastly, in chapter 5 section 5.5, we analyze the difference between the MPC-proposed controls vs the current operation of the library through the Wasserstein distance – also called the earth mover distance. The Wasserstein distance can be added as a constraint to the MPC formulation to limit actions that diverge the system behaviour too far away from the conventional controls to stay within a trusted region. As more data is collected, this region would expand, shift and gradually allow the system to approach a safe optimal policy.

The far-reaching goal is to optimally operate the built environment to improve comfort within buildings and reduce our impact on the environment through the reliance on renewable energy sources. Through better understanding the occupant, better data collection through IoT devices and sensors, through better analytics and leveraging domain expertise mixed with machine learning tools for modelling and controls, through better system design, integration

and inter-building energy distribution networks and, finally, through better utility energy and communication platforms integrating grid-level renewable power generation with electrical storage – chemical or potential and either centralized or distributed virtually through a network of grid-connected electric vehicles – I believe we can make a net-positive difference.

6.1 Thesis Contributions

The contributions of the thesis are listed below:

1. Approach and analysis methodologies applied to a net-zero energy building: Chapter 3.

2. A novel approach to analyze building data to derive quantities/features suitable to calibrate a low-order model offering a scalable and mass-applicable approach. The model and data pre-processing are derived together: Chapter 4 sections 4.3.2 and Appendix B.1. Calibration metrics suitable for longer prediction horizons with a visualization to assess stability are developed: Chapter 4 section 4.3.3.

3. The design and selection of a low-order model based on the system characteristics is performed: Chapter 4 sections 4.3.4, 4.3.5, 4.3.6 and 4.3.7.

4. A general and generic formulation of applying MPC is proposed. This approach considers model parameters as distributions and uses different sampling models for exogenous inputs: ambient temperature, cloudiness based on day types and consumption based on day of week. See: Chapter 5 section 5.4 and Appendix sections B.5 and B.6.

5. A sampling and iterative-based approach is detailed resulting in a robust control profile: Chapter 5 section 5.5.

6. The use of the Wasserstein distance metric to assess how different MPC proposed controls are from current practice; opens an avenue to apply trust-region based controls: Chapter 5 section 5.5.1.

Bibliography

ACEC (2016). Varennes Net-Zero Library. https://www.acec.ca/events_awards/cce_awards/2016/awards_excellence/a6.html. 45

Aduda, K., T. Labeodan, W. Zeiler, G. Boxem, and Y. Zhao (2016, April). Demand side flexibility: Potentials and building performance implications. *Sustainable Cities and Society 22*, 146–163. http://linkinghub.elsevier.com/retrieve/pii/S2210670716300245. 2, 14, 54, 86

Afram, A. and F. Janabi-Sharifi (2014). Theory and applications of HVAC control systems - A review of model predictive control (MPC). *Building and Environment 72*, 343 – 355. http://www.sciencedirect.com/science/article/pii/S0360132313003363. 11, 55

Afram, A., F. Janabi-Sharifi, A. S. Fung, and K. Raahemifar (2017, April). Artificial neural network (ANN) based model predictive control (MPC) and optimization of HVAC systems: A state of the art review and case study of a residential HVAC system. *Energy and Buildings 141*, 96–113. http://linkinghub.elsevier.com/retrieve/pii/S0378778816310799. 32

Amara, F., K. Agbossou, A. Cardenas, Y. Dubé, and S. Kelouwani (2015). Comparison and Simulation of Building Thermal Models for Effective Energy Management. *Smart Grid and Renewable Energy 06*(04), 95–112. http://www.scirp.org/journal/doi.aspx?DOI=10.4236/sgre.2015.64009. 18

Andriamamonjy, A., R. Klein, and D. Saelens (2019, April). Automated grey box model implementation using BIM and Modelica. *Energy and Buildings 188-189*, 209–225. https://linkinghub.elsevier.com/retrieve/pii/S0378778818325878. 24

ASHRAE (2002). Guideline 14-2002, Measurement of Energy and Demand Savings. *American Society of Heating, Ventilating, and Air Conditioning Engineers, Atlanta, Georgia*. 62

ASHRAE (2015). *ASHRAE Handbook - HVAC Applications*. Atlanta, GA: American Society of Heating, Refrigerating and Air-Conditioning. 11

ASHRAE (2016). *ANSI/ASHRAE Standard 62.1-2016: Ventilation for Acceptable Indoor Air Quality*. ASHRAE. 19

Athienitis, A., M. Stylianou, and J. Shou (1990). A methodology for building thermal dynamics studies and control applications. *ASHRAE Transactions 96*(Conf-9006117). 11, 55

Athienitis, A. K. E. and W. E. O'Brien (2015). *Modeling, Design, and Optimization of Net-Zero Energy Buildings* (1 ed.). Berlin, Germany: Ernst & Sohn. 14, 42, 43, 88

Bacher, P. and H. Madsen (2011, July). Identifying suitable models for the heat dynamics of buildings. *Energy and Buildings 43*(7), 1511–1522. `https://linkinghub.elsevier.com/retrieve/pii/S0378778811000491`. 21

Bahakim, S. S. and L. A. Ricardez-Sandoval (2014, April). Simultaneous design and MPC-based control for dynamic systems under uncertainty: A stochastic approach. *Computers & Chemical Engineering 63*, 66–81. `http://linkinghub.elsevier.com/retrieve/pii/S0098135414000040`. 31

Balaji, B., Y. Agarwal, M. Berges, D. Culler, R. Gupta, M. B. Kjærgaard, M. Srivastava, K. Whitehouse, A. Bhattacharya, G. Fierro, J. Gao, J. Gluck, D. Hong, A. Johansen, J. Koh, and J. Ploennigs (2016). Brick: Towards a Unified Metadata Schema For Buildings. In *Proceedings of the 3rd ACM International Conference on Systems for Energy-Efficient Built Environments - BuildSys '16*, Palo Alto, CA, USA, pp. 41–50. ACM Press. `http://dl.acm.org/citation.cfm?doid=2993422.2993577`. 82, 116

Bernal, W., M. Behl, T. X. Nghiem, and R. Mangharam (2012). MLE+: a tool for integrated design and deployment of energy efficient building controls. In *Proceedings of the Fourth*

ACM Workshop on Embedded Sensing Systems for Energy-Efficiency in Buildings, pp. 123–130. ACM. 23

Bertsekas, D. P. (1995). *Dynamic programming and optimal control*, Volume 1. Athena scientific Belmont, MA. 33

Blum, D., F. Jorissen, S. Huang, Y. Chen, J. Arroyo, K. Benne, V. Gavan, L. Rivalin, L. Helsen, D. Vrabie, M. Wetter, M. Sofos, and Y. Li (2019). Prototyping the BOPTEST Framework for Simulation-Based Testing of Advanced Control Strategies in Buildings. 24, 111

Blum, D. H. and M. Wetter (2017). MPCPy: An Open-Source Software Platform for Model Predictive Control in Buildings. San Francisco, CA. IBPSA. 24

Bohlin, T. and S. F. Graebe (1995). Issues in nonlinear stochastic grey box identification. *International journal of adaptive control and signal processing 9*(6), 465–490. 18

Borrelli, F., A. Bemporad, and M. Morari (2012). *Predictive control: for linear and hybrid systems*. `http://www.control.ee.ethz.ch/~stdavid/BBMbook_Cambridge_newstyle.pdf`. 14

Bourdeau, M., X. q. Zhai, E. Nefzaoui, X. Guo, and P. Chatellier (2019, July). Modeling and forecasting building energy consumption: A review of data-driven techniques. *Sustainable Cities and Society 48*, 101533. `https://linkinghub.elsevier.com/retrieve/pii/S2210670718323862`. 21

Boyd, S. (2008). EE364b Lecture 16: Model predictive control. `https://www.youtube.com/watch?v=1A734g96Npk`. 13

Boyd, S. P. and L. Vandenberghe (2004). *Convex optimization*. Cambridge, UK ; New York: Cambridge University Press. 14

Brastein, O., D. Perera, C. Pfeifer, and N.-O. Skeie (2018, June). Parameter estimation for grey-box models of building thermal behaviour. *Energy and Buildings 169*, 58–68. `https://linkinghub.elsevier.com/retrieve/pii/S0378778817331791`. 25

Brick (2020, May). Brick: A uniform metadata schema for buildings. https://brickschema.org/. 82, 116

Bucking, S., A. K. Athienitis, and R. Zmeureanu (2014). Multi-Objective Optimal Design of a Near Net Zero Energy Solar House. *ASHRAE Transactions 120*, 224. http://search.proquest.com/openview/75fbfe3794f5d656afe7672928079b32/1?pq-origsite=gscholar. 15

Bucking, S. and V. Dermardiros (2018, February). Distributed evolutionary algorithm for co-optimization of building and district systems for early community energy masterplanning. *Applied Soft Computing 63*, 14–22. http://linkinghub.elsevier.com/retrieve/pii/S1568494617306580. 7

Bucking, S., V. Dermardiros, and A. K. Athienitis (2016). The effect of hourly primary energy factors on optimal net-zero energy building design. Hamilton, Ontario. 3, 12, 54

Buonomano, A., G. De Luca, U. Montanaro, and A. Palombo (2016, June). Innovative technologies for NZEBs: An energy and economic analysis tool and a case study of a non-residential building for the Mediterranean climate. *Energy and Buildings 121*, 318–343. https://linkinghub.elsevier.com/retrieve/pii/S0378778815302243. 54

Camacho, E. F. and C. Bordons (2007). *Model Predictive control*. Advanced Textbooks in Control and Signal Processing. London: Springer London. http://link.springer.com/10.1007/978-0-85729-398-5. 14

Candanedo, J., V. Dehkordi, and M. Stylianou (2013, November). Model-based predictive control of an ice storage device in a building cooling system. *Applied Energy 111*, 1032–1045. http://linkinghub.elsevier.com/retrieve/pii/S0306261913005047. 23

Candanedo, J. A. (2011). *A Study of Predictive Control Strategies for Optimally Designed Solar Homes*. Ph. D. thesis, Concordia University. http://citeseerx.ist.psu.edu/viewdoc/download?doi=10.1.1.633.1851&rep=rep1&type=pdf. 19

Candanedo, J. A., A. Allard, and A. K. Athienitis (2011). Predictive Control of Radiant

Floor Heating and Transmitted Irradiance in a Room with High Solar Gains. *ASHRAE Transactions 117*(2). 11, 55

Candanedo, J. A. and A. K. Athienitis (2010). Simplified linear models for predictive control of advanced solar homes with passive and active thermal storage. `http://docs.lib.purdue.edu/cgi/viewcontent.cgi?article=1029&context=ihpbc`. 21

Candanedo, L. M. I. (2010). *Modelling and evaluation of the performance of building-integrated open loop air-based photovoltaic/thermal systems*. PhD Thesis, Concordia University. `https://spectrum.library.concordia.ca/979429/`. 88, 152

Cengel, Y. A., A. J. Ghajar, and H. Ma (2011). *Heat and Mass Transfer: Fundamentals & Applications* (4th ed.). McGraw-Hill. 146

Christiano, P., Z. Shah, I. Mordatch, J. Schneider, T. Blackwell, J. Tobin, P. Abbeel, and W. Zaremba (2016, October). Transfer from Simulation to Real World through Learning Deep Inverse Dynamics Model. *arXiv:1610.03518 [cs]*. `http://arxiv.org/abs/1610.03518`. 32

Chwif, L., M. R. P. Barretto, and R. J. Paul (2000). On simulation model complexity. In *Proceedings of the 32nd conference on Winter simulation*, pp. 449–455. Society for Computer Simulation International. `http://dl.acm.org/citation.cfm?id=510448`. 19

Cigler, J. and S. Prívara (2010). Subspace identification and model predictive control for buildings. In *Control Automation Robotics & Vision (ICARCV), 2010 11th International Conference on*, pp. 750–755. IEEE. `http://ieeexplore.ieee.org/xpls/abs_all.jsp?arnumber=5707821`. 21

CNRC-NRC (2015). *National Building Code of Canada*. Canadian Commission on Building and Fire Codes. 19

Coakley, D., P. Raftery, and M. Keane (2014, September). A review of methods to match building energy simulation models to measured data. *Renewable and Sustainable Energy Reviews 37*, 123–141. `http://linkinghub.elsevier.com/retrieve/pii/S1364032114003232`. 20, 29

Coffey, B. (2012). *Using building simulation and optimization to calculate lookup tables for control*. Ph. D. thesis, University of California, Berkeley. https://escholarship.org/uc/item/1202p562.pdf. 26

Coffey, B., F. Haghighat, E. Morofsky, and E. Kutrowski (2010, July). A software framework for model predictive control with GenOpt. *Energy and Buildings 42*(7), 1084–1092. http://linkinghub.elsevier.com/retrieve/pii/S0378778810000290. 13, 26

Costa-Carrapiço, I., R. Raslan, and J. N. González (2020, March). A systematic review of genetic algorithm-based multi-objective optimisation for building retrofitting strategies towards energy efficiency. *Energy and Buildings 210*, 109690. https://linkinghub.elsevier.com/retrieve/pii/S0378778819319462. 29

Denholm, P. and M. Hand (2011, March). Grid flexibility and storage required to achieve very high penetration of variable renewable electricity. *Energy Policy 39*(3), 1817–1830. http://linkinghub.elsevier.com/retrieve/pii/S0301421511000292. 5, 14, 54

Dermardiros, V. (2015). *Modelling and Experimental Evaluation of an Active Thermal Energy Storage System with Phase-Change Materials for Model-Based Control*. Ph. D. thesis, Concordia University. http://spectrum.library.concordia.ca/980456/. 5

Dermardiros, V. and A. K. Athienitis (2015, November). Comparison of PCM-active thermal storage systems integrated in building enclosures. Bern, Switzerland. 5

Dermardiros, V., A. K. Athienitis, and S. Bucking (2019). Energy Performance, Comfort and Lessons Learned from an Institutional Building Designed for Net-Zero Energy. *ASHRAE Transactions 125, Part 1*. 2, 55, 88

Dermardiros, V., S. Bucking, and A. K. Athienitis (2019). A Simplified Building Control Environment with a Reinforcement Learning Application. In *Proceedings of IBPSA 2019, Rome, Italy*. https://github.com/vderm/SimplifiedBldgControlEnv. x, 33, 119

Dermardiros, V., Y. Chen, and A. K. Athienitis (2015, November). Modelling of an Active PCM Thermal Energy Storage for Control Applications. *Energy Procedia 78*, 1690–1695. http://linkinghub.elsevier.com/retrieve/pii/S1876610215019931. 5, 19

Dermardiros, V., Y. Chen, A. Daoud, and A. K. Athienitis (2016). Development of reduced-order thermal models of building-integrated active PCM-TES. *ASHRAE Transactions OR-16-021*, 267–277. 5

Dermardiros, V., C. Vallianos, S. Bucking, and A. K. Athienitis (2017, August). Model-Based Control of a Hydronic Radiant Slab for Peak Load Reduction. San Francisco, CA. xiv, xv, 41, 50, 56, 144, 146, 149

Dhariwal, P., C. Hesse, O. Klimov, A. Nichol, M. Plappert, A. Radford, J. Schulman, S. Sidor, Y. Wu, and P. Zhokhov (2017). OpenAI Baselines. `https://github.com/openai/baselines`. 32

Diamond, S. and S. Boyd (2016). CVXPY: A Python-Embedded Modeling Language for Convex Optimization. *Journal of Machine Learning Research 17*(83), 1–5. 94

DiLaura, D. L., G. R. Steffy, R. G. Mistrick, and K. W. Houser (Eds.) (2011). *The IESNA lighting handbook: reference and application* (10th ed.). Illuminating Engineering. 142

Domahidi, A., E. Chu, and S. Boyd (2013). ECOS: An SOCP solver for embedded systems. In *2013 European Control Conference (ECC)*, pp. 3071–3076. IEEE. 94

Drgoňa, J., D. Picard, M. Kvasnica, and L. Helsen (2018, May). Approximate model predictive building control via machine learning. *Applied Energy 218*, 199–216. `https://linkinghub.elsevier.com/retrieve/pii/S0306261918302903`. 27

Duffie, J. A., W. A. Beckman, and N. Blair (2020). *Solar Engineering of Thermal Processes, Photovoltaics and Wind*. John Wiley & Sons. 90, 161

Dumoulin, R. (2019, April). Integrated Modelling and Analysis of a Heat Pump BIPV/T System with Thermal Storage for Load Shifting. Master's thesis, Concordia University, Montreal, Canada. `https://spectrum.library.concordia.ca/985975/`. xi, 43

EERE (2017, October). Confronting the Duck Curve: How to Address Over-Generation of Solar Energy. `https://www.energy.gov/eere/articles/confronting-duck-curve-how-address-over-generation-solar-energy`. x, 4

EIA (2017, April). Rising solar generation in California coincides with negative wholesale electricity prices - Today in Energy. https://www.eia.gov/todayinenergy/detail.php?id=30692. x, 4

Erickson, V. L., M. Carreira-Perpiñán, and A. E. Cerpa (2011). OBSERVE: Occupancy-based system for efficient reduction of HVAC energy. In *Information Processing in Sensor Networks (IPSN), 2011 10th International Conference on*, pp. 258–269. IEEE. http://ieeexplore.ieee.org/xpls/abs_all.jsp?arnumber=5779043. 30

Fonti, A., G. Comodi, S. Pizzuti, A. Arteconi, and L. Helsen (2017, May). Low Order Grey-box Models for Short-term Thermal Behavior Prediction in Buildings. *Energy Procedia 105*, 2107–2112. https://linkinghub.elsevier.com/retrieve/pii/S1876610217306446. 22

Foreman-Mackey, D., D. W. Hogg, D. Lang, and J. Goodman (2013). emcee: The MCMC Hammer. *PASP 125*, 306–312. 63

Gamble, C. and J. Gao (2018, August). Safety-first AI for autonomous data centre cooling and industrial control. https://www.deepmind.com/blog/article/safety-first-ai-autonomous-data-centre-cooling-and-industrial-control. 120

Garrett, A. and J. R. New (2016). Suitability of ASHRAE Guideline 14 Metrics for Calibration. *ASHRAE Transactions*. 20, 23, 24

Goodfellow, I., Y. Bengio, and A. Courville (2016). *Deep Learning*. MIT Press. 6

Google (2020, May). Places API: Place Details. https://developers.google.com/places/web-service/details. 90

Graves, L. (2017, October). World's cheapest prices submitted for Saudi Arabia's first solar project. *The National AE*. https://www.thenational.ae/business/energy/world-s-cheapest-prices-submitted-for-saudi-arabia-s-first-solar-project-1.663842. 3

Gunay, H. B., J. Bursill, B. Huchuk, W. O'Brien, and I. Beausoleil-Morrison (2014, December). Shortest-prediction-horizon model-based predictive control for individual offices.

Building and Environment 82, 408–419. http://linkinghub.elsevier.com/retrieve/pii/S0360132314003035. 30

Gunay, H. B., W. O'Brien, and I. Beausoleil-Morrison (2016, April). Control-oriented inverse modeling of the thermal characteristics in an office. *Science and Technology for the Built Environment*, 1–20. http://www.tandfonline.com/doi/full/10.1080/23744731.2016.1175893. 22

Haystack (2020, May). Project Haystack: An Open Source initiative to streamline working with IoT Data. https://project-haystack.dev/. 82, 116

Heidarinejad, M., J. G. Cedeño-Laurent, J. R. Wentz, N. M. Rekstad, J. D. Spengler, and J. Srebric (2017, July). Actual building energy use patterns and their implications for predictive modeling. *Energy Conversion and Management 144*, 164–180. https://linkinghub.elsevier.com/retrieve/pii/S0196890417303096. 21

Henze, G. P., A. R. Florita, M. J. Brandemuehl, C. Felsmann, and H. Cheng (2010). Advances in Near-Optimal Control of Passive Building Thermal Storage. *Journal of Solar Energy Engineering 132*(2), 021009. http://SolarEnergyEngineering.asmedigitalcollection.asme.org/article.aspx?articleid=1473771. 22

Herzog, S. and D. Ostwald (2013, February). Experimental biology: Sometimes Bayesian statistics are better. *Nature*. doi:10.1038/494035b. 30

Hottel, H. C. (1976). A simple model for estimating the transmittance of direct solar radiation through clear atmospheres. *Solar energy 18*(2), 129–134. 166

Hovgaard, T. G., S. Boyd, L. F. Larsen, and J. B. Jørgensen (2013, August). Nonconvex model predictive control for commercial refrigeration. *International Journal of Control 86*(8), 1349–1366. http://www.tandfonline.com/doi/abs/10.1080/00207179.2012.742207. 25

Hu, M. (2015, March). A data-driven feed-forward decision framework for building clusters operation under uncertainty. *Applied Energy 141*, 229–237. https://linkinghub.elsevier.com/retrieve/pii/S030626191401304X. 29

Hu, M., F. Xiao, J. B. Jørgensen, and R. Li (2019, May). Price-responsive model predictive control of floor heating systems for demand response using building thermal mass. *Applied Thermal Engineering 153*, 316–329. https://linkinghub.elsevier.com/retrieve/pii/S1359431118361921. 16

Jensen, S. O., A. Marszal-Pomianowska, R. Lollini, W. Pasut, A. Knotzer, P. Engelmann, A. Stafford, and G. Reynders (2017, November). IEA EBC Annex 67 Energy Flexible Buildings. *Energy and Buildings 155*, 25–34. http://linkinghub.elsevier.com/retrieve/pii/S0378778817317024. 5, 14, 54

Jia, R. and C. Spanos (2017, July). Occupancy modelling in shared spaces of buildings: a queueing approach. *Journal of Building Performance Simulation 10*(4), 406–421. https://www.tandfonline.com/doi/full/10.1080/19401493.2016.1267802. 30

Kabessa, N. (2017, December). Power Ledger's Disruptive Decentralized Energy Market. x, 2

Kamthe, S. and M. P. Deisenroth (2017, June). Data-Efficient Reinforcement Learning with Probabilistic Model Predictive Control. *arXiv:1706.06491 [cs, stat]*. http://arxiv.org/abs/1706.06491. 33

Kavlak, G., J. McNerney, and J. E. Trancik (2018). Evaluating the causes of cost reduction in photovoltaic modules. *Energy Policy 123*, 700 – 710. http://www.sciencedirect.com/science/article/pii/S0301421518305196. 2

Kelman, A. D. and F. Borelli (2011). Bilinear Model Predictive Control of a HVAC System Using Sequential Quadratic Programming. Milano, Italy, pp. 9869–9874. 15, 21, 30

Krzywinski, M. and N. Altman (2013). Points of significance: Importance of being uncertain. *Nature Methods 10*, 809–810. 30

Kuznetsova, E., Y.-F. Li, C. Ruiz, and E. Zio (2014, September). An integrated framework of agent-based modelling and robust optimization for microgrid energy management. *Applied Energy 129*, 70–88. https://linkinghub.elsevier.com/retrieve/pii/S0306261914003766. 29

Laperrière, A. and R. Brassard (2011). Three elements electric water heater. x, 6

Lazos, D., A. B. Sproul, and M. Kay (2014, November). Optimisation of energy management in commercial buildings with weather forecasting inputs: A review. *Renewable and Sustainable Energy Reviews 39*, 587–603. http://linkinghub.elsevier.com/retrieve/pii/S136403211400505X. 30

LeCun, Y., Y. Bengio, and G. Hinton (2015, May). Deep learning. *Nature 521*(7553), 436–444. http://www.nature.com/doifinder/10.1038/nature14539. 6

Lee, J. H. (2011, June). Model predictive control: Review of the three decades of development. *International Journal of Control, Automation and Systems 9*(3), 415–424. http://link.springer.com/10.1007/s12555-011-0300-6. 13, 14

Lehmann, B., D. Gyalistras, M. Gwerder, K. Wirth, and S. Carl (2013, March). Intermediate complexity model for Model Predictive Control of Integrated Room Automation. *Energy and Buildings 58*, 250–262. http://linkinghub.elsevier.com/retrieve/pii/S0378778812006561. 21

Levenberg, K. (1944). A method for the solution of certain non-linear problems in least squares. *Quarterly of applied mathematics 2*(2), 164–168. 63

Liu, S. and G. Henze (2004). Impact of modeling accuracy on predictive optimal control of active and passive building thermal storage inventory. In *ASHRAE Transactions*, Volume 110 PART 1, pp. 151–163. https://www.scopus.com/inward/record.uri?eid=2-s2.0-2442529922&partnerID=40&md5=f66de9eb5e19fab41b90119b47e787f7. 29

Ljung, L. (1987). *System Identification Theory for User*. University of Linkoping, Sweden: Prentice Hall Englewood Cliffs, NJ. 23

Lund, P. D., J. Lindgren, J. Mikkola, and J. Salpakari (2015, May). Review of energy system flexibility measures to enable high levels of variable renewable electricity. *Renewable and Sustainable Energy Reviews 45*, 785–807. http://linkinghub.elsevier.com/retrieve/pii/S1364032115000672. 5

Ma, J., J. Qin, T. Salsbury, and P. Xu (2012, January). Demand reduction in building energy systems based on economic model predictive control. *Chemical Engineering Science 67*(1), 92–100. http://linkinghub.elsevier.com/retrieve/pii/S0009250911005240. 23

Ma, Y., J. Matusko, and F. Borrelli (2015, January). Stochastic Model Predictive Control for Building HVAC Systems: Complexity and Conservatism. *IEEE Transactions on Control Systems Technology 23*(1), 101–116. http://ieeexplore.ieee.org/document/6802411/. 30

Ma, Z., J. D. Billanes, and B. N. Jørgensen (2017). User needs, motivation and barriers for application of Energy Flexibility in Buildings. Technical report. 55

Maasoumy, M., M. Razmara, M. Shahbakhti, and A. S. Vincentelli (2014, July). Handling model uncertainty in model predictive control for energy efficient buildings. *Energy and Buildings 77*, 377–392. http://linkinghub.elsevier.com/retrieve/pii/S0378778814002771. 29

Machairas, V., A. Tsangrassoulis, and K. Axarli (2014, March). Algorithms for optimization of building design: A review. *Renewable and Sustainable Energy Reviews 31*, 101–112. http://linkinghub.elsevier.com/retrieve/pii/S1364032113007855. 15

Macogep (2014, April). Varennes library wins UDI Award for Excellence in the "Innovation" category. http://www.macogep.com/en/nouvelle/varennes-library-wins-udi-award-for-excellence-in-the-innovation-category/. 45

Magnier, L. and F. Haghighat (2010, March). Multiobjective optimization of building design using TRNSYS simulations, genetic algorithm, and Artificial Neural Network. *Building and Environment 45*(3), 739–746. http://linkinghub.elsevier.com/retrieve/pii/S0360132309002091. 15

Marquardt, D. W. (1963). An algorithm for least-squares estimation of nonlinear parameters. *Journal of the society for Industrial and Applied Mathematics 11*(2), 431–441. 63

Massa Gray, F. and M. Schmidt (2018, April). A hybrid approach to thermal building modelling using a combination of Gaussian processes and grey-box models. *Energy and Buildings 165*, 56–63. https://linkinghub.elsevier.com/retrieve/pii/S0378778817332942. 25

Mavrotas, G., D. Diakoulaki, K. Florios, and P. Georgiou (2008, July). A mathematical programming framework for energy planning in services' sector buildings under uncertainty in load demand: The case of a hospital in Athens. *Energy Policy 36*(7), 2415–2429. https://linkinghub.elsevier.com/retrieve/pii/S0301421508000104. 29

May-Ostendorp, P., G. P. Henze, C. D. Corbin, B. Rajagopalan, and C. Felsmann (2011, February). Model-predictive control of mixed-mode buildings with rule extraction. *Building and Environment 46*(2), 428–437. http://linkinghub.elsevier.com/retrieve/pii/S0360132310002477. 15, 26, 27

Mlecnik, E. (2018). Opportunities and barriers for asset managers integrating energy flexibility. In *International Sustainable Energy Conference 2018*. 55

Montgomery, R. and R. McDowall (2008). *Fundamentals of HVAC control systems*. Atlanta, GA: Elsevier. 11

Morales, J. M., A. J. Conejo, H. Madsen, P. Pinson, and M. Zugno (2014). *Integrating Renewables in Electricity Markets*, Volume 205 of *International Series in Operations Research & Management Science*. Boston, MA: Springer US. http://link.springer.com/10.1007/978-1-4614-9411-9. 14, 54

Moriyama, T., G. De Magistris, M. Tatsubori, T.-H. Pham, A. Munawar, and R. Tachibana (2018, August). Reinforcement Learning Testbed for Power-Consumption Optimization. *arXiv:1808.10427 [cs]*. http://arxiv.org/abs/1808.10427. 33

Moroşan, P.-D., R. Bourdais, D. Dumur, and J. Buisson (2010, September). Building temperature regulation using a distributed model predictive control. *Energy and Buildings 42*(9), 1445–1452. http://linkinghub.elsevier.com/retrieve/pii/S0378778810000915. 21

Moslehi, K. and R. Kumar (2010). A reliability perspective of the smart grid. *IEEE Transactions on Smart Grid 1*(1), 57–64. 5

Nagy, A., H. Kazmi, F. Cheaib, and J. Driesen (2018). Deep Reinforcement Learning for Optimal Control of Space Heating. pp. 8. 33

Naveros, I., C. Ghiaus, D. Ruíz, and S. Castaño (2015, December). Physical parameters identification of walls using ARX models obtained by deduction. *Energy and Buildings 108*, 317–329. https://linkinghub.elsevier.com/retrieve/pii/S0378778815302620. 25

Newville, M., T. Stensitzki, D. B. Allen, M. Rawlik, A. Ingargiola, and A. Nelson (2016). LMFIT: Non-linear least-square minimization and curve-fitting for Python. *Astrophysics Source Code Library*. 63

Nguyen, A.-T., S. Reiter, and P. Rigo (2014, January). A review on simulation-based optimization methods applied to building performance analysis. *Applied Energy 113*, 1043–1058. http://linkinghub.elsevier.com/retrieve/pii/S0306261913007058. 23, 25, 29

NRCan (2016). National Energy Use Database (NEUD). http://oee.nrcan.gc.ca/corporate/statistics/neud/dpa/home.cfm. 45

NREL (2014, September). Cost Control Strategies for Zero Energy Buildings: High-Performance Design and Construction on a Budget. Technical report, National Renewable Energy Laboratory (NREL), Golden, CO. 146

Nuzzo, R. (2014, February). Scientific method: Statistical errors. *Nature*, 150–152. 30

of Canada, G. (2015, September). Public weather forecast bulletins. https://www.canada.ca/en/environment-climate-change/services/types-weather-forecasts-use/public/guide/bulletins.html. 90

Oldewurtel, F., A. Parisio, C. N. Jones, D. Gyalistras, M. Gwerder, V. Stauch, B. Lehmann, and M. Morari (2012, February). Use of model predictive control and weather forecasts for energy efficient building climate control. *Energy and Buildings 45*, 15–27. http://linkinghub.elsevier.com/retrieve/pii/S0378778811004105. x, 13, 21

OpenAI (2018). OpenAI Five. https://blog.openai.com/openai-five/. 32

OpenAI, M. Andrychowicz, B. Baker, M. Chociej, R. Jozefowicz, B. McGrew, J. Pachocki, A. Petron, M. Plappert, G. Powell, A. Ray, J. Schneider, S. Sidor, J. Tobin, P. Welinder, L. Weng, and W. Zaremba (2018, August). Learning Dexterous In-Hand Manipulation. *arXiv:1808.00177 [cs, stat]*. http://arxiv.org/abs/1808.00177. 32

Paris, B., J. Eynard, S. Grieu, T. Talbert, and M. Polit (2010, October). Heating control schemes for energy management in buildings. *Energy and Buildings 42*(10), 1908–1917. https://linkinghub.elsevier.com/retrieve/pii/S0378778810001891. 17

Parisio, A., D. Varagnolo, M. Molinari, G. Pattarello, L. Fabietti, and K. H. Johansson (2014). Implementation of a Scenario-based MPC for HVAC Systems: an Experimental Case Study. Cape Town, South Africa, pp. 599–605. IFAC. 25

Pedregosa, F., G. Varoquaux, A. Gramfort, V. Michel, B. Thirion, O. Grisel, M. Blondel, P. Prettenhofer, R. Weiss, V. Dubourg, and others (2011). Scikit-learn: Machine learning in Python. *The Journal of Machine Learning Research 12*, 2825–2830. http://dl.acm.org/citation.cfm?id=2078195. 46

Pinto, L., J. Davidson, and A. Gupta (2016, October). Supervision via Competition: Robot Adversaries for Learning Tasks. *arXiv:1610.01685 [cs]*. http://arxiv.org/abs/1610.01685. 33

Pinto, L., J. Davidson, R. Sukthankar, and A. Gupta (2017, March). Robust Adversarial Reinforcement Learning. *arXiv:1703.02702 [cs]*. http://arxiv.org/abs/1703.02702. 33

Prívara, S., Z. Váňa, E. Žáčeková, and J. Cigler (2012, December). Building modeling: Selection of the most appropriate model for predictive control. *Energy and Buildings 55*, 341–350. https://linkinghub.elsevier.com/retrieve/pii/S0378778812004446. 19, 20, 62

Qin, S. J. and T. A. Badgwell (2003). A survey of industrial model predictive control technology. *Control engineering practice 11*(7), 733–764. http://www.sciencedirect.com/science/article/pii/S0967066102001867. 13, 14

Rastogi, P., M. E. Khan, and M. Andersen (2017). Gaussian-Process-Based Emulators for Building Performance Simulation. San Francisco, CA. IBPSA. 32

Rawlings, J. B. and D. Q. Mayne (2009). *Model predictive control: theory and design*. Madison, Wis: Nob Hill Pub. 14

Reddy, T. A., I. Maor, and C. Panjapornpon (2007). Calibrating Detailed Building Energy Simulation Programs with Measured Data - Part I: General Methodology. *13*(2), 22. 30

Reynders, G., J. Diriken, and D. Saelens (2017, July). Generic characterization method for energy flexibility: Applied to structural thermal storage in residential buildings. *Applied Energy 198*, 192–202. https://linkinghub.elsevier.com/retrieve/pii/S0306261917304555. 14, 54

Reynders, G., R. A. Lopes, A. Marszal-Pomianowska, D. Aelenei, J. Martins, and D. Saelens (2018). Energy flexible buildings: An evaluation of definitions and quantification methodologies applied to thermal storage. *Energy and Buildings 166*, 372 – 390. http://www.sciencedirect.com/science/article/pii/S037877881732947X. 2, 14, 86

Ricardez-Sandoval, L. A. (2012, August). Optimal design and control of dynamic systems under uncertainty: A probabilistic approach. *Computers & Chemical Engineering 43*, 91–107. http://linkinghub.elsevier.com/retrieve/pii/S0098135412001044. 31

Runge, J., P. Nowack, M. Kretschmer, S. Flaxman, and D. Sejdinovic (2019). Detecting and quantifying causal associations in large nonlinear time series datasets. *Science Advances 5*(11). https://advances.sciencemag.org/content/5/11/eaau4996. 156

Rätz, M., A. P. Javadi, M. Baranski, K. Finkbeiner, and D. Müller (2019, November). Automated data-driven modeling of building energy systems via machine learning algorithms. *Energy and Buildings 202*, 109384. https://linkinghub.elsevier.com/retrieve/pii/S0378778819316585. 18, 29

Sanchez-Gonzalez, A., N. Heess, J. T. Springenberg, J. Merel, M. Riedmiller, R. Hadsell, and P. Battaglia (2018, June). Graph networks as learnable physics engines for inference and control. *arXiv:1806.01242 [cs, stat]*. http://arxiv.org/abs/1806.01242. 33

Sanchez-Sanchez, K. B. and L. A. Ricardez-Sandoval (2013, April). Simultaneous Design and Control under Uncertainty Using Model Predictive Control. *Industrial & Engineering Chemistry Research 52*(13), 4815–4833. http://pubs.acs.org/doi/10.1021/ie302215c. 31

Scattolini, R. (2009, May). Architectures for distributed and hierarchical Model Predictive Control – A review. *Journal of Process Control 19*(5), 723–731. http://linkinghub.elsevier.com/retrieve/pii/S0959152409000353. 27

Schaarschmidt, M., A. Kuhnle, and K. Fricke (2017). TensorForce: A TensorFlow library for applied reinforcement learning. https://github.com/reinforceio/tensorforce. 32

SciPy (2019, December). Bivariate spline approximation over a rectangular mesh. https://docs.scipy.org/doc/scipy/reference/generated/scipy.interpolate.RectBivariateSpline.html. 165

Shaikh, P. H., N. B. M. Nor, P. Nallagownden, I. Elamvazuthi, and T. Ibrahim (2014, June). A review on optimized control systems for building energy and comfort management of smart sustainable buildings. *Renewable and Sustainable Energy Reviews 34*, 409–429. http://linkinghub.elsevier.com/retrieve/pii/S1364032114001889. 15, 18, 55

Silver, D., J. Schrittwieser, K. Simonyan, I. Antonoglou, A. Huang, A. Guez, T. Hubert, L. Baker, M. Lai, A. Bolton, Y. Chen, T. Lillicrap, F. Hui, L. Sifre, G. van den Driessche, T. Graepel, and D. Hassabis (2017, October). Mastering the game of Go without human knowledge. *Nature 550*(7676), 354–359. http://www.nature.com/doifinder/10.1038/nature24270. 32

Smarra, F., A. Jain, T. de Rubeis, D. Ambrosini, A. D'Innocenzo, and R. Mangharam (2018, April). Data-driven model predictive control using random forests for building energy optimization and climate control. *Applied Energy*. http://linkinghub.elsevier.com/retrieve/pii/S0306261918302575. 32

St-Jacques, M., S. Bucking, and W. O'Brien (2020, October). Spatially and temporally sensitive consumption-based emission factors from mixed-use electrical grids for building

electrical use. *Energy and Buildings 224*, 110249. https://linkinghub.elsevier.com/retrieve/pii/S0378778819337387. 12

SWOB-ML (2020, May). Weather information database. https://dd.weather.gc.ca/observations/swob-ml/. 90

The-AlphaStar-Team (2019, October). AlphaStar: Grandmaster level in StarCraft II using multi-agent reinforcement learning. 32

Thieblemont, H., F. Haghighat, R. Ooka, and A. Moreau (2017, October). Predictive control strategies based on weather forecast in buildings with energy storage system: A review of the state-of-the art. *Energy and Buildings 153*, 485–500. http://linkinghub.elsevier.com/retrieve/pii/S0378778816320333. 28

Thomas, N. (2017, March). DeepMind and National Grid in AI talks to balance energy supply. https://www.ft.com/content/27c8aea0-06a9-11e7-97d1-5e720a26771b. 5

Torcellini, P., S. Pless, M. Deru, and D. Crawley (2006). Zero energy buildings: a critical look at the definition. *National Renewable Energy Laboratory and Department of Energy, US*. http://www.biomassthermal.org/programs/documents/118_ZEBCriticalLookDefinition.pdf. 41

USDOE (2019). Spawn-of-EnergyPlus (Spawn). https://www.energy.gov/eere/buildings/downloads/spawn-energyplus-spawn. 24

Viot, H., A. Sempey, L. Mora, J. Batsale, and J. Malvestio (2018a, August). Model predictive control of a thermally activated building system to improve energy management of an experimental building: Part II - Potential of predictive strategy. *Energy and Buildings 172*, 385–396. https://linkinghub.elsevier.com/retrieve/pii/S0378778818311460. 22

Viot, H., A. Sempey, L. Mora, J. Batsale, and J. Malvestio (2018b, August). Model predictive control of a thermally activated building system to improve energy management of an experimental building: Part I—Modeling and measurements. *Energy and Buildings 172*, 94–103. https://linkinghub.elsevier.com/retrieve/pii/S0378778818311435. 22

Wang, H. and Z. J. Zhai (2016, September). Advances in building simulation and computational techniques: A review between 1987 and 2014. *Energy and Buildings 128*, 319–335. http://linkinghub.elsevier.com/retrieve/pii/S0378778816305692. 19

Wei, Y., X. Zhang, Y. Shi, L. Xia, S. Pan, J. Wu, M. Han, and X. Zhao (2018, February). A review of data-driven approaches for prediction and classification of building energy consumption. *Renewable and Sustainable Energy Reviews 82*, 1027–1047. https://linkinghub.elsevier.com/retrieve/pii/S136403211731362X. 29

Wetter, M. (2009). Modelica-based modelling and simulation to support research and development in building energy and control systems. *Journal of Building Performance Simulation 2*(2). https://doi.org/10.1080/19401490902818259. 13

WGBC (2013). The Business Case for Green Building. Technical report, World Green Building Council. 12, 34

Wolisz, H., T. M. Kull, D. Müller, and J. Kurnitski (2020, January). Self-learning model predictive control for dynamic activation of structural thermal mass in residential buildings. *Energy and Buildings 207*, 109542. https://linkinghub.elsevier.com/retrieve/pii/S037877881833456X. 16

Wolpert, D. H. and W. G. Macready (1997). No free lunch theorems for optimization. *IEEE transactions on evolutionary computation 1*(1), 67–82. 6

Yamaguchi, Y., N. Shigei, and H. Miyajima (2015). Air Conditioning Control System Learning Sensory Scale Based on Reinforcement Learning. In *Proceedings of the International MultiConference of Engineers and Computer Scientists*, Volume 1. 33

Yan, B., X. Li, W. Shi, X. Zhang, and A. Malkawi (2017). Forecasting Building Energy Demand under Uncertainty Using Gaussian Process Regression: Feature Selection, Baseline Prediction, Parametric Analysis and a Web-based Tool. San Francisco, CA. IBPSA. 31

Yuan, S. (2016). *A study of hybrid ventilation in an institutional building for predictive control*. Ph. D. thesis, Concordia University. http://spectrum.library.concordia.ca/981756/. xviii, 143, 145

Zakaria, A., F. B. Ismail, M. H. Lipu, and M. Hannan (2020, January). Uncertainty models for stochastic optimization in renewable energy applications. *Renewable Energy 145*, 1543–1571. https://linkinghub.elsevier.com/retrieve/pii/S0960148119311012. 29

Zhao, H.-X. and F. Magoulès (2012, August). A review on the prediction of building energy consumption. *Renewable and Sustainable Energy Reviews 16*(6), 3586–3592. http://linkinghub.elsevier.com/retrieve/pii/S1364032112001438. 20, 30, 32

Žáčeková, E., S. Prívara, and Z. Váňa (2011, November). Model predictive control relevant identification using partial least squares for building modeling. Melbourne, Australia, pp. 6. 20, 62

Appendix A

Varennes Library Supplementary Information

A.1 Lighting

In high-performance buildings, the relative consumption of the HVAC system is reduced compared to the rest of the loads. Lighting can become a proportionally larger consumer only to be superseded by plug loads, and so paying attention to controlling lighting level can lead to worth-while energy savings.

The library features T8 fluorescent luminaires equipped with a digital addressable lighting interface (DALI) where each luminaire can be dimmed individually and controlled by sector. When the library was first opened, the lighting was set to a minimum of 800 lux everywhere. Since then, lighting was reduced following Illuminating Engineering Society of North America (IESNA) guidelines (DiLaura et al., 2011). Two main tasks are conducted in a library: (1) office work and reading, and (2) browsing the library book shelves/stacks. IESNA recommends 300-500 lux for office work and library reading; and 200-500 lux for the library shelves. However, when lighting was reduced, occupants complained that it was too dim, possibly because of strong contrast between the daylit areas and the book stacks.

The library is open to employees much earlier that to clients. During that period, the lighting in areas designated for clientele can be switched off or sparsely lit. Photosensors dim luminaires when daylight is present. After the 5^{th} year of operation, many ballasts

began failing and their repair was unsuccessful because the ballast lost their addressability and dimming features. The building manager replaced the luminaires with LED luminaires since they last longer, are more economical to operate, can be dimmed efficiently and do not contain harmful elements like mercury.

A.2 Natural Ventilation

The library has motorized operable windows installed along the length of the building, see Figure A.1. The windows open to let in fresh air and is used for free-cooling. Due to concerns with vandalism, the windows remain shut during the night.

In a complimentary study, Yuan (2016) has proposed a window opening strategy based on exterior air water content and temperature, see Figure A.2. The ambient air is acceptable if the admitted air does not raise the indoor air relative humidity above 70% at 22°C. In her study, she allows ambient air down to 8°C to be admitted for pre-cooling when the building is unoccupied – night-time free-cooling strategy.

Applying the proposed ranges to the library, we note a window opening rate increase from 9.0 to 9.4% going from the current control program to Yuan's most conservative scenario: see Table A.1, *Yuan Case 1* where the exterior conditions are closest to interior conditioned air. By increasing the range of acceptable air, window use can be increased to almost 29%. However, admitting the lower bound 8°C air should only be considered in unoccupied hours otherwise it will lead to thermal discomfort near the windows. By utilizing longer natural ventilation and night-time pre-cooling strategies during the cooling season, the cooling load can be reduced. To address the concern for vandalism, night-time pre-cooling can be applied to the upper level only.

The challenge of natural ventilation is to be able to utilize it alongside the HVAC system to reduce the overall energy use.

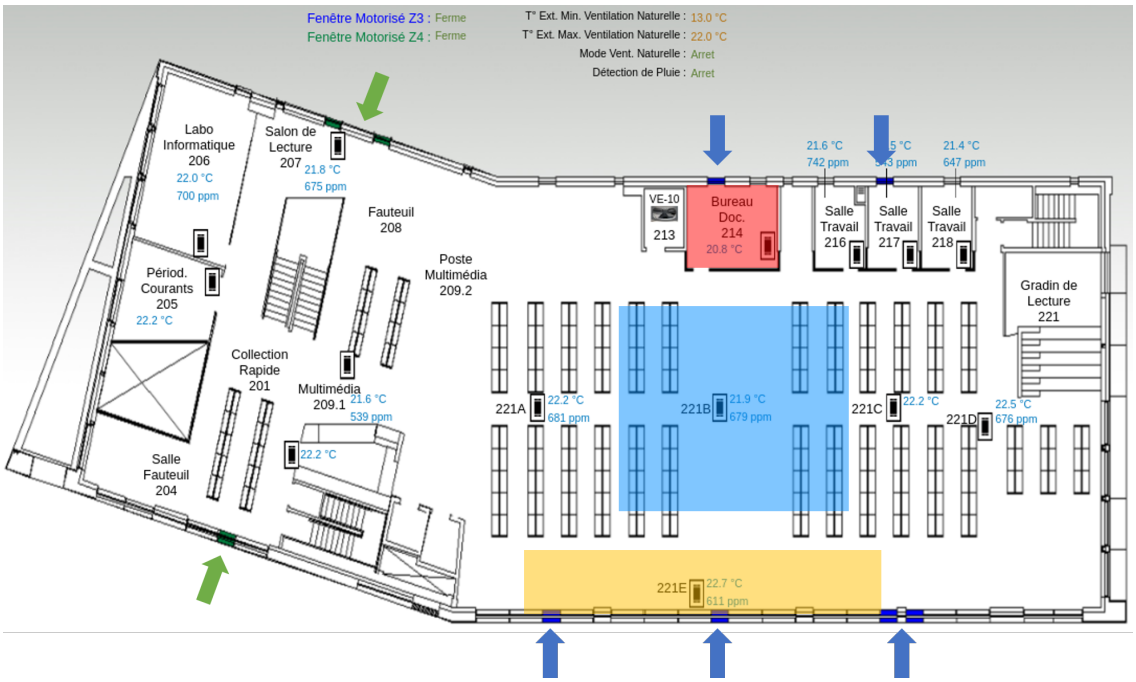

Figure A.1: Library second floor plan view showing operable motorized windows, same coloured arrows operate together.

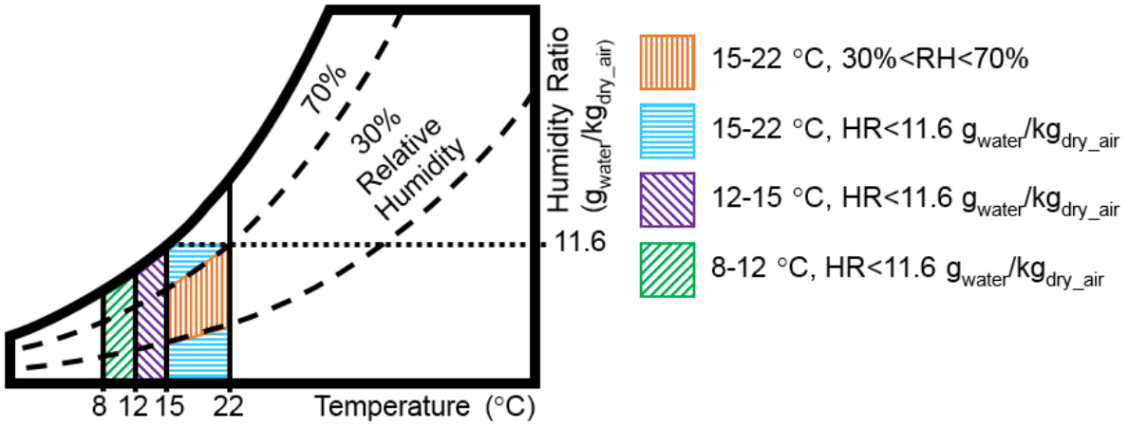

Figure A.2: Psychrometric chart showing proposed conditions for allowing exterior air. Cases mapped to colour and hatch: {1: orange vertical, 2: cyan horizontal, 3: purple NW to SE, 4: green NE to SW}.

A.3 Hydronic Radiant Slab Control Strategy

We have completed a preliminary study (Dermardiros et al., 2017) on how to apply an optimization-based MPC strategy on the radiant slab on an archetype zone.

Table A.1: Natural ventilation current use and potential use (Yuan, 2016). Windows automatically close upon rain detection. Data from February 20, 2016 to February 20, 2017.

Cases	Conditions		% in Effect	% if Combined	
Yuan	Closed		71.4		
1	15-22°C	30-70% RH	9.43		
2	15-22°C	W < 11.6 g/kg	6.09	15.52	(1+2)
3	12-15°C	W < 11.6 g/kg	5.61	21.13	(1+2+3)
4	8-12°C	W < 11.6 g/kg	7.47	28.6	(1+2+3+4)
Current	Closed		90.96		
	13-22°C	Fresh air need	9.04		

The hydronic radiant slab is the primary source of space conditioning in the east, south and west perimeter zones of the Varennes library. It is supplemented by the air system which also brings in the required fresh air based on occupancy and demand. The current controls for the radiant slab function based on two operational modes: heating or cooling. If the zone is in cooling mode, no heating can be supplied to that zone and vice-versa. There are opportunities to reduce the overall energy consumption of a zone with radiant slabs by either pre-heating or pre-cooling in anticipation of a future load, such as occupancy or solar gains.

Conventionally, hydronic radiant slabs are controlled through inlet-oulet temperature differentials and based on ambient conditions correlations. Predictive measures are seldom applied which can be beneficial for peak demand reduction and shifting. The MPC algorithm here replicates a pre-cooling strategy in anticipation of mid-day solar gains.

Based on a model of the radiant slab and on future forecasts, MPC will determine the operational trajectory the system needs to follow to minimize a cost function. For a case where heating is needed in the morning and cooling in the afternoon, it is possible that the lowest energy optimal is to cool the slab in the morning in anticipation of solar gains at noon but use the diffusers for heating in the morning. This strategy was found by the optimization routine. The method also dramatically reduced the peak electrical demand by as much as 50% by pre-emptively cooling the slab instead of simply reacting to solar gains – as is the current case. The preliminary study did not consider the electricity production in its optimization function and so higher savings can be anticipated when included.

The study was to take and model a cross-section of the library that would include the areas served with a radiant slab and areas served strictly with the air system. The section

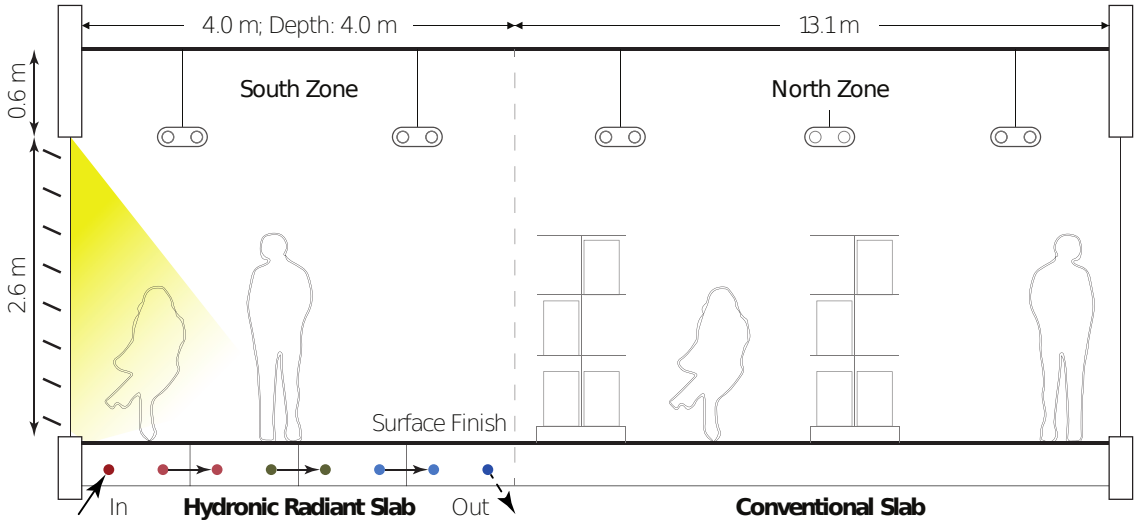

Figure A.3: Library cross-section (Dermardiros et al., 2017).

shown in Figure A.3 represents a slice of the library oriented North-South; it is also shown in Figure 3.1 panel 4. The section serves as an archetype zone of an institutional building that allows deep daylight penetration and cross ventilation through the use of motorized windows on both sides. The U.S. National Renewable Energy Laboratory's Research Support Facility (NREL RSF) features a similar concept (NREL, 2014).

The two zones – with and without radiant slab – are modelled with single conductances representing the influence of the exterior conditions and with single capacitances representing the effective thermal storage effect of the walls, air and furniture in the space. The HVAC system is modelled as a simple constant air volume system where the HVAC system is a node and is connected to the zone air node with conductance representing the air changes per hour. The southern slab containing the piping is discretized in smaller parts. First, the slab surface is partitioned into 4 sections depth-wise from the window. These 4 sections are discretized into 2-dimensional volumes: 5 nodes in width and 4 in depth. The concrete depth is 75 mm for the base scenario. Along the direction of fluid flow, the temperatures are assumed constant within a node of a section. The fluid exiting a section after having transferred energy to the slab enters the following section. The analogous electrical circuit equivalent of the thermal network is shown and explained in Figure A.4. The temperature of the fluid travelling through a slab section follows an exponential regime (Cengel et al., 2011,

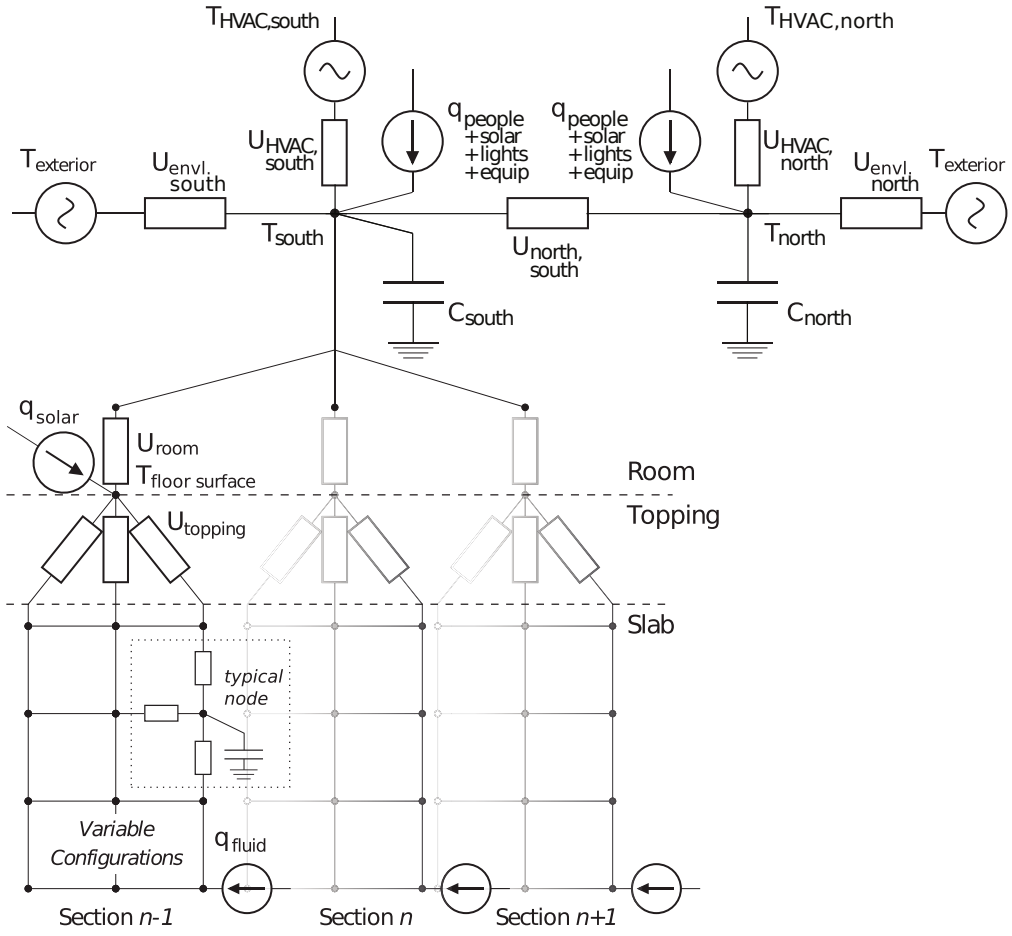

Figure A.4: Circuit representation of library section, surface finish and slab. Each zone is represented by a single node with a single capacitance representing the effective thermal mass of the walls and furniture. It is connected to the exterior ambient air via an effective windowed wall conductance. The slab is separated in 4 sections. Each section is represented by a 5*4 (width*depth) 2-D grid. All the nodes have a capacitance representing the concrete volume and are connected to one another. The side and bottom boundary of the slab are adiabatic. The heat input from the fluid flow is connected to the bottom corner. The slab top nodes are connected by conductors representing the topping material and merge into the slab section's floor surface node. The floor surface receives part of the solar gains passing through the window and connect to the zone air node through a combined convective and radiative conductance. The north zone does not have an active slab.

see chap. 8).

The MPC scheme will maintain the setpoint profile by employing future predictions of

the weather and attempt to minimize a predefined cost function. For this study, the future predictions are deterministic. There are three control variables: the north and south air and water temperatures. They are optimized over the longer (8 hour) prediction horizon, but only the control sequences within the shorter (1 hour) control horizon are applied. Once the control horizon trajectory is applied, the process is repeated.

All the thermal nodes in the model were initialized at 19°C. The first day served as a warm-up period and is not shown in any of the results. Looking at the results for the base scenario of a vinyl tile covered 75 mm concrete hydronic slab in Figure A.5, we can observe that the setpoints are generally respected. Since the simulated days were clear and although the exterior temperature was frigid, cooling is required for the south zone. The extracted heat from the room would be transferred to adjacent zones requiring heating in winter. The slab water inlet temperature is mostly at around room temperature, although there are periods of cooling that begin in anticipation of the peak solar gains.

This optimized operation was able to reduce the peak energy demand by 50% for this case. However, this study was simplified and real-world results would defer. This served as an initial step to apply MPC into the library and to analyze which modelling approach to follow. The cost functions in the paper had decaying terms – more importance attributed to closer actions – to compensate for the perfect knowledge assumptions taken. In the thesis, this was forgone in favour of uncertain predictions and utilizing a sampling-based approach. The renewable generation was also later considered.

A.4 Ground-Source Heat-Pump Ground Interactions

The building's heating and cooling is supplied from four ground-source heat-pumps (GSHP) connected to eight 152 m [400'] deep boreholes with combined cooling capacity equalling 30 tons. The radiant slab acts more as a short-term thermal storage system whereas the ground is more of a long-term or seasonal system. Preliminary heat interactions with the ground revealed a yearly imbalance in the range of -65,000 kWh, see Figure A.6, which signifies that the ground is heating over time, *i.e.* the building is cooling dominated. Typically in Quebec, buildings are heating-dominated. The library's orientation and window design

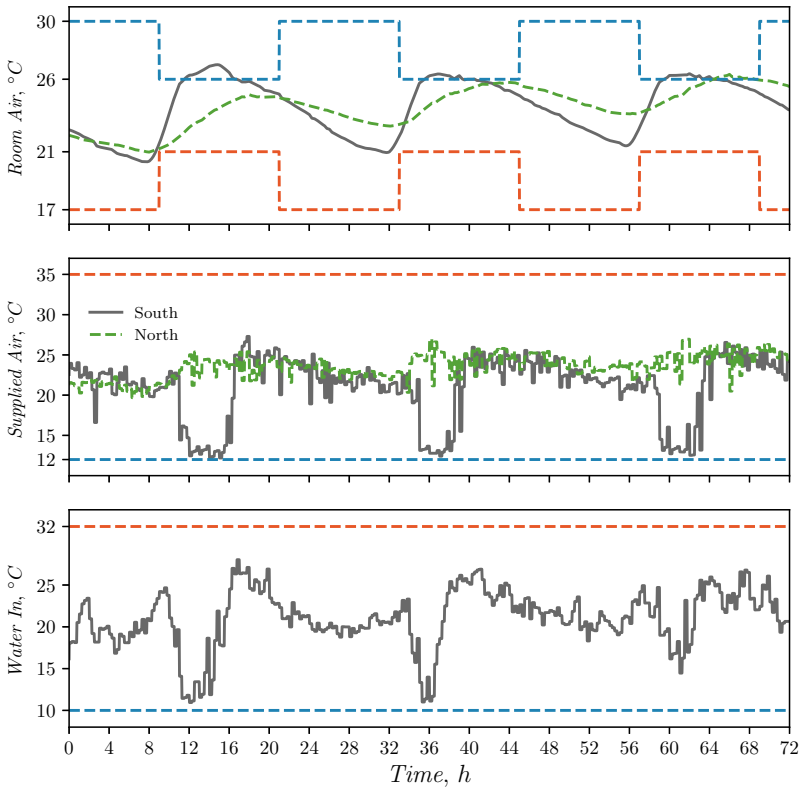

Figure A.5: Optimal supplied air and radiant slab inlet temperatures for a sunny winter day. Supplied water is colder to absorb solar gains and move to northern side of the library (Dermardiros et al., 2017).

allows for better passive solar heat gains and the heat recovery from the BIPV/T system reduces the need for pre-heating. On a yearly basis, the heating load is less than the cooling load because of these factors. How this imbalance will play a role in the future capacity of the geothermal system will be monitored. Natural ventilation and better radiant slab control strategies can mediate the effects. Installation of motorized shades can reduce solar gains and diminish cooling loads. Should there be a need for seasonal control strategies will need to be investigated.

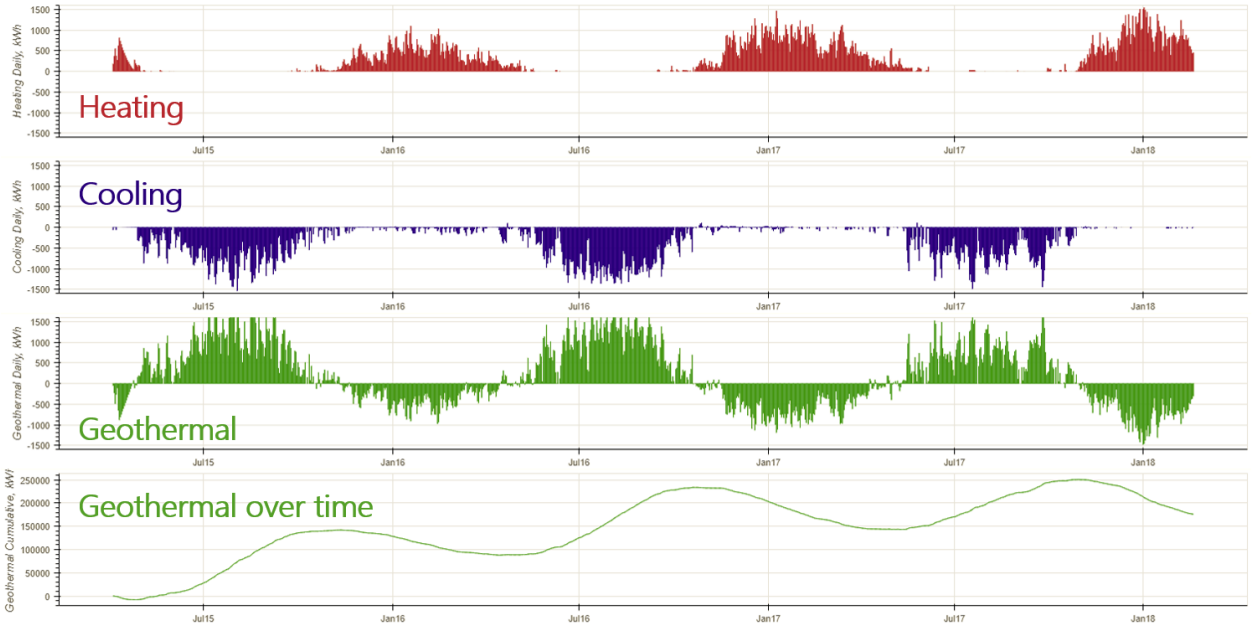

Figure A.6: Heating and cooling loads and resulting cumulative energy balance towards the ground.

A.5 Building-Integrated Photovoltaic and Thermal System

The Varennes library features a building-integrated photovoltaic and thermal recovery (BIPV/T) system. Aside being a highly efficient and well-insulated building, the on-site renewables contribute on making this building a net-zero energy building (NetZEB). This section details the BIPV/T system, what its typical behaviour is in winter, the detection of loss of performance that was later remedied, and the design and application of an on-site solar irradiance measurement station. In appendix B.4, details of a simplified linear model to estimate the electrical production used in the MPC formulation in chapter 5 is described.

A.5.1 System Overview

The library has a 110.5 kWp roof-mounted building-integrated photovoltaic (BIPV) array. From the total 711 m^2 [425 panels] PV area, 428 m^2 [258 panels] is naturally vented through a 150 mm [6”] air gap between the PV panels and metal roofing. The remaining 280 m^2

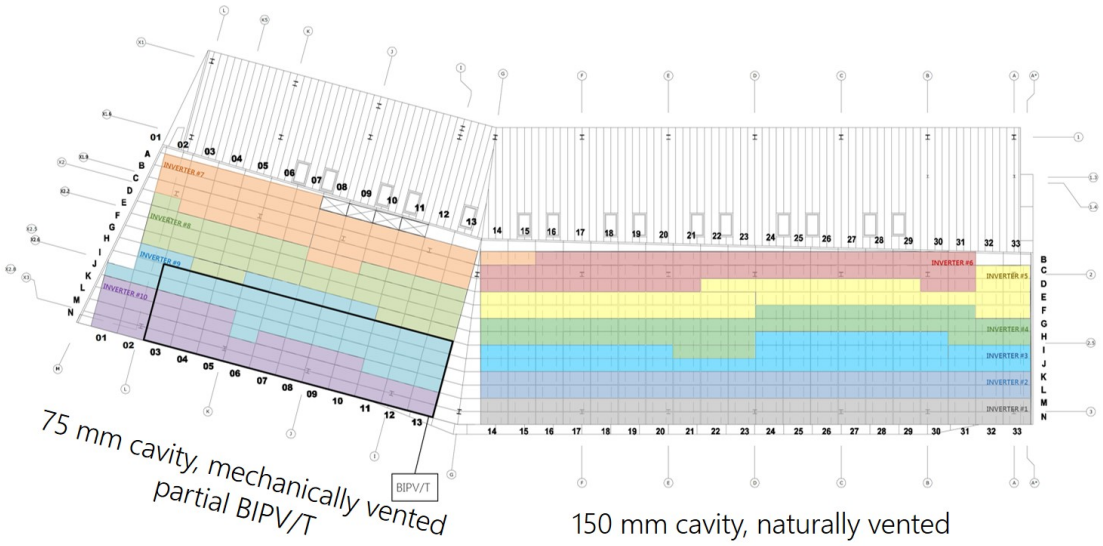

Figure A.7: BIPV/T roof showing panels connected to inverters identified by colour.

[167 panels] is fan-assisted and vented through a narrower 70 mm [2.8”] air gap. Air flow behind the panels serves to reduce overheating and to increase production efficiency. From a 173 m^2 [66 panels] portion of the forced air area, heat from the PV panels is recovered through outdoor air flowing in the cavity under the panels which is used as fresh air. This airflow to the fresh air intake is controlled through variable speed fans during the heating season, see Figure 3.2 – this system is known as BIPV/thermal (BIPV/T) as it produces useful heat in addition to electricity.

A.5.2 Production on a Cold Sunny Day

As an example, for a typical cold sunny day, 220 kWh can be harvested as solar heat. On average, 6835 kWh have been harvested per heating season (November to April). On approximately 50% of the occupied time the BIPV/T system harvested above 2 kW of heat and 14% of the occupied time above 10 kW of heat. The BIPV/T portion covers 16% of the roof; if the whole roof were BIPV/T, 6.5x more heat could theoretically be recovered and potentially fed to a thermal micro-grid to assist neighbouring buildings in heating, however injecting excess heat to the ground would further increase the imbalance of season heat transfer, see Appendix section A.4. The BIPV/T system was designed to maintain an air

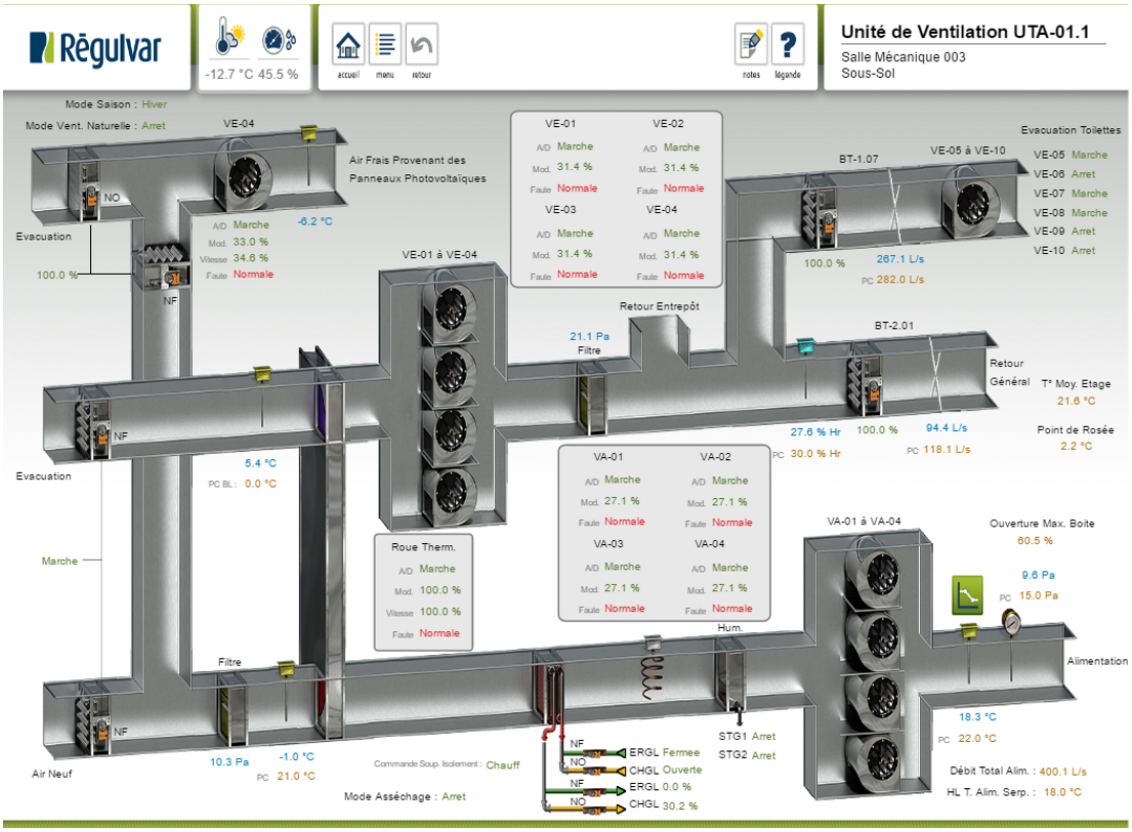

Figure A.8: BIPV/T control graphical user interface. Left-most ducting shows BIPV/T heat recovery being supplemented with the fresh air supply.

velocity within the air channel near 1 m/s as it was found to be a good compromise between maximizing heat transfer while reducing pressure loss (Candanedo, 2010, chap. 3). In summer, the mechanical ventilation under the panels is turned on for a minimum of 30 minutes whenever the air at the end of the cavity reaches 25°C. This air is exhausted directly to the outside since there is no need to harvest heat during summer.

A.5.3 Loss of Production

Expertise in the installation and configuration of photovoltaic arrays was lagging in Quebec since grid-purchased electricity remains relatively inexpensive and there is not yet a strong push towards on-site renewables.

Ten 10 kW inverters convert the DC output from the photovoltaic system to AC to be used by the building or exported to the grid. The inverters were slightly undersized with

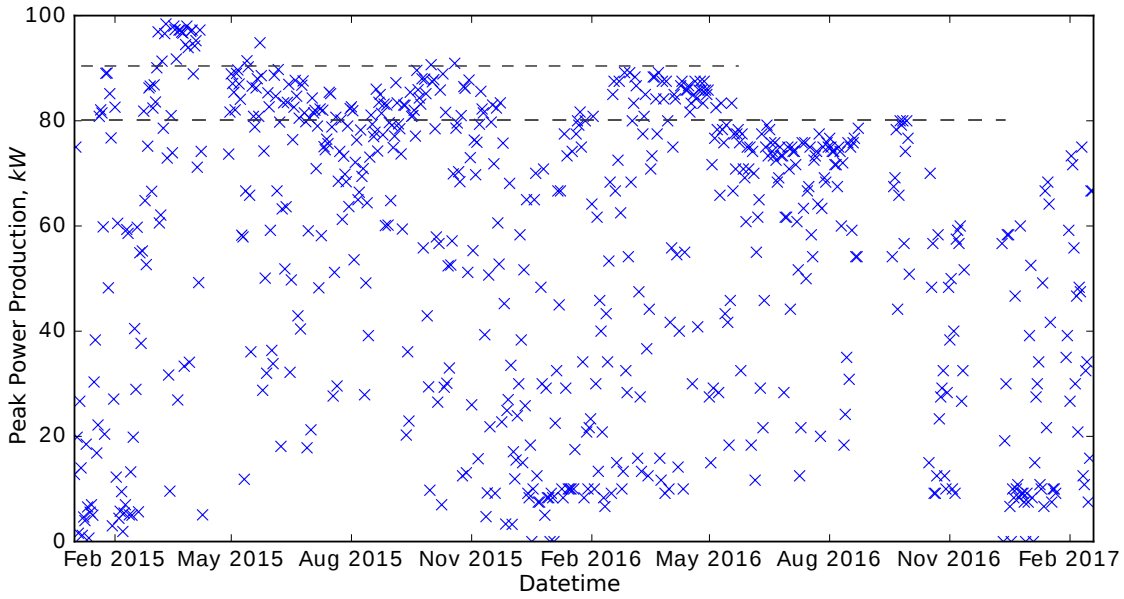

Figure A.9: Daily Electrical Peak Power Production. Around June 2015 the peak no longer crosses 90 kW, and around May 2016 the peak no longer crosses 80 kW. A new controller was installed on February 2017 to monitor individual inverters.

the aim to achieve higher yields during average days. The daily peak production for the whole history of the building is plotted in Figure A.9 and shows that the installed 110.5 kWp power was never achieved due to losses in wiring and conversion. Tracking the peaks, past June 2015, they reach a maximum of 90 kW. Similarly, past May 2016, the daily peaks do not surpass 80 kW. After a site visit, we noticed that two inverters were not functioning whereas a third was functioning erratically. These inverters were connected to larger strings of PVs. Poorly functioning inverters have since been replaced. We suspect the inverters are breaking down due to a combination of (1) a much larger production than their rated 10 kW caused overloading, (2) the maximum power point tracker (MPPT) had failed, (3) the PV strings were not wired correctly, and/or (4) the inverter settings were incorrect and led to failures. A dedicated controller has been installed since February 2017 to monitor the individual inverters; only aggregate amounts were logged beforehand. We can observe similar trends by looking at the daily energy production in Figure A.10. Further rewiring and correction were also commissioned in a follow-up study from CanmetENERGY-Varennes highlighting the need for improving the familiarity of these systems and to warrant better

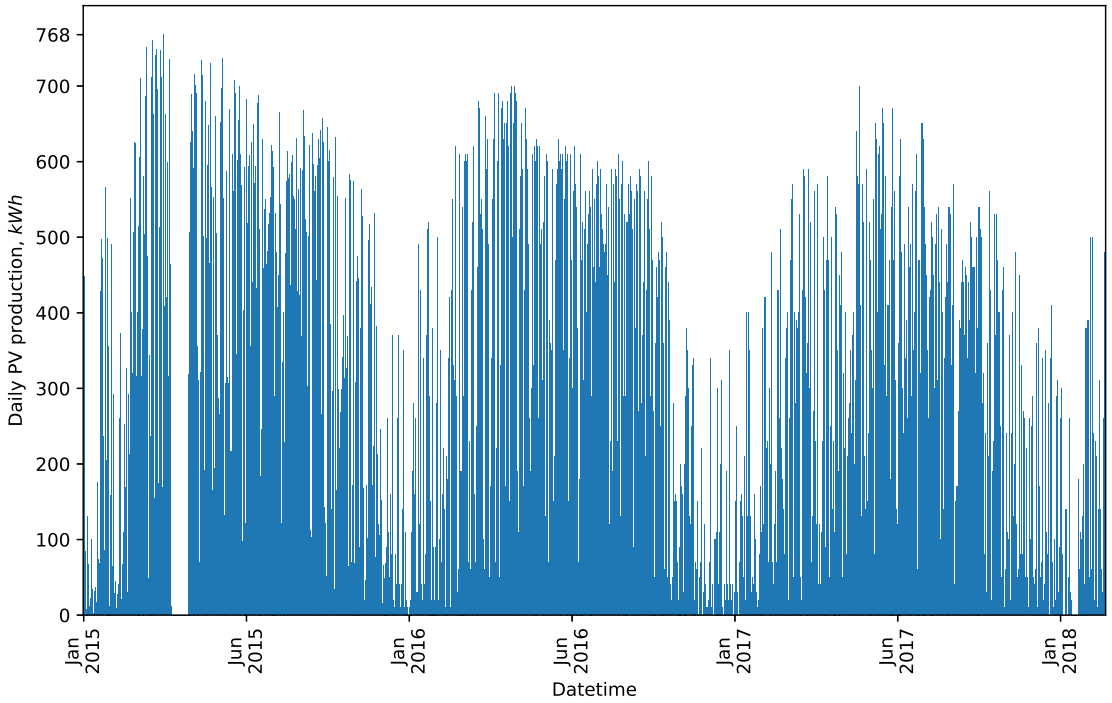

Figure A.10: Daily Electrical Energy Production.

training of electricians and installers.

A.5.4 Solar Irradiance Measurements

Three sources of solar irradiance values are available near the library: (1) the Montreal international airport (IATA: YUL, ICAO: CYUL), (2) the St-Hubert airport (IATA: YHU, ICAO: CYHU), and (3) CanmetENERGY-Varennes PV research measurement station. The airports offer radiation data in 1-hour intervals and is too crude for a detailed analysis when the rest of the collected data has a 5-minute to 15-minute resolution. CanmetENERGY is located 8 km from the library. To assure the data collected there corresponds closely to the library's on-site conditions, I designed and built a solar-battery-powered data-logger with an instrument amplifier connected to two pyranometers (LI-COR LI-200R with 400 to 1100 nm range) sitting on a 3D-printed customized mount, see Figure A.11. Data was collected in the summer period and showed a strong correlation with data obtained from CanmetENERGY. Due to considerations outside the scope of expertise, the data from the data-loggers cannot be used since temperature corrections due to the change of the resistance

(a) Small PV panel charging control box battery seen on the right of the pole

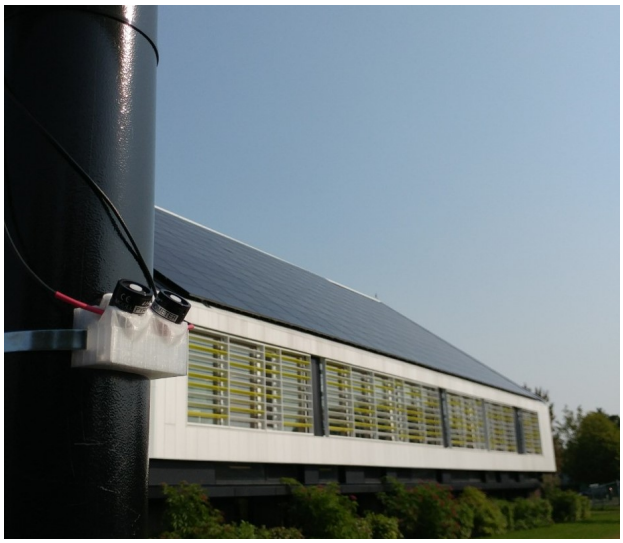

(b) Two pyranometers installed on a custom-designed 3D-printed mount with angles matching library roof panels

Figure A.11: On-site pyranometer measurement, instrument amplifier and data-logger setup. Data collected used to compare values obtained from CanmetENERGY Varennes located nearby.

of the gain-setting resistor on the instrument amplifier was not considered. As of summer 2019, CanmetENERGY has installed a weather station on the library's site with two infrared thermal cameras directed to the two BIPV/T roof sections.

Appendix B

Supplementary Models and Details

B.1 Causal Effects between Input Features

Runge et al. (2019) has developed a method to, beyond simple correlations, determine the causal effects within variables and have made it available through their Python package `tigramite`[1]. The proposed method was used on the Varennes library data that would be used to fit partially the 3rd-order model to keep the graphs simple. Figure B.1 shows the relationship of the points to one another through time; arrows depicting the direction of causality – the numbers on the arrows represent the significant time lags to consider whereas the colours of the dots represent the self-correlation through time.

Solar radiation (GHI) is affecting the room air temperature of the space above the radiant slab, which is on the southern perimeter. Not having known its orientation, it may have been inferred based on this correlation. Solar radiation also affects exterior temperature. Focusing on the heat sources, they are all interdependent because of a common thermal loop and this does show up in the correlation analysis. Due to the common loop, this methodology is unable to strongly separate their individual effects to their attributed zones. The analysis was carried considering a maximum time lag effect of 8 steps – 2 hours – and the maximum reported significant time lag in the 10% significance threshold is 2 – 30 minutes – for the radiant slab; 15 minutes for the air systems. This means that an applied heat to a thermal node takes at most 30 minutes to be felt by a zone. The pipes in the radiant slab are close

[1] `https://github.com/jakobrunge/tigramite/`

to the surface. At the 10% sigma level, the exterior temperature is shown to not influence the interior temperature. For a well-insulated and air-tight building like the library, the exterior temperature is only felt through the fresh air into the air handling unit, and for this particular building, that effect is also lessened due to having a demand-driven system which utilizes heat recovery from the BIPV/T system.

The modelling approach herein is based on predicting one timestep at a time. Should we have used an approach to predict a longer sequence, we would have limited it to 2 past steps and 2 future steps since there is no strong evidence to go longer and warrant a more complicated model.

B.2 State-Space Model Matrices

This section details the different ordered – in space – state-space models used in this work. The general state-space formulation – 1st-order in time – is given:

$y(t) = x(t+1) = Ax(t) + Bu(t) + Cw(t)$, where:

$y(t)$ model output, which is the same as what goes back in for the following timestep (recursive).

$x(t)$ system variables to track, *e.g.* zone temperature.

$u(t)$ controllable variables, *e.g.* heating/cooling stages, fan, damper position, or other.

$w(t)$ exogenous inputs, *e.g.* weather and time indicators.

A, B, C state and input matrices.

The state and input matrices are designed for the different models.

B.2.1 1st-Order Model

The 1st-order model in its state-space representation can be described by the following equations:

$\mathrm{x} = \left\{ T_{air} \right\}^T$

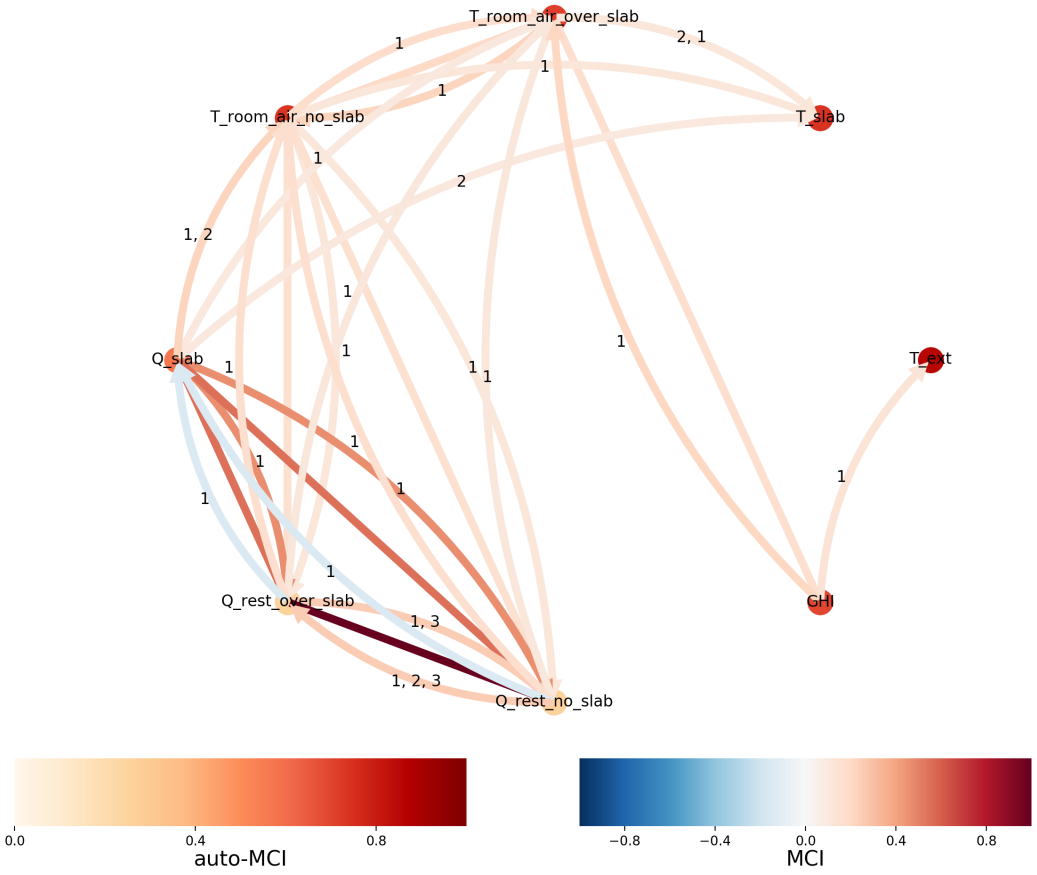

Figure B.1: Input causality graphs: 10% significance, data from January 7 to February 14, 2018.

$$
\begin{aligned}
\mathrm{u} &= \left\{ Q_{total} \right\}^T \\
\mathrm{w} &= \left\{ T_{ext} \quad \mathrm{Cons}_{\mathrm{\emptyset HVAC}} \quad \mathrm{GHI} \right\}^T \\
\mathrm{A} &= \left[1 - \frac{U_{air,ext}\Delta t}{C_{air}} \right] \\
\mathrm{B} &= \left[\frac{\Delta t}{C_{air}} \right] \\
\mathrm{C} &= \left[\frac{U_{air,ext}\Delta t}{C_{air}} \quad \frac{\alpha_{gains}\Delta t}{C_{air}} \quad \frac{\alpha_{sol}\Delta t}{C_{air}} \right] \\
\mathrm{A}_{black} &= \left[a_{1,1} \right] \\
\mathrm{B}_{black} &= \left[b_{1,1} \right]
\end{aligned}
$$

$\mathrm{C}_{black} = \begin{bmatrix} c_{1,1} & c_{1,2} & c_{1,3} \end{bmatrix}$

Where,

$\mathbf{U_{air,ext}}$ Library effective wall conductivity between $\mathrm{T_{air}}$ and $\mathrm{T_{ext}}$.

$\mathbf{C_{air}}$ Library air effective thermal capacitance; includes the air, furniture, the walls.

$\alpha_{\mathbf{gains}}$ Factor converting electrical consumption net of HVAC equipment to internal gains.

$\alpha_{\mathbf{sol}}$ Factor converting GHI to solar gains within the library.

B.2.2 2nd-Order Model

The 2nd-order model in its state-space representation can be described by the following equations:

$$\mathrm{x} = \begin{Bmatrix} T_{slab} & T_{air} \end{Bmatrix}^T$$

$$\mathrm{u} = \begin{Bmatrix} Q_{slab} & Q_{air} \end{Bmatrix}^T$$

$$\mathrm{w} = \begin{Bmatrix} T_{ext} & \mathrm{Cons}_{\emptyset\mathrm{HVAC}} & \mathrm{GHI} \end{Bmatrix}^T$$

$$\mathrm{A} = \begin{bmatrix} 1 - \frac{U_{air,slab}\Delta t}{C_{slab}} & \frac{U_{air,slab}\Delta t}{C_{slab}} \\ \frac{U_{air,slab}\Delta t}{C_{air}} & 1 - \frac{U_{air,slab}\Delta t}{C_{air}} - \frac{U_{air,ext}\Delta t}{C_{air}} \end{bmatrix}$$

$$\mathrm{B} = \begin{bmatrix} \frac{\Delta t}{C_{slab}} & 0 \\ 0 & \frac{\Delta t}{C_{air}} \end{bmatrix}$$

$$\mathrm{C} = \begin{bmatrix} 0 & 0 & \frac{\alpha_{sol}\Delta t}{C_{slab}} \\ \frac{U_{air,ext}\Delta t}{C_{air}} & \frac{\alpha_{gains}\Delta t}{C_{air}} & 0 \end{bmatrix}$$

$$\mathrm{A}_{black} = \begin{bmatrix} a_{1,1} & a_{1,2} \\ a_{2,1} & a_{2,2} \end{bmatrix}$$

$$\mathrm{B}_{black} = \begin{bmatrix} b_{1,1} & 0 \\ 0 & b_{2,2} \end{bmatrix}$$

$$\mathrm{C}_{black} = \begin{bmatrix} c_{1,1} & c_{1,2} & c_{1,3} \\ c_{2,1} & c_{2,2} & c_{2,3} \end{bmatrix}$$

$\mathbf{U_{air,slab}}$ Effective conductivity between the air $\mathrm{T_{air}}$ and radiant slab $\mathrm{T_{slab}}$.

$\mathbf{U_{air,ext}}$ Effective conductivity between the air $\mathrm{T_{air}}$ and exterior $\mathrm{T_{ext}}$.

C_{slab} Radiant slab effective thermal capacitance.

C_{air} Library air effective thermal capacitance; includes the air, furniture, the walls.

B.2.3 3rd-Order Model

The 3rd-order model in its state-space representation can be described by the following equations:

$$\mathrm{x} = \begin{Bmatrix} T_{slab} & T_{air-south} & T_{air-north} \end{Bmatrix}^T$$

$$\mathrm{u} = \begin{Bmatrix} Q_{slab} & Q_{air-south} & Q_{air-north} \end{Bmatrix}^T$$

$$\mathrm{w} = \begin{Bmatrix} T_{ext} & \mathrm{Cons}_{\text{øHVAC}} & \mathrm{GHI} \end{Bmatrix}^T$$

$$\mathrm{A} = \begin{bmatrix} 1 - \frac{U_{air-S,slab}\Delta t}{C_{slab}} & \frac{U_{air-S,slab}\Delta t}{C_{slab}} & 0 \\ \frac{U_{air-S,slab}\Delta t}{C_{air-S}} & 1 - \frac{U_{air-S,slab}\Delta t}{C_{air-S}} - \frac{U_{air-S,ext}\Delta t}{C_{air-S}} - \frac{U_{air-N,air-S}\Delta t}{C_{air-S}} & \frac{U_{air-N,air-S}\Delta t}{C_{air-S}} \\ 0 & \frac{U_{air-N,air-S}\Delta t}{C_{air-N}} & 1 - \frac{U_{air-N,air-S}\Delta t}{C_{air-N}} - \frac{U_{air-N,air-S}\Delta t}{C_{air-N}} \end{bmatrix}$$

$$\mathrm{B} = \begin{bmatrix} \frac{\Delta t}{C_{slab}} & 0 & 0 \\ 0 & \frac{\Delta t}{C_{air-south}} & 0 \\ 0 & 0 & \frac{\Delta t}{C_{air-north}} \end{bmatrix}$$

$$\mathrm{C} = \begin{bmatrix} 0 & 0 & \frac{\alpha_{sol}\Delta t}{C_{slab}} \\ \frac{U_{air-south,ext}\Delta t}{C_{air-south}} & \frac{\alpha_{gains-south}\Delta t}{C_{air-south}} & 0 \\ \frac{U_{air-north,ext}\Delta t}{C_{air-north}} & \frac{\alpha_{gains-north}\Delta t}{C_{air-north}} & 0 \end{bmatrix}$$

$U_{\text{air-south, slab}}$ Effective conductivity between the south air $T_{\text{air-south}}$ and radiant slab T_{slab}.

$U_{\text{air-south, ext}}$ Effective conductivity between the south air $T_{\text{air-south}}$ and exterior T_{ext}.

$U_{\text{air-north, ext}}$ Effective conductivity between the north air $T_{\text{air-north}}$ and exterior T_{ext}.

$U_{\text{air-north, air-south}}$ Effective conductivity between the north and south air $T_{\text{air-north}}$ & $T_{\text{air-south}}$.

C_{slab} Radiant slab effective thermal capacitance.

$C_{\text{air-south}}$ South-side library air above radiant slab effective thermal capacitance.

$C_{\text{air-north}}$ North-side library air *not* above radiant slab effective thermal capacitance.

$\alpha_{\textbf{gains-[side]}}$ Factor converting electrical consumption net of HVAC equipment to internal gains where [side] corresponds to either north or south.

B.3 Monte Carlo Posterior Fit Sampling

This section shows the Monte Carlo sampling outputs for the 3 models. Each dot in the plots represents one sample and if there are adequate number of samples, a contour plot is used instead for clarity. Within the contour plots, a darker colour represents a higher density of points. The last plot on each row shows a density plot for that corresponding parameter. The 1st-order model is shown in Figure B.2, the 2nd-order in Figure B.3, and the 3rd-order in Figure B.4.

B.4 Photovoltaic Power Generation Projected Solar Linear Model

The PV AC generation is calculated from solar radiation data obtained from CanmetENERGY and projected onto the PV arrays per unit square, according to geometric correlations (Duffie et al., 2020). The PV AC generation can be modelled as a linear function using the projected values, see Equations B.1 and B.2. This part remains separated from energy model but is input in the optimization in chapter 5.

$$\text{PVgen} = \alpha_{\text{projected2PVpower}} \text{I}_{\text{proj}} \tag{B.1}$$

The PV array – 425 panels – is separated into two areas with different orientations: a due south – 167 panels, $\psi = 0$ °– and south-east – 258 panels, $\psi = -14$ °east of south – section. Both sections have the same tilt – $\beta = 37$ °. The solar projection onto the whole array per unit area is as follows:

$$\text{I}_{\text{proj}} = \text{DHI}\frac{1 + cos(\beta)}{2} + \text{DNI}(\frac{167}{425}cos(\theta_S) + \frac{258}{425}cos(\theta_{SE})) \tag{B.2}$$

Where,

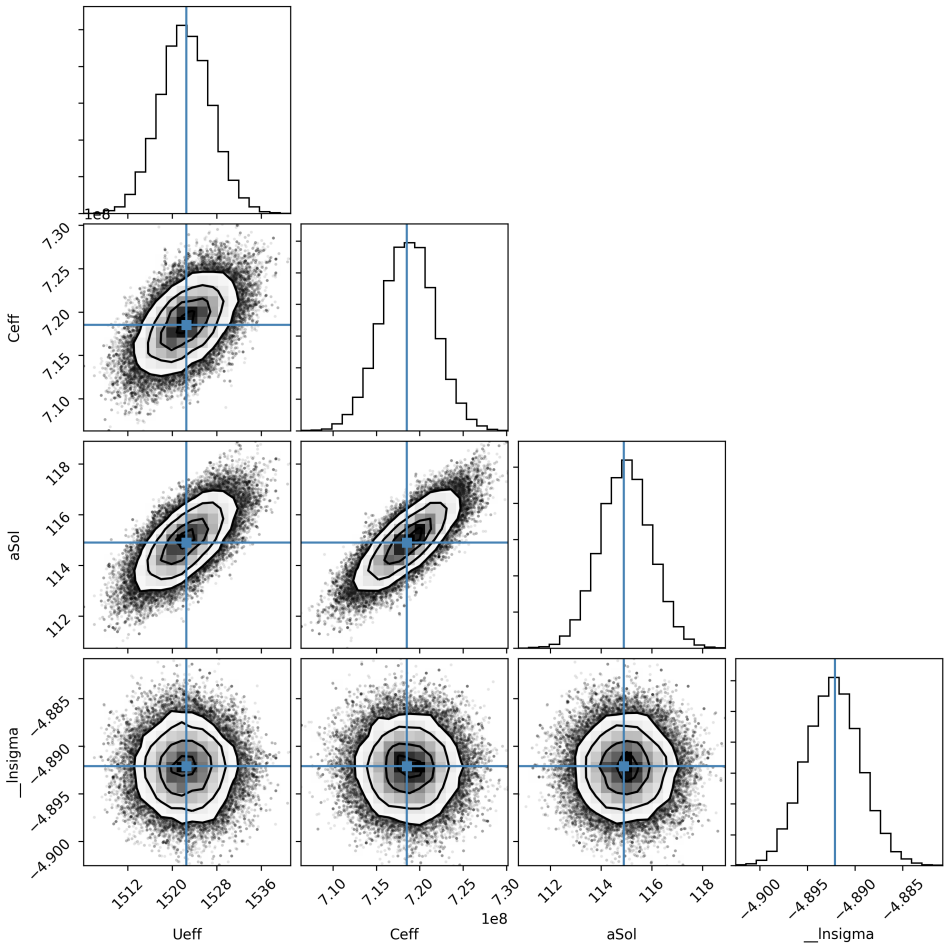

Figure B.2: 1st-order `emcee` Monte Carlo sampling output after first fit using `lmfit`. Settings: timestep: 15-min, decay factor: 0.2, prediction horizon: 6 hours, train data: 4 weeks. Posterior parameter distributions for the effective conductance and capacitance, and the solar gain coefficient shown. Distributions appear normal and unimodal and therefore stable around the best estimate. Lnsigma is a coefficient used for sampling.

DHI diffuse horizontal irradiance (W/m^2),

DNI direct normal irradiance (W/m^2),

θ incidence angle between the normal to the panels and the Sun's rays, calculated using solar angle equations,

ψ surface azimuth angle (west of south is positive),

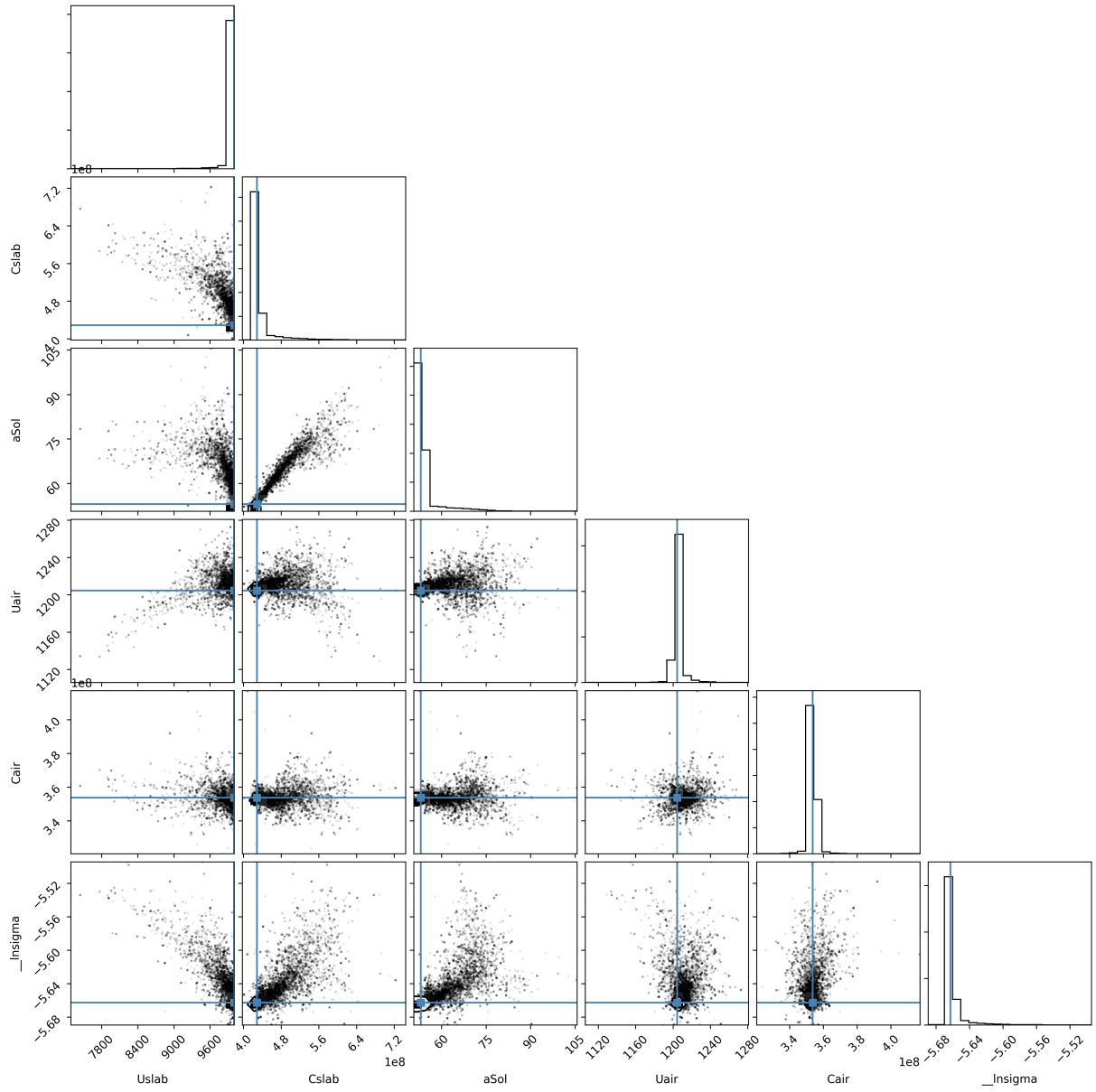

Figure B.3: 2nd-order `emcee` Monte Carlo sampling output after first fit using `lmfit`. Settings: timestep: 15-min, decay factor: 0.2, prediction horizon: 6 hours, train data: 4 weeks, importance: 50/50. Posterior parameter distributions for the conductances and capacitances for the slab and air nodes, and the solar gain coefficient shown. Distributions appear unimodal but with fatter tails. Lnsigma is a coefficient used for sampling.

β surface tilt angle relative to horizontal.

Collected data is used to fit the α coefficient by minimizing the mean squared error

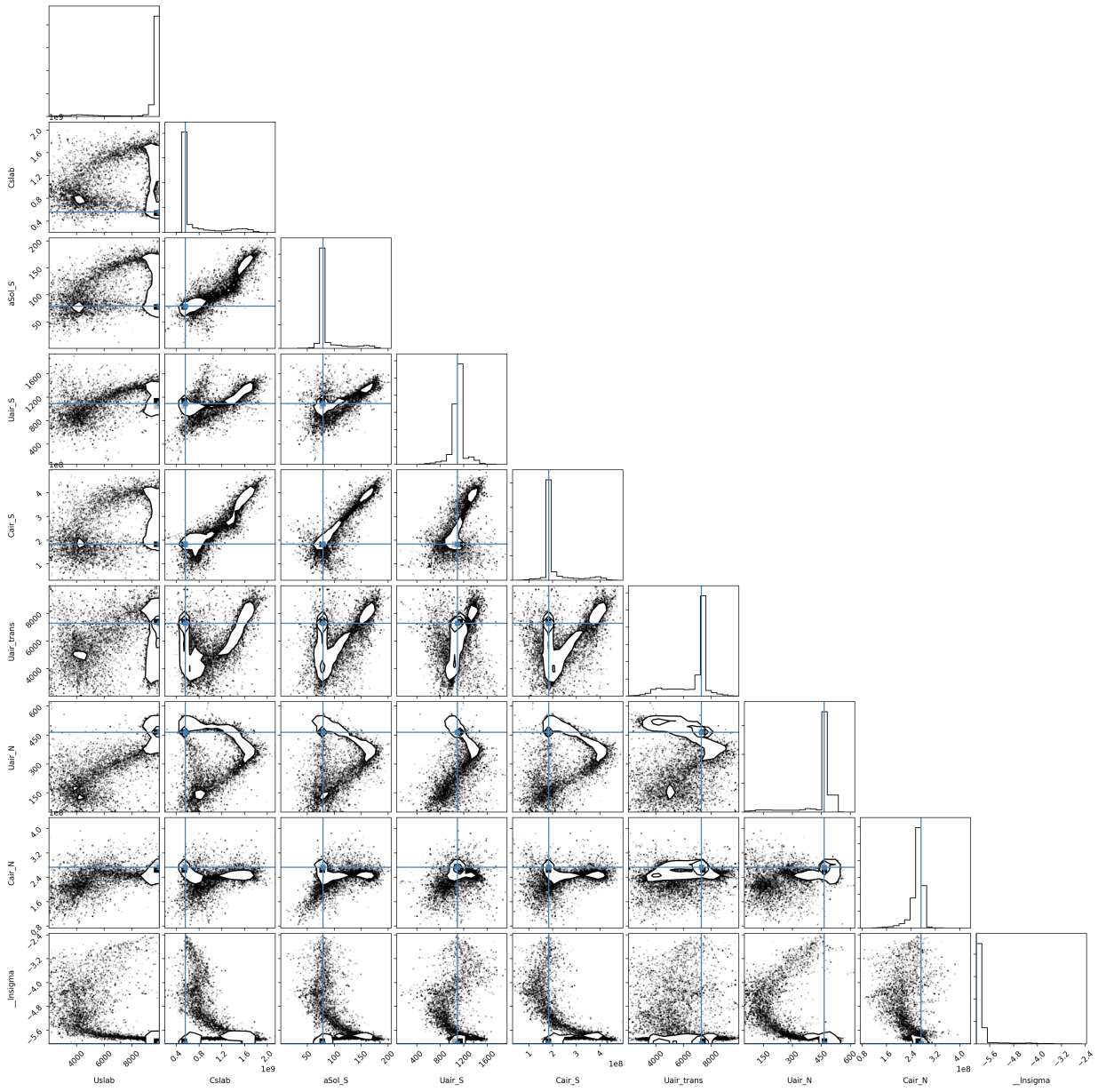

Figure B.4: 3rd-order `emcee` Monte Carlo sampling output after first fit using *lmfit*. Settings: timestep: 15-min, decay factor: 0.2, prediction horizon: 6 hours, train data: 4 weeks, 33/33/33 importance. Posterior parameter distributions for the conductances and capacitances for the slab and both air nodes, the conductance connecting both zones, and the solar gain coefficient shown. Distributions appear slightly bimodal and may contain combinations of equifinality. Lnsigma is a coefficient used for sampling.

between actual and predicted values, and is reported in Table 5.1 and shown in Figure 5.4 in section 5.3.1.

B.5 Exterior Ambient Temperature Forecast Noised Model

To have a realistic noise in the exterior ambient temperature predictions, forecast data was collected and analyzed to derive a model to describe this uncertainty as a function of forecast length. Collected data from the local airport (IATA: YUL, ICAO: CYUL) from January 2015 to October 2016 are considered. The predicted ambient temperatures are aligned to what happened in the future to calculate the differences, shown in Figure B.5 for hours with at least 50 samples. This analysis serves to better understand how off and how accurate these predictions are and the errors serve to add a sensible amount of noise to temperature predictions in a live application.

With the differences at various hours collected, their covariance can be calculated, see Figure B.6 left. Since not every prediction hour has enough samples to generate the full covariance matrix, the missing values were interpolated using a bivariate spline approximation (SciPy, 2019).

Lastly, noise samples are generated from a multivariate normal distribution with mean 0 and the covariance calculated and interpolated above, see Figure B.6. The noise would be added to the temperature predictions from the weather source.

B.6 Solar Radiation Cloudiness Sampling Model

Solar radiation prediction is very difficult. In this section, a simplified approach is proposed where the type of day would be predicted and a profile with the magnitude of solar radiation would be sampled from normalized historical data.

The k-means clustering is applied assuming the existence of 3 clusters or types of days: overcast, partially cloudy and clear sunny days. Applying clustering naively on collected data, a seasonal variation – length of day – instead of the intraday variances is observed, as

shown in Figure B.7.

To remedy this behaviour, collected solar radiation data are compared to a sunny day using the Hottel clear sky model (Hottel, 1976). Comparing the clear sky model to collected data, both did not agree perfectly and a one-year periodic calibration function was used to scale the amplitude. To remove the seasonal bias, the beginnings and ends of each day was cut short. Figure B.8 shows the clustering applied to the ratios and a calendar corresponding to those clusters are shown in Figure B.9.

Finally, the objective of the clustering approach is to predict the solar radiation cluster for the next day, sample a ratio curve from Figure B.8, fill the morning and evenings where the ratio was cut with normally distributed noise with variance equalling that of the cluster's,

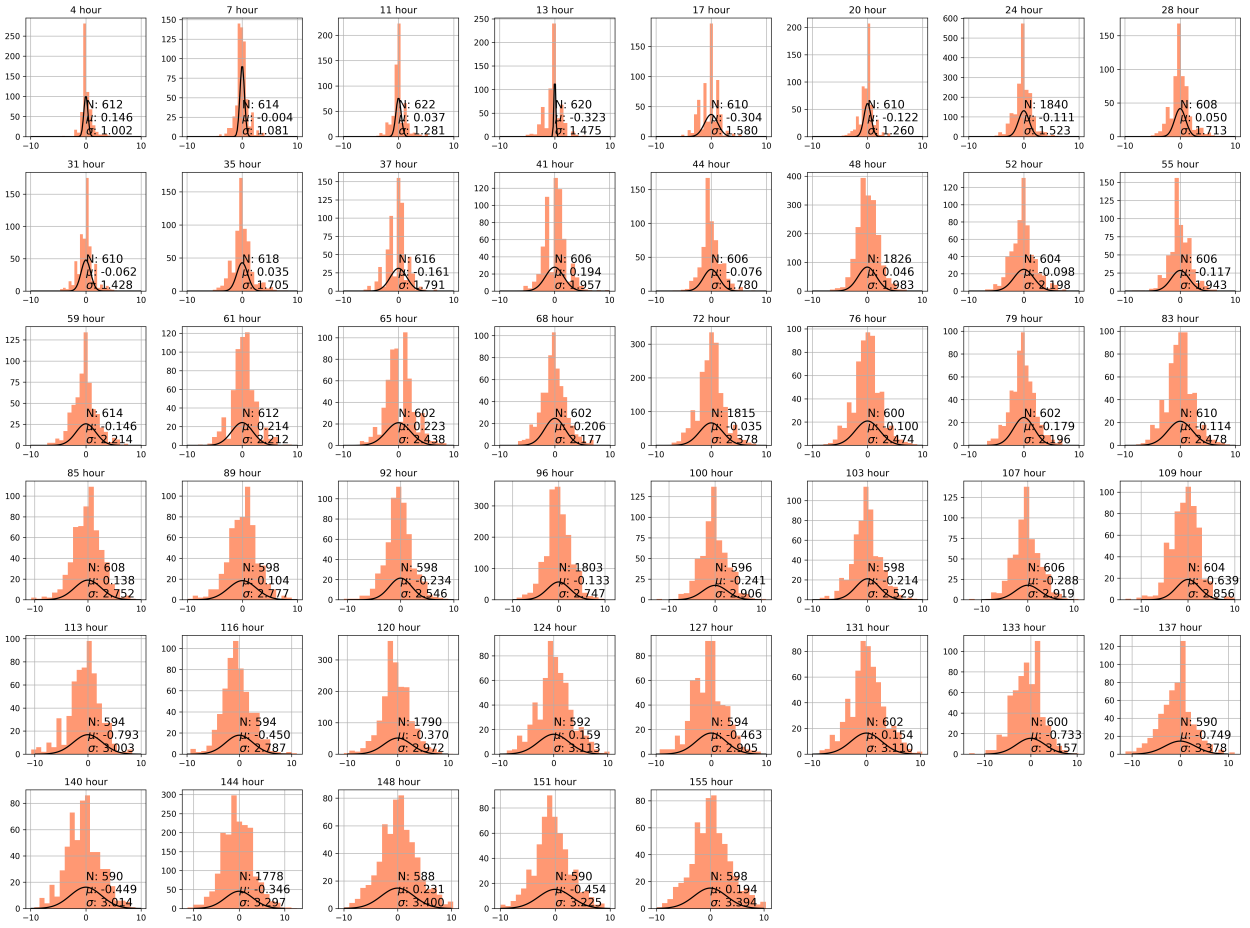

Figure B.5: Ambient temperature prediction error for various look-ahead periods. Periods are noted in the subplot titles.

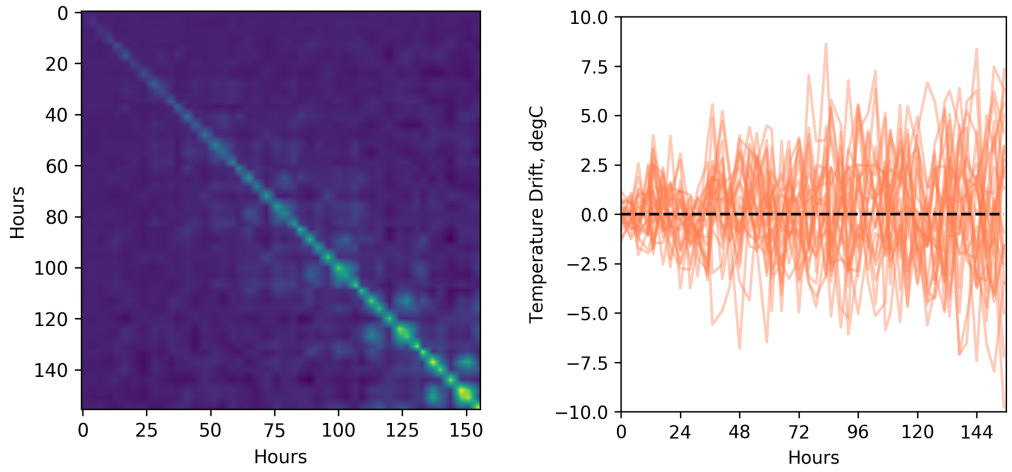

(a) Error covariance, brighter colour signifies stronger variance

(b) Prediction noise

Figure B.6: Ambient temperature covariance and forward noise.

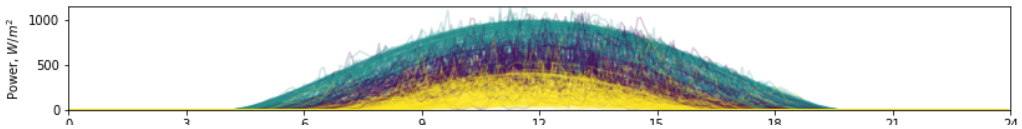

Figure B.7: GHI clustering using raw data.

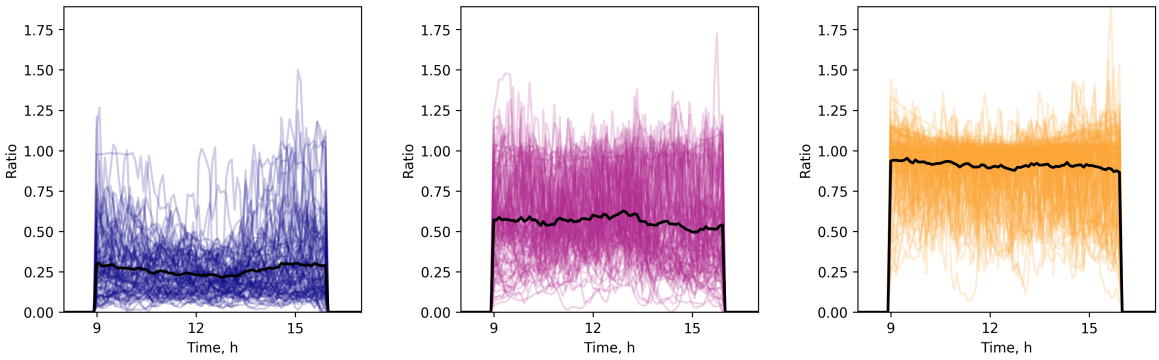

(a) Overcast

(b) Partially cloudy

(c) Sunny

Figure B.8: GHI ratio clustering.

and, last, multiply this filled ratio to the corrected Hottel clear sky output to obtain a likely radiation profile. The analysis was done on 5-minute interval data and can be resampled to longer intervals by randomly picking an appropriate number of points, *e.g.* to resample to 15-minutes, one of the three 5-minute points is sampled. As a comparison, we have

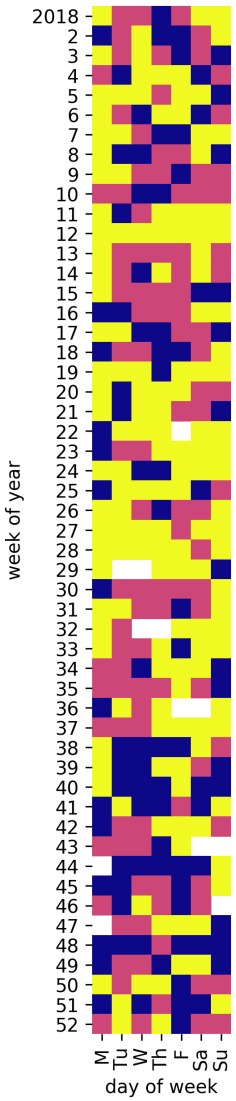

Figure B.9: Solar day type clustering calendar.

also simulated with using normally distributed noise with variance equalling that of the cluster's. The noise-based, sample-based and resampled sample-based approaches are shown in Figure B.10. The sampled solar radiation can then be used in the building energy and photovoltaic production models.

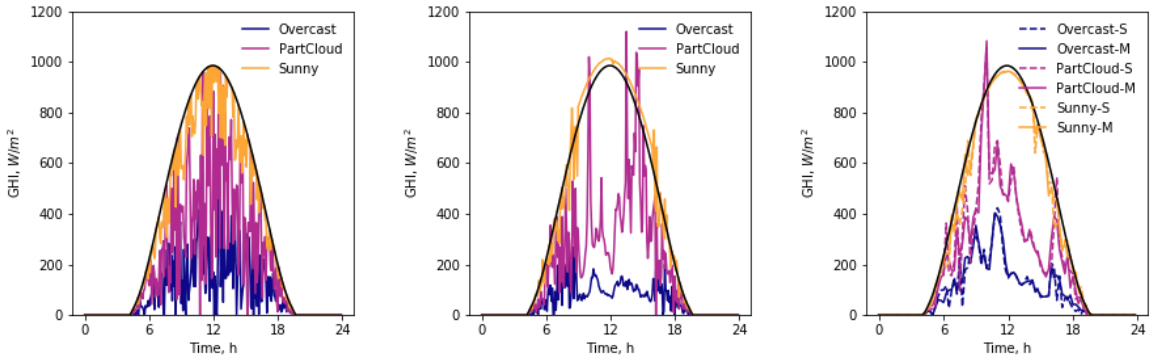

(a) Gaussian noise

(b) Sampled ratio noise with Gaussian noise extrapolation

(c) Sampled ratio noise with Gaussian noise extrapolation, resampled to 15 minutes

Figure B.10: GHI for sunny, partially cloudy and overcast days.

Appendix C

Publication Contributions and Significance

The following is a list of the contributions completed as part of this PhD dissertation categorized per main topics.

Papers [Journal: 2; Conference: 1, 2, 4; Poster: 1, 2] explore methods of optimal operation for the library, describe its operation and assesses the energy flexibility of the building. **Personal contribution** Lead on the data collecting and processing for the building. Performed the exploratory data analysis, analyzed its early performance and suggested improvements. ASHRAE journal paper was written to highlight the key features that got the building to be net-zero and receive a LEED Gold certification. International policies for climate change incentivize these types of buildings and the interplay of the HVAC system with the renewable generation must be better mastered. For co-authored publications, I offered explanation of the design intent and for the detailed specifications, data and scripts to aid in their respective end goals.

Papers [Journal: 1, 3; Conference: 5,6] analyze the performance of a novel phase-change material based expandable thermal storage solution that would be installed as a retrofit measure: part of the HVAC system or into the building envelope. **Personal contribution** The design of the storage solution is my brainchild. This is work continuing from my Master's where modelling of the thermal storage was carried out and validated using experiments that I designed and ran. The studies features this storage solution to be used to reduce the peak

demand of a building through MPC. For the co-authored papers, I provided support for the parts utilizing the phase-change material through explaining the thermal cycling procedure and offered help with the programming implementation.

Papers [Journal: 4; Conference: 7] simulate and optimize the design of a net-zero energy building taking into consideration the primary energy factor of the grid where instead of relying on electricity price, a building that can operate while clean energy sources would be available would be optimal. **Personal contribution** I was responsible of collecting and cleaning public energy data from the Ontario grid; I wrote a script to automate the procedure. I designed an approach to use surrogate deep learning models instead of EnergyPlus for design exploration offering a 100x speedup, however, that approach was largely abandoned.

Paper [Conference: 3] is an exploratory idea to design a reinforcement learning based optimal controller that can be mass-applied to residential buildings. **Personal contribution** First, I designed and implemented a reinforcement learning (RL) agent class that can learn with experience. I also created controllers utilizing ON/OFF staging and PID loops to be able to compare the predictive method to the conventional ones typically present in homes. Second, I built a generic and general physics-based environment to train the RL agent. The environment parameters can be tuned with collected data and randomized to cover a wide range of possible instances. The model would learn on these cases and would perform *well-enough* to be mass-applied and its policy would be refined *in situ*.

C.1 Articles Published in Refereed Journals

1. Morovat, N., Candanedo, J.A., Athienitis, A.K., **Dermardiros, V.** (2019). Simulation and performance analysis of an active PCM-heat exchanger intended for building operation optimization. *Energy and Buildings.*

2. **Dermardiros, V.**, Athienitis, A.K., Bucking, S. (2019). Energy performance, comfort and lessons learned from an institutional building designed for net-zero energy. *ASHRAE Transactions* 125, Part 1.

3. Papachristou, A.C., Vallianos, C.A., **Dermardiros, V.**, Athienitis, A.K., Candanedo,

J.A. (2018). A numerical and experimental study of a simple model-based predictive control strategy in a perimeter zone with phase-change material. *Science and Technology for the Built Environment.*

4. Bucking, S., **Dermardiros, V.** (2017). Distributed evolutionary algorithm for co-optimization of building and district systems for early community energy masterplanning. *Applied Soft Computing Journal*, Volume 63 (Feb 2018): 14-22.

C.2 Conference Proceedings

1. Amara, F., **Dermardiros, V.**, Athienitis, A.K., Buonomano, A. (2020). Energy Flexibility Modelling and Implementation for an Institutional Net-zero Energy Solar Building and Design Application. 2020 Summer Study on Energy Efficiency in Buildings: Efficiency – The Core of a Clean Energy Future. American Council for an Energy-Efficient Economy. Pacific Grove, CA, 2020-08-17 to 21.

2. Amara, F., **Dermardiros, V.**, Athienitis, A.K. (2019). Energy flexibility for an institutional building with integrated solar system: Case study analysis. 2019 IEEE Electrical Power and Energy Conference (EPEC). Montreal, Quebec, Canada.

3. **Dermardiros, V.**, Bucking, S., Athienitis, A.K. (2019). A simplified building controls environment with a reinforcement learning application. IBPSA Building Simulation 2019 conference, Rome, Italy, 2019-09-02 to 04.

4. **Dermardiros, V.**, Vallianos, C., Athienitis, A.K., Bucking, S. (2017). Model-based control of a hydronic radiant slab for peak load reduction. IBPSA Building Simulation 2017 conference, San Francisco, CA, USA, 2017-08-07 to 09.

5. Avagliano, G., Buonomano, A., Cellura, M., **Dermardiros, V.**, Guarino, F., Palombo, A. (2017). Buildings integrated phase-change materials: modelling and validation of a novel tool for the energy performance analysis. BSA 2017 Proceedings, Bolzano, Italy, 2017-02-08 to 10.

6. **Dermardiros, V.**, Athienitis, A.K. (2016). Building-Integrated PCM-TES for peak load reduction. eSim 2016. (May 2016).

7. Bucking, S., **Dermardiros, V.**, Athienitis, A.K. (2016). The effect of hourly primary energy factors on optimal net-zero energy building design. eSim 2016. (May 2016).

C.3 Non-Refereed Contributions

1. Amara, F., **Dermardiros, V.**, Athienitis, A.K. (2019). Energy Flexibility for an Institutional Net-Zero Energy Building in a Cold Climate (Poster). 2019 IEEE Electrical Power and Energy Conference (EPEC). Montreal, Quebec, Canada. 2019-10-16 to 18.

2. **Dermardiros, V.**, Vallianos, C., Dumoulin, R., Kapsis, K., Athienitis, A.K. (2016). On Demand Side Management and Grid Interaction for Institutional Net-Zero Energy Buildings in Canada (Poster). 7th International Conference on Integration of Renewable and Distributed Energy Resources, Niagara Falls, Canada, 2016-10-24 to 28.